Removal of Engineered Nanomaterials Using Polyelectrolytes

高分子電解質を用いた人工ナノマテリアルの除去

SOENARYO Tirto

Doctor of Engineering
Graduate School of Environmental Studies, Nagoya University

2018

Acknowledgements

This thesis was written based on the research activities conducted on Murata -Zinchenko Laboratory in Nagoya University from 2015 until 2018. This thesis can be written not only by my own strength, but the help of a lot of people. Thus, I would like to express my gratitude to them.

Firstly, I would like to present this thesis to my parents and my family since they were and are the ones who care much about my education. Without their support and encouragement, this thesis would never be realized. Through the hardship, I can spend my doctorate life without any lacking.

Secondly, I would like to express my gratitude to my academic supervisor, Anatoly Zinchenko. Without his supervising, I would not get any idea about how to use polyelectrolytes for environmental purposes, what is important in doctorate life and how to write a proper paper. I still have difficulty to express my opinion scientifically. Nonetheless, it is so much better now.

I would not forget about the help of Prof. Shizuaki Murata who guided me with his own way. It was very unique way to make me realize that I was lacking certain part in my research. The two of them make a unique combination that will be left in my memories.

Next, I would like to express my gratitude to all people who helped me to get chemicals, do measurement and get some data. Like any other stories, their parts might not be big, but crucial in my thesis and experiment.

I would like to express my gratitude to all members of Indonesian association members for filling the days I spent in Nagoya. Especially to my best friends who I met in Nagoya, Bill

Mangindaan for spending a lot of time with me doing silly things, going to many trips and discussing some topics, Anthony Santoso for sharing his food treasures with me and for Jovano Erris Nugroho for being my first friend and having some fun together. Special thanks to the “Kindahausen” uncle and aunty and Ms. Kasmiati for providing Indonesian food for me.

I also wanted to express my gratitude to my gossip friends, Indra Oliver Candra Hadyiswanto and Sri Rahayu, who are always there for me during ups and downs from undergraduate.

I also wanted to express my gratitude for the M2 students of my lab, Wakahara Akihiro, Taniguchi Shota and Inagaki Eisuke, who graduated one year earlier than me for filling my Ph.D. life with a lot of joy. I hoped that I could understand Japanese better so I could exchange a lot of idea with you guys. However, I loved the silly chitchatting with my broken Japanese.

For helping me with my financial, I am really grateful to Japan Tobacco Asia Scholarship. Through their help, I can at last finish my Ph.D. without financial problem. Moreover, through them, I met a lot of wonderful friends and I could experience a lot kind of Japanese culture.

Lastly, I would like to express my gratitude to my current supervisor in Micron Memory Japan, Ayumu Matsuoka who still supports me to finish the final part of my Ph.D. life as well as some of my mates in this company who cheer me up, Tachta Erlangga, Oat (Chaiyanan Kulchaisit), Taichi Watanabe and Taichi Osato.

I feel that they are still a lot of them that I cannot write here. However, I am truly grateful for everyone. Thank you for being a part of my life journey.

Table of Contents

Nomenclature

APTES: 3- aminopropyltriethoxy- silane (99%)

C_{60}-OH: hydroxylated fullerenes

CMC: carboxymethyl celluloses

CNT-OH: hydroxlated multi-walled carbon nanotubes

DLS: dynamic light scattering

ENM : engineered nanomaterials

FM: fluorescence spectroscopy

IPEC: interpolyelectrolyte complexes

Mvis: molecular weight calculated through viscosity (using Mark-Houwink Equation)

Mw: molecular weight

NaAlg: sodium alginate

NP: nano particles

PAANa: sodium polyacrylates/ polyacrylic acids, sodium salt

PDADMAC: polydiallyldimethylammonium chloride ($(C_8H_{16}NCl)_n$)

PEG: polyethylene glycol

RBITCS: rhodamine-B isothiocyanate (RBITC)

SNURs: significant new use rules

TEM: transmission electron microscopy

TSCA: toxic substance control act

Abstract

Engineered nanomaterials (ENM) are a part of nanotechnology that boosts development of materials in various fields due to their unique chemical and physical properties. They consist of materials in dimension between 1 nm to 100 nm and various shapes (rod, nanotube and sphere are the most common). As application of ENM is progressively growing, so is the ENM production. However, starting from 2000s, there have been many reports pointing out on the toxicity of ENM and various possible scenarios of the environment contamination caused by ENM. Although several countries, such as countries in European Union and USA, are getting more concerned about the potential environmental issues associated with ENM and established a number of regulations regarding handling of ENM, the rapid advancement of ENM manufacturing technology yielding various types of ENM with new specific properties renders it difficult to establish proper handling regulations that can be implemented equally well to all types of ENM. Thus, it is highly likely, especially for developing countries, to treat some types of ENM in the same manner as bulk materials even though they behave differently. Consequently, many past studies predict that concentration of ENM in the environment will dramatically increase in the near future. There are several countermeasures that can be implemented and those include proper handling of ENM production, proper management of ENM containing waste and remediation of ENM-contaminated environment. This Ph.D. project focuses on the utilization of polyelectrolytes (PE) in such countermeasure methods. More specifically, PE are used for ENM entrapment followed by either direct removal from a contaminated media or localization and retention. Two main environmental remediation methods have been developed in this study: (1) a method by utilizing abundant natural polymer, chitosan, for decontamination of water from during water treatment, and (2) a

method by utilizing inter-polyelectrolyte complexes to immobilize ENM in porous media as a simple model of soil.

The development of ENM removal method utilizing chitosan as a single coagulant was a substantial improvement of the previously proposed strategy based on interpolyelectrolyte complexes (IPEC) that entrap ENM dispersed in water during co-precipitation. In this method, by adjustment of pH from acidic to mild basic, precipitation of chitosan entraps dispersed ENM into bulky insoluble floc. Using this method, more than 90% of ENM can be entrapped into chitosan floc. Moreover, this method can be applied to various types of ENM, such as hydroxylated fullerene (C_{60}-OH), hydroxylated carbon nanotubes (CNT-OH), gold nanoparticles (gold NP) and silica nanoparticles (silica NP). The influences of parameters that affect the efficiency of the removal process, such as PE concentration and PE molecular weight, ENM size, ionic strength, settling time as well as separation method were systematically investigated.

Besides water, soil is one of the sinks for various kinds of contamination, including ENM. In this study, we established a method to prevent ENM diffusion and spreading over a porous media (sand) by utilizing interpolyelectrolyte complexes (IPEC). Hydroxylated fullerene, hydroxylated carbon nanotubes, gold nanoparticles, and silica nanoparticles were successfully entrapped and immobilized with almost 100% retention efficiency using this method. We also investigated critical parameters affecting ENM diffusion in the porous media in the absence and in the presence of IPEC such as PE solubility as well as solution ionic strength, polycation-polyanion ratio in IPEC, incubation time, PE concentration, PE molecular weight and the pore size of the media.

Finally, we also tested both methods under conditions simulating natural environment and showed that both developed methods can be easily implemented and applicable to various types of ENM.

From a broader perspective, this study contributes two efficient and robust methods for ENM decontamination to a scant number of hitherto developed ENM-treatment methods, and, on the other hand, further broadens the scope of polyelectrolyte applications for pollution treatment in the field of environmental science.

Chapter 1

General Introduction

1.A. Introduction to Engineered Nanomaterials.

Around the end of 20th century, nanotechnology was a breath of fresh air in the development of science and engineering. Starting from the idea stated by the father of nanotechnology as well as a Nobel Prize recipient, Richard Feynman, nanotechnology is developing into an interdisciplinary technology.[1] One part of it is the production and application of engineered nanomaterials (ENM). ENM are one type of material with at least one dimension (length, width, height or diameter) between 1 to 100 nm.[2] If we were to compare it with a tennis ball (diameter: ca. 6.86 cm), nanomaterial is around one millionth of it (**Figure 1.1**). Because of their small size, ENM have larger surface area to their bulk counterparts, and possess unique properties. Those features of ENM attract people to research them as well as utilize their unique physico-chemical properties to develop products that are useful for daily life.

Various types of research about ENM are currently being conducted. Currently, not only researches about new ENM, but also development in manufacturing method of existing ENM as well as surface modification/ treatment method of ENM and applicability of ENM in many fields of expertise, are being seek further. For instance of the recent development of ENM, in 2004, carbon dots were discovered during carbon nanotubes purification.[3] Afterwards, new methods to synthesize them and utilize their electrochemiluminescence features were discovered and developed further by scientists.[4] Another example is the development of polymer-based NP, polyplex, which can be utilized for cancer treatment.[5]

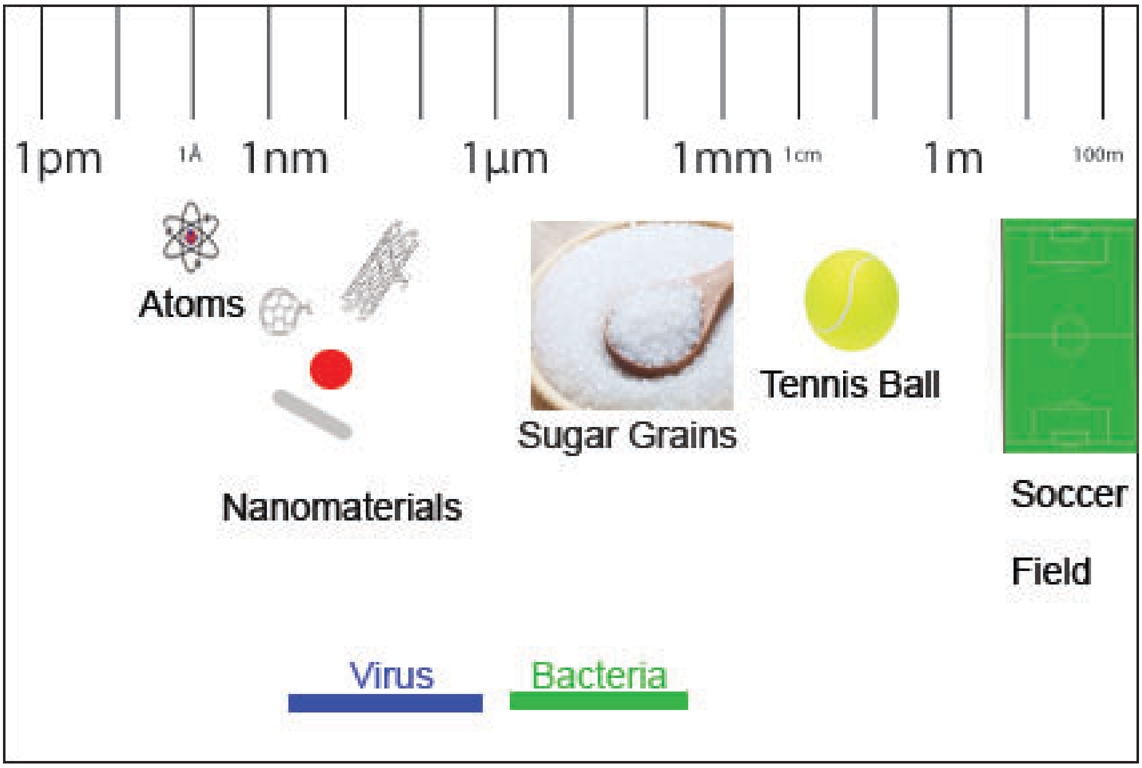

Figure 1.1. Size comparison of engineered nanomaterials and some common goods. The data are derived from several sources.[6–8]

ENM are being used for not only high-specification application, such as car body, but also daily life goods, such as bandages and sunscreen lotions. Due to vast applicability of ENM, there are a lot of products (**Figure 1.2**) containing ENM in the market and the number is still growing. In addition, the number of production of ENM is predicted to grow around 25% each year. [9,10] This rapid growth of ENM will boost the development of nanotechnology, which will boost the development of other technologies, such as agricultural, automobile, medical, etc. Further discussion about ENM is provided in **Chapter 2**.

Figure 1.2. Daily products that are containing ENM. ©2006 David Hawxhurst, Woodrow Wilson International Center for Scholars. Found in an article authored by Steph.[11]

1.B. Introduction to Environmental Contamination by Engineered Nanomaterials.

Although the manufacturing of ENM is developing rapidly, the regulation regarding safety and handling is developing in slower pace.[12,13] For instance, Japanese government is still under investigation of the danger of nanomaterials and supporting voluntary gathering regarding the risk of nanomaterials from industries.[14,15] On the other hand, under Toxic Substance Control Act (TSCA), USA government requests the manufacturers of nanomaterials to report to the government about the safety of the nanomaterials included prior to manufacturing. Moreover, under Significant New Use Rules (SNURs), the government also asked the manufacturers to report regarding the new use of certain existing nanomaterials, especially carbon-based ones.[14,15] It can be said that USA and Japan are concerned about the danger of ENM to health and environment, but they still have difficulty to implement handling regulations to all available and future ENM. Thus, the lack of balance between the development of ENM and the handling regulation of ENM develops concerns about ENM contamination to the environment.

Recent studies showed that ENM have high mobility in environment,[16] capability to be adsorbed by organisms and bioaccumulated,[17–19] capability to cause harm to human cells and animals,[20–28] plants,[27,29,30] and organisms.[27,31] With the current upsurge of ENM production and ENM-related activities, the threat of ENM to environment and health of living being will exacerbate gradually. Thus, in addition to the knowledge about fate of ENM in environment, reliable methods to prevent ENM from contaminating environment, remove them from environment, and recover them after usage are vital. The discussion about nanotoxicity of ENM is provided further in **Chapter 2**.

1.C. Introduction to Remediation Methods of Engineered-Nanomaterial-Contaminated Environment

Naturally-occurring nanomaterials, such as volcanic ash and dust, and nano-sized virus have been in existence in environment since long time ago.[32] On the other hand, anthropogenic nanomaterials or ENM did not exist until recently and were recently developed. Nonetheless, their concentration will spike in the same manner as our daily usage of ENM-containing products rises. Accordingly, we will find several novel materials contaminating air, water, and soil in certain concentration that may impose risk to our health.

ENM contamination to soil and water may become worse in the future as both are the sink for many types of contaminants, including ENM.[33–36] Furthermore, ENM can be transferred through the act of eating to the higher organisms in food chain (bioaccumulation). [17–19] Thus, their contamination is threatening human health indirectly.[36] Hence, remediation methods of soil and water are tremendously important part of development of nanotechnology.

Remediation of water can be done through various physical, chemical, or biological methods.[37] However, the most widely-used method to supply clean water in water treatment plant is water treatment system, in which, contaminated water is treated over several steps (**Figure 1.3**). The simplest one (consisting of only primary treatment) usually consists of 2 steps which are coagulation (and flocculation) and sedimentation. Nonetheless, if higher removal efficiency is needed, filtration is adapted as an additional process (**Figure 1.4**). In first step, general contaminants are forced to bind to each other/ coagulate by neutralizing the charge of the substances, to produce bulkier and denser ones, which are commonly called floc. After the formation of flocs, those flocs precipitate due to gravitation.[38–40] This process is commonly supplemented by filtration to further enhance the separation efficiency of dissolved contaminants from mother liquid.[40] Composition of the filters can be sands, charcoals or man-made polymers. The components of the filter can determine filter's pore size (more than 1 µm-pore size for natural filters, such as charcoals and smaller for man-made ones) which limits the size of dissolved contaminants that can be removed. The discussion about ENM contamination of water and its remediation method is available in **Chapter 4**.

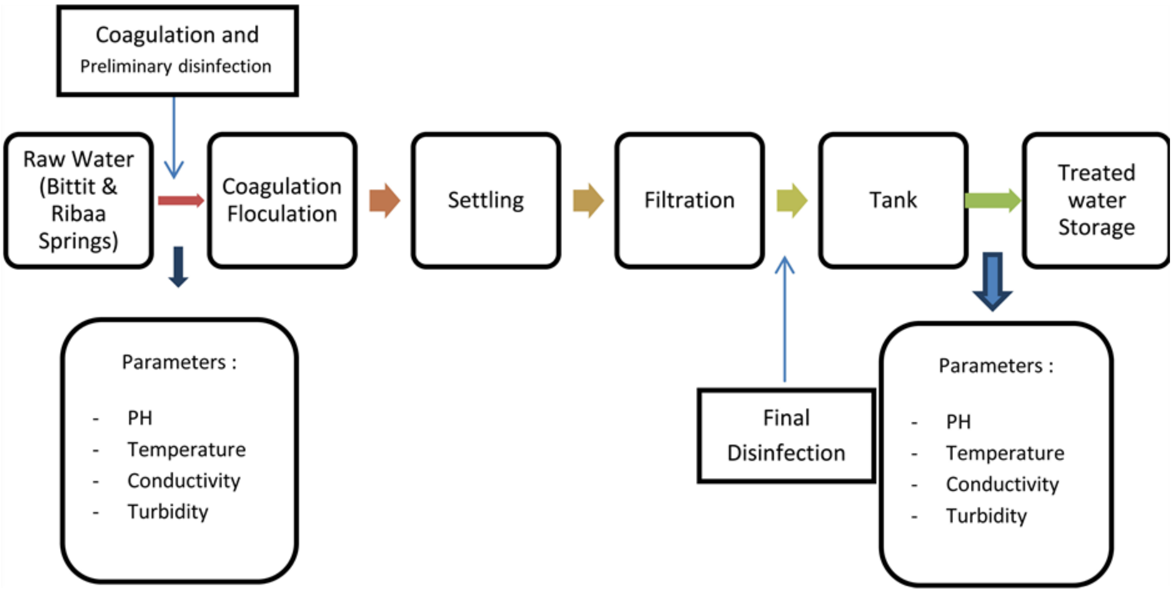

Figure 1.3. Scheme of water treatment plant. Reproduced from Farhaoui, M.; Derraz, M. Review on Optimization of Drinking Water Treatment Process. J. Water Resour. Prot. 2016, 08 (08), 777–786.[41]

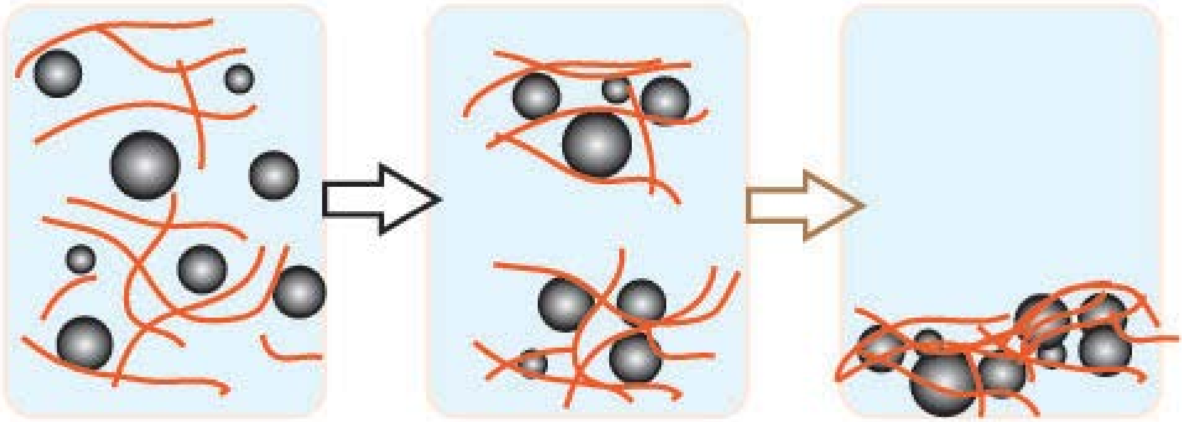

Figure 1.4. Coagulation of dispersed particulate matter (black spheres) by polymer coagulants. Impurities are adsorbed by coagulants to form denser and bigger flocs. Due to their heavy weight, those formed flocs precipitate naturally (this natural precipitation is called sedimentation).

Since ENM can be more mobile in environment than existing contaminants, ENM penetration to environment will be highly likely, even though it is still debatable (**Chapter 4.A.3**). On that account, development of water treatment system is crucial, especially coagulation and flocculation methods, which are readily applicable. Answering such needs, our group has been developing methods as a countermeasure to ENM contamination of water, such as calcium-carbonate-entrapment method[42] and interpolyelectrolyte-complex (IPEC) method.[19]

Chapter 4 of this thesis explains about a new method, which is developed from IPEC method, to coagulate ENM utilizing infamous biodegradable polymers, chitosan.[43]

Similar to method of remediation of water, soil can be remediated physically (and thermally), chemically and biologically.[37,44] However, soil treatment method depends on the type of contaminants that are about to be cleaned from the contaminated site. For instance, heating of contaminants can be applied to solve the problem of organic solvent contaminants and electro-kinetic separation is to solve contamination by heavy-metal ion.[37] Even though the studies about remediation of soil was quite advanced for some common contaminants, such as heavy metal ions, the investigation about soil remediation due to ENM contamination, is still lacking. Currently most of research about ENM contamination is about the mobility of ENM in porous media (**Chapter 5.A.I**) and most of the recent findings show that the porous media can be penetrated easily by ENM. Therefore, an effective method to solve ENM-contamination is distinctive and development of the method is vital.

Developed by Russian scientists to remediate the radioactive-contaminated soil during Chernobyl accident, polyelectrolytes were used to entrap those contaminants in soil.[45–47] As utilization of polyelectrolytes of both charges showed a good entrapment efficiency for ENM-contaminated water treatment,[19] IPEC can be an efficient method to entrap ENM in soil. In this research, such method was developed for the remediation treatment of ENM contaminated soil. The discussion about ENM contamination of porous media (soil) and their remediation method is available in **Chapter 5.**

1.D. Objectives of This Research

Nanotechnology is developing rapidly, and it has been implemented in our daily lives. Unknowingly, ENM-containing products are being used in various aspects of life, not only medicine, but also car accessories, hygiene products, food, etc. This fact demonstrates that ENM, an emergent environmental contaminant, contamination to environment are becoming more serious. In addition, ENM is found to be harmful for environment and living organisms in it, including human beings. To reduce the impact of ENM to environment and health of organisms, including human beings, in this research, two methods are presented as follows:

1. Remediation of ENM-contaminated water by coagulation with natural PE, chitosan. Acid-soluble chitosan adsorbed water-dispersed ENM and precipitated due to adjustment of pH to basic condition. This study is discussed further in **Chapter 4**.
2. Remediation of ENM-contaminated soil by entrapment of ENM in soil with IPEC method. In this method, polycation-polyanion-salt solution was added into ENM-contaminated sand column. Due to formation of IPEC, ENM could be trapped in sand column. This study is discussed in **Chapter 5**.

Chapter 2

Engineered Nanomaterials Around Us and Their Toxicity

2.A. Overview of Nanomaterials

A nanometer is one out of one billion meter and nanomaterials are literally materials which are on that scale.[2] Thus, nanomaterials are on the same scale as virus which cannot be seen with naked human eye and it is necessary for us to use transmission electron microscopy (TEM) to observe those nanomaterials in details. Though ENM products become widespread at the beginning of 21st century, nanomaterial's existence in nature has been since a long time ago, such as smoke, viruses, activated cells, etc.[32]

As a counterpart of naturally-occurring nanomaterials, ENM which were discovered in the latter half of 20th century, are developing rapidly and widely due to their unique physiochemical properties.[2] ENM behave differently from their bulk counterparts due to two phenomena resulted from their small structures. Those properties are high surface area to volume ratio, which affects reactivity, and quantum confinement, which affects their psychochemical properties.[1,48–51] Besides, ENM have less defects compared to bulk materials due to their small sizes.

2.A.I. ENM Classifications

ENM were applied in various products ranging from simple daily products, such as band-aid, to the high technology products, such as aircraft body and the technology is developing continuously. It is not uncommon that each of those products requires certain type of ENM so there are various types of ENM being produced. Nonetheless, those ENM can be classified into several categories depending on the constituent materials. [2,52,53]

1. Carbon-based ENM, such as carbon nanotubes (CNT) and fullerene.
2. Metal ENM, such as gold nanoparticles (NP) and silver NP.
3. Metal-oxide/ ceramic ENM, such as titanium dioxide NP and zirconium dioxide NP.
4. Polymeric ENM.
5. Semiconductor NP (Quantum Dots)

Those ENM can be classified further depending on their shape, such as spheres, rods, tubes, etc.

2.A.II. ENM Applications

Each application of ENM requires ENM with particular properties. For instance, since silver NP demonstrates antimicrobial properties, silver NP perform well for medicine-related goods, such as adhesive bandages. Each type of ENM and their applications are as follows (refer to **Table 2.1** for each ENM and their applicable fields):

Table 2.1. Common ENM and their fields of application

Type of ENM	Application Fields	Ref.
Titanium dioxide NP (TiO_2)	Biomedicine, cosmetics, electronics, paint, environmental remediation, food, clothes, energy, structure	2,10,28,34,52,54–58
Silicon dioxide NP (SiO_2)	Biomedicine, electronics	10,52,59,60
Zinc oxide NP (ZnO_2)	Biomedicine, environmental remediation, cosmetics	2,10,52,57,58
Iron oxide NP (Fe_2O_3)	Biomedicine, environmental remediation, energy, catalyst	52,61,62
Fullerene (C_{60})	Electronics, cosmetics, structure	10,52,54,63
Quantum dots (CdS, CdSe, CdTe)	Energy, biomedicine, electronics	64,65
Carbon black (C_n)	Tire	66,67
Gold NP (Au)	Biomedicine, sensor	52,58,68–70
Silver NP (Ag)	Biomedicine, sensor, fabric, cosmetics	2,52
Cerium oxide NP (CeO_2)	Energy, agriculture, environment remediation	2,71
Aluminum oxide NP (Al_2O_3)	Structure, environmental remediation (membrane)	52,72,73

1. Carbon-based ENM.

The representative of this group is fullerene, carbon nanotubes, graphene, carbon dots and carbon black. As listed in **Table 2.1**, most applications of materials in this groups are related to electrical and mechanical due to their high stiffness and high thermal and electrical conductivity.[2,74] The shape and the size of this type of ENM greatly vary. CNT is a tube-shaped with diameter of less than 10 nm for single-walled and 5-40 nm for multi-walled and length of a few micrometers. CNT have a very high length to diameter aspect ratio. Fullerene is a ball-like structure with diameter less than 1 nm. It can aggregate easily and form bundles. Graphene is a sheet-like structure with high aspect ratio between width/ length to thickness.[74] Carbon dot is a nanoparticle of diameter of less than 10 nm consisting of carbon atom. Different from other type of carbon-based ENM, carbon dots are a good fluorescent so it is being extensively researched for bioimaging and related fields.[3,75] Among the currently-available carbon-based ENM, the production of CNT and carbon black is still the highest.[76] Compared to other types of ENM, the amount of production of this type of ENM is still relatively small compared to metal oxide ENM (less than 10%).[76,77]

2. Metal oxide ENM

This type of ENM is one of the most applied in the daily life products.[76] Titanium dioxide (TiO_2) NP, silicon dioxide (SiO_2) NP, and zirconium dioxide (ZnO_2) NP belong to this group. These ENM are usually applied in the field of biomedicine, environmental remediation, cosmetics and electronics due to their excellent photochemical properties, unique electrical properties and magnetic properties.[2,78] Metal oxide ENM is the most produced ENM due to their various applicable fields.[76,77]

3. Metal ENM

Gold NP and silver NP are the representative of this type of ENM. As both silver and gold NP have antibacterial properties, they are manufactured to maintain the hygiene of medical-related goods and hygiene-related goods.[2] However, for the same reason, metal ENM are considered more toxic to human and animal cells.[2,79] Thus, handling of metal ENM needs to be extensively studied and regulated.

4. Other type of ENM

There are various ENM that are not included into the categories above. Those are quantum dots, polymeric ENM, etc. Polymeric ENM are relatively new and sought after due to their biodegradability and safety. Thus, this type of ENM is commonly used in biomedical field.[52] Quantum dots are mainly applied in the field of biomedicine due to their fluorescence properties.[64] However, as little as 0.2 mg/mL of quantum dot concentration can induce cytotoxicity.[80]

2.B. Manufacturing of Engineered Nanomaterials

There are various methods to manufacture ENM. However, they can be divided into 2 kinds of approaches. The first approach is top-down approach, which is a manufacturing method of ENM in which the ENM is manufactured from their bulk counterparts.[2,10,21] The method can be a physical method, such as milling and photolithography or chemical method, such as chemical cutting.[2,10] The second approach is bottom-up approach, which is a manufacturing method in which the ENM is produced from their building chemicals. Firstly, the ENM nucleuses are produced and then they grow until the required dimensions reached.[2,10,21] The examples of this approach is the synthesis of silica NP by Shakiba[78] and gold NP by Frens[81].

Since ENM have aggregation problems that limit their applicability, in several researches of ENM bottom-up synthesis, surface modification was incorporated during the synthesis. For example, in the production of gold NP, gold was synthesized by reduction of gold (III) chloride with citrate. In this process, citrate does not act only as a reduction agent, but also as a surface modification agent.[81] In other process, the reduction agent used is sodium borohydride (NaBH4) and the surface protecting agent is cetyltrimethylammonium bromide (CTAB).[82] Surface modification is discussed further in the following section.

2.C. Surface Modification of Engineered Nanomaterials

ENM own excellent physical and chemical properties so this type of materials is getting widespread nowadays. However, due to the agglomeration of pristine ENM, they are usually not implemented in the products in pristine form. Surface treatment and modification of ENM are commonly implemented to improve ENM solubility and compatibility between ENM and other phase.[83–86] The surface treatment to ENM to improve their applicability is usually called functionalization.[87,88]

Several methods are being studied to alter the surface charge of ENM. Those methods can be divided into 2 types of modification that are implemented to ENM nowadays, covalent and non-covalent modification.[83,85,89] Covalent bonding modification is a type of modification, the modifiers of which, are chemically bonded to the ENM, for example: grafting of hydroxyl groups grafted into fullerene. Non-covalent bonding modification is a type of modification, the modifiers of which are not linked chemically through a covalent bond to the ENM, for example: the utilization of CTAB to cap gold NP.[82] The bonding formed is Van der Walls, hydrogen bond and electrostatic interaction.[9091] This research did not focus on the surface modification of ENM. However, since surface modification is usually implemented in the manufacturing of ENM-containing products, all ENM in this research are surface-modified. CNT-OH and C_{60}-OH were hydroxylated, meanwhile, gold NP were capped with citrate ions and silica NP were capped with triton X-100 (non-ionic surfactant, $(C_{14}H_{22}O(C_2H_4O)_n)$).

2.D. Life Cycle of Engineered Nanomaterials

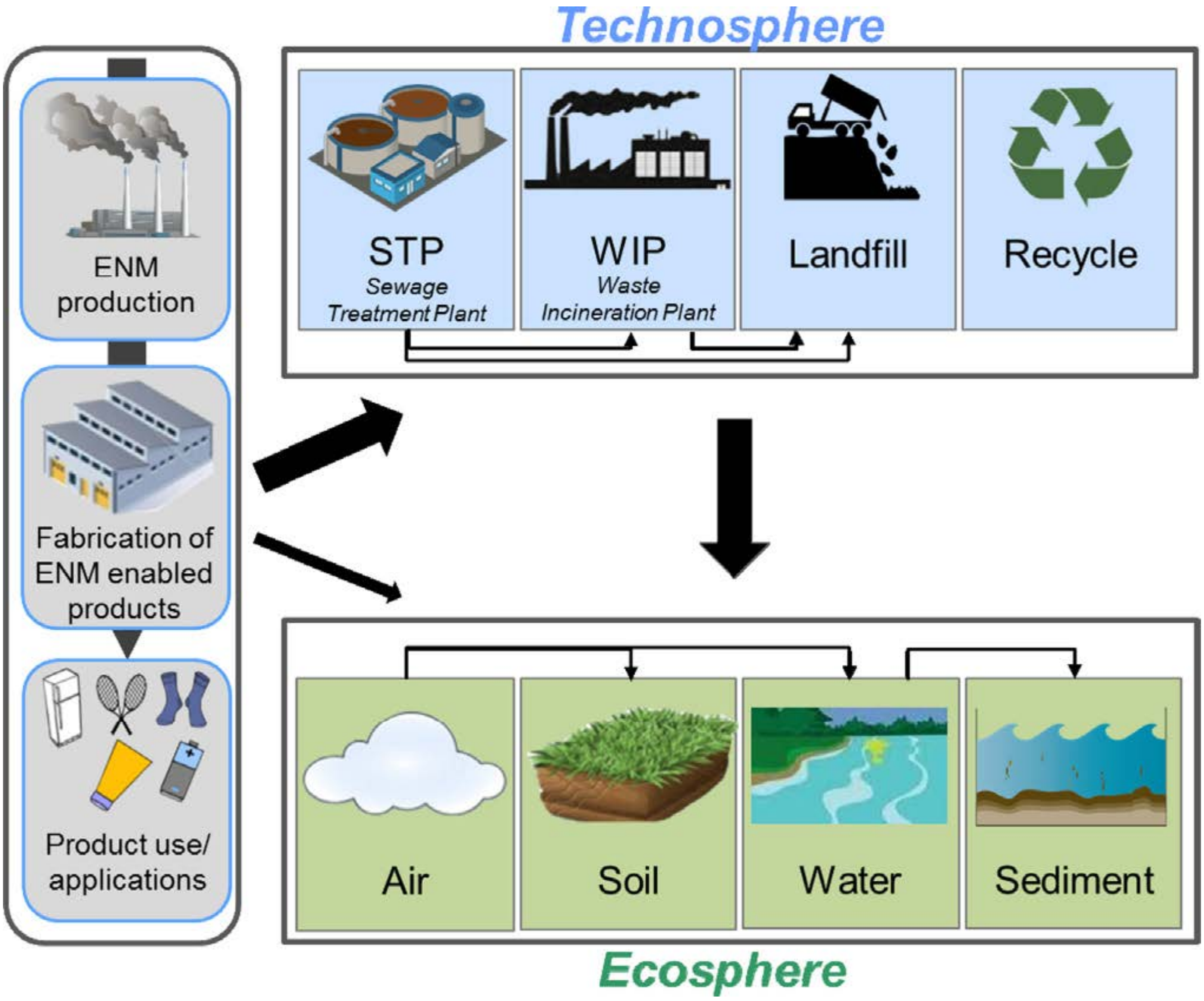

Figure 2.1. General life cycle of engineered nanomaterials. Reproduced from T. Y. Sun et al, *Environ. Pollut.*, 2014, **185**, 69–76[92] with permission from Elsevier. (license number: 4421200435713

Figure 2.1 shows the general flow of ENM from production to their end-of-life (life cycle of ENM). ENM are manufactured in an ENM-manufacturing company and the products are sent to other company that produces ENM-containing products, such as sunscreens or rackets. Afterwards, those ENM-containing products are sent to market and bought by costumers to be used. Most of those ENM products which reach their end of life are disposed and enter the waste-related treatment plant, meanwhile, a small part of it may enter environment directly during certain incident, for example some release of Ag NP during the usage of clothes.[21,93]

In the end of their lifetime, ENM products are treated in wastewater plants or waste treatment plants. In those plants, ENM are captured in the sludge of wastewater treatment or mixed with the ashes from the incineration plants. Those sludges are usually applied to the agricultural plots in certain countries[94] or end up in the landfill together with the products from other waste treatment plants.[95] Through this way, ENM can transport into soil and water body. Small parts of ENM can be transported by the wind or brought up during evaporation of water and contaminate air.[21,93,95]

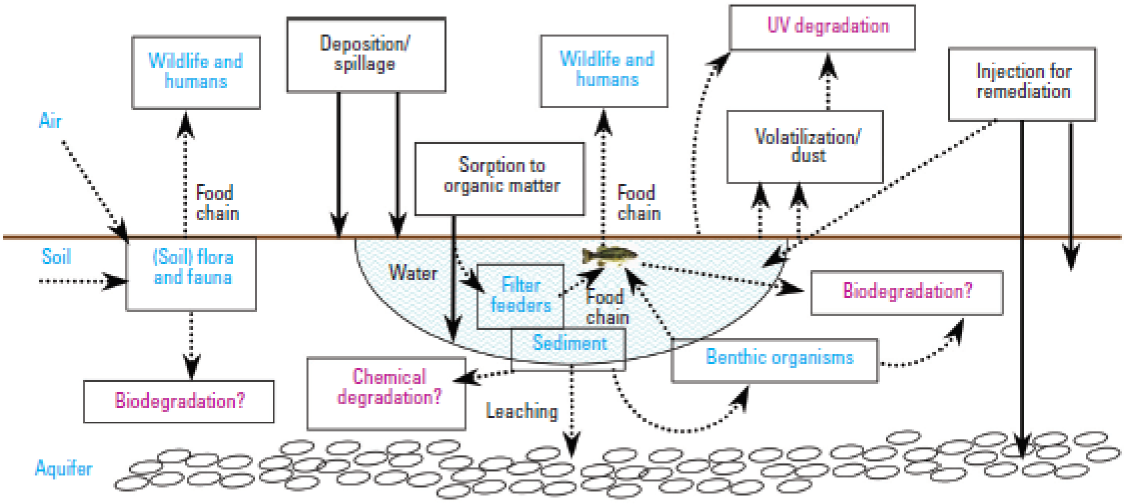

Figure 2.2. Various exposure routes and uptake of to ENM in the environment. Reproduced from Oberdörster, G. et al, Environ. Health Perspect., 2005, 113, 823–839.[32]

ENM are mobile in nature (air, water and soil) so they can migrate from one place to another place, for instance, ENM can travel from soil to ground water and reach sea.[16] Besides, ENM can be digested by some animals as well as taken up by plants and they can accumulate in the body of those living organisms. Furthermore, those animals and plants can be eaten by other animals in the higher food chain or humans. This phenomenon is called bioaccumulation.[17–19] Thus, humans are at risk of ENM uptake. ENM can enter human body through various means, such as ingestion, skin contact, inhalation, and wear of implants.[36] Various routes of exposure and uptake in the environment were discussed in detail by Oberdörster, G. et al.(**Figure 2.2**)[32]

2.E. Nanotoxicity

As dust, one type of natural NP, can become the cause of lung-related diseases,[96] ENM are found to be harmful to environment and health of living beings in it according to recent researches. There are a lot of researches and reviews regarding nanotoxicity, study of which is called nanotoxicology, and almost all types of ENM were shown to cause some problems to health of living organisms or plants or human beings.[32,36,70,97,98] **Table 2.2** summarizes some types of ENM and their possible harmful side effects.

Table 2.2. Common ENM and their harmful side effects.

Type of ENM	Toxicology Data	Ref.
Titanium dioxide NP (TiO_2)	Pathological lesions, lung tumor, disruption to growth and reproduction, inflammatory, reactive oxygen species (ROS), respiratory distress	2,10,28,34,52,54–58
Silicon dioxide NP (SiO_2)	Pulmonary inflammation, ROS, disruption to cell membrane, apoptosis	10,52,59,60
Zinc oxide NP (ZnO_2)	Pulmonary inflammation, disruption to reproduction, reactive oxygen species (ROS), oxidative stress, cellular damage, toxicity to lung	2,10,52,57,58
Iron oxide NP (Fe_2O_3)	Altered cellular response	52,61,62
Fullerene (C_{60})	Cytotoxic to human cells, bioaccumulation, brain damage, reproduction problem, death.	10,52,54,63

Table 2.2. Common ENM and their harmful side effects. (Continued)

Quantum dots (CdS, CdSe, CdTe)	Cell death, DNA damage	64,65
Carbon black (C_n)	Damage to lung	66,67
Gold NP (Au)	Oxidative stress, mitochondrial damage	52,58,68–70
Silver NP (Ag)	Reactive Oxygen Species (ROS) in cells, reproductive toxicity,	2,52
Cerium oxide NP (CeO_2)	Cell membrane damage, bioaccumulation, reactive oxygen stress (ROS), disturbance in plant defense system	2,71
Aluminum oxide NP (Al_2O_3)	Oxidative stress, reactive oxygen stress (ROS), cell membrane damage	52,72,73
Carbon nanotubes (CNT)	Respiratory problems, Chrohn's disease, cancer, blood clot, health disease, oxidative injury.	2,52,99,100
Polymeric NP	No toxicological data	52,101

In the review done by Buzea, C. et al,[36] they showed that each path of entry to human body can cause different type of disease to human body. For instance, inhalation of ENM can cause adverse effect to respiratory system. Digestion of ENM can cause Chron's disease, cancer, ulcerative colitis. Injection of ENM can cause allergic reactions. Wear of implant in the body can cause autoimmune disease. Meanwhile, the danger of dermal uptake of ENM is still on debate. Moreover, it is reported that ENM can transport inside blood vein if the size is smaller than 30 nm and they can cause cytotoxicity to cell.

Chapter 3

Application of Polyelectrolytes to Remediate Environmental Problems

3.A. Introduction to Polyelectrolytes

In the macromolecule world, macromolecules, which consist of repeating units, are called polymers. Among those polymers, there are some which can maintain their charges in certain condition, which are called polyelectrolytes (PE).[102] Thus, polyelectrolytes are macromolecule substances (polymers) which contain positive or negative charges if dissolved in ionizable solvent.[103] Positively-charged PE are called polycations and negatively-charged PE are called polyanions. In addition, PE that contain both charges are called polyampholytes. PE properties are heavily affected by functional groups grafted to the backbone and are sensitive to ionic strength of the solution.[103]

There are 3 types of PE depending on the availability in nature: natural PE, chemically-modified natural PE and synthetic PE.[102,103] Natural PE are PE which are available in nature as they are. To acquire them, certain extraction method is required. Examples of this type of PE are DNA and cellulose. Chemically-modified natural PE are PE which are obtained after chemically processing natural PE. Examples of this type of PE are chitosan and carboxymethyl cellulose. Synthetic PE are man-made PE which are polymerized from their monomers.[102,103]

PE are extensively studied in many field such as water treatment and mineral extraction, but the main field that applied PE is biomedical and pharmaceutical.[102–106] Some examples of PE are shown in **Figure 3.1** which shows the PE that were used in the study.

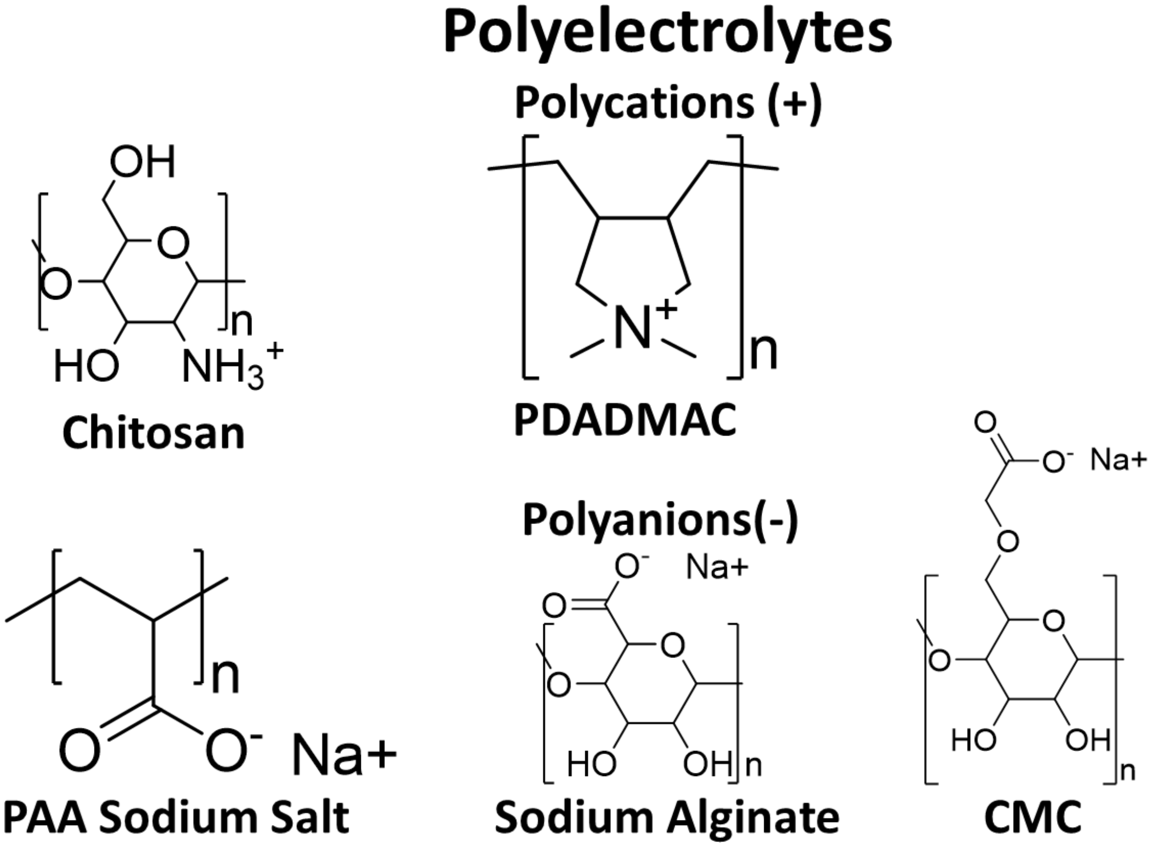

Figure 3.1. Chemical structures of typical polyelectrolytes (polycations and polyanions) that are applied in this study. PDADMAC is poly(diallydimethylamonium chloride). PAANa is polyacrylic acid, sodium salt. CMC is carboxymethyl cellulose.

There are 2 polycations and 3 polyanions that were used in the experiments:

1. Chitosan

Chitosan is a derivative from chitin that can be extracted from the shell of crustaceans, such as shrimp so it can be obtained from fishery industry waste. Chitin and their derivatives are the second most abundant natural polymers on earth after cellulose. Moreover, chitosan is not toxic and biodegradable so it is relatively safe for environmental applications.[107,108] Due to their amino functional group, chitosan is a weak polycation and commonly dissolved in weak acid, such as acetic acid.[109] In this study, chitosan was utilized to entrap ENM contaminating water.[43]

2. Poly(diallydimethylamonium chloride)/ PDADMAC

PDADMAC is a synthetic polycation which has high charge density. It can be easily dissolved in water. Due to its property, PDADMAC is usually applied in water treatment process.[110] In this study, paired with polyanions, PDADMAC was utilized to entrap ENM in porous media.

3. Polyacrylonitrile, sodium salt/ PAANa

PAANa is the sodium salt of polyacrylonitrile and a synthetic polyanion. In this study, PAANa was the main polyanion used to entrap ENM in porous media together with PDADMAC.

4. Carboxymethyl cellulose/ CMC

CMC is one of the derivatives of cellulose which is the most abundant natural polymers on earth. Due to carboxymethyl functional groups, CMC contains negative charges. Since it is one of derivatives of natural polymers, CMC is relatively safe and biodegradable.[108] In this study, CMC was applied together with PDADMAC to immobilize ENM on the surface of porous media.

5. Alginic acid, sodium salt/ sodium alginate/ NaAlg

NaAlg is the sodium salt of alginate which can be extracted from brown algae and it belongs to natural polyanion. Since it is extracted from brown algae, sodium alginate ix safe and environmentally friendly.[108] In this study, NaAlg was paired with PDADMAC to entrap ENM on porous media.

3.B. Interpolyelectrolyte Complexes (IPEC)

If positively-charged PE combine with negatively-charged PE, they form complexes which can be water-soluble, colloidal or insoluble depending on the stoichiometry of the IPEC.[103] Polyelectrolytes in aqueous solution have electrical double layers which constrain the motion of counterions surrounding them. Complexation of polyelectrolytes due to charge neutralization of those PE disrupt the double layers surrounding PE and release the counterions. Thus, the entropy increases and the formation of the complexes is promoted.[111]

IPEC properties can be affected by various factors and one of those factors are ionic strength.[104,105] In slightly higher ionic strength solution, formed IPEC tends to swell larger than the one formed in non-ionic solution. In even higher concentration of salt, the turbidity of the IPEC solution is gone. In very high salt concentration, IPEC are no longer formed due to electrostatic screening of both polycation and polyanion.

3.C. Application of Polyelectrolytes for Environment Remediation

Even though there are many IPEC applications which are biomedical-related, there are some examples that IPEC were studied and applied for environmental protection purposes. For examples, chitosan was suggested to be applied in wastewater industry as coagulant.[112] Other than chitosan, there are a lot of PE which are used to remediate heavy-metal ion polluted water.[19,46,110,113] On another case, IPEC were used to remediate soil which was contaminated by radiation. IPEC were applied to reduce the erosion of contaminated soil by water and wind. Thus, contaminated soil cannot migrate to other area and the contamination can be localized in one specific area. [45–47]

Chapter 4

Utilization of Natural Polyelectrolytes Chitosan to Remove Engineered Nanomaterials from Water

Most of the content in this chapter is reproduced and modified from Soenaryo, T.; Zinchenko, A.; Murata, S. Removal of Carbon Nanomaterials by Co-Precipitation with Chitosan: A Facile Method for Water Pre-Treatment. *Environ. Sci. Water Res. Technol.* 2018, *4* (2), 265–271[43] with permission from the Royal Society of Chemistry

4.A. Introduction to ENM Contamination to Water

4.A.I. Engineered Nanomaterials and their Water Contamination

Water is needed by many living beings and even 60% of human bodies contain water. Thus, natural water bodies are precious resources for lives. In nature, water is not as pure as the water used for research (distilled water/ milli-Q water), it contains various salts and natural organic matters.[110,114] In addition to the currently dissolved matters in water, water can absorb any kinds of chemical from outside. Thus, water is like an estuary of many kinds of contaminant flow, including the new emerging engineered nanomaterials.

As nanomaterials become more widespread, production scale and variety of commercial products utilizing nanoparticles (NP) are rapidly growing [2,12,115–118]. Due to utilization of ENM in manufactured products, ENM are already found in wastewaters from industries and households[12,117–119]. For instance, in 2009, Gottschalk et al reported that ca. 4 µg/ L of titanium dioxide NP, ca. 40 ng/L of silver NP, ca. 10 ng/L of CNT-OH and ca. 4 ng/L of fullerene were found in the sewage treatment plant effluent in Switzerland.[120] On the other hand, it is well established that certain classes of ENM are toxic for humans (**Table 2.2**)[116,117,121] plants, and animals in soil[26,27,30,58,122] and water[23–25,115,123,124]. Due to lack of regulations, ENM production is poorly controlled[12,13] and accumulation of ENM in water and soil is being increasingly concerned[95,125].

4.A.II. Capacity of Current Water Treatment to Remediate ENM Contamination

Treatment of water is an essential technology to prevent nanoparticles intake into living organisms and there have been many studies on ENM removal efficiency by conventional water treatment technologies (**Table 4.1**). The removal efficiency depended strongly on type of nanomaterial and applied method, but, in most of cases, a significant amount of ENM escape during the current water treatment process was found. Obviously, an improvement of water treatment is required to provide cleaner and safer water[115]. In this regard, the filtration was proposed as a pre-treatment step targeting ENM contamination[12,117,126,127]. Nonetheless, filtration has some shortcomings related to (i) necessity of water pre-treatment to minimize the membrane fouling[117,128,129], (ii) high external pressures for filtering out the nanoscale matter[128], (iii) effects of water demineralizing which makes it unhealthy[130], and, finally, (iv) additional costs to build filtration treatment facility which is not available in most of water treatment plants[129]. Development of efficient coagulants, on the other hand, can help improving the removal rates of ENM using current water treatment technologies.

In general, co-precipitation treatment is a suitable strategy for entrapment of a substantial portion of nanoscale matter into a bulky precipitate. Recently, we have shown that formation of insoluble inter-polyelectrolyte complexes[19] or inorganic precipitate[42] in a solution of ENM is accompanied by incorporation of a substantial fraction of ENM into a precipitate that can be easily removed. As both these methods use a pair of reactants forming precipitate, the ratio of the reactants plays a critical role in the efficiency of ENM entrapment and removal. Here, we propose a single-reactant-based, environmentally-friendly procedure for ENM removal by co-precipitation with a derivative of an abundant natural polymer, chitosan.

Table 4.1. Comparison of the results on breakthrough of different types of ENM in various porous media.

Opinion	Type of ENM	Method	Result	Ref.
Basic water treatment is sufficient to remove most of ENM	TiO_2	Jar test	Artificial ground water: 95 – 100% removal. Artificial surface water: more than 90% removal ($Al_2(SO_4)_3$, Fe_2SO_4), 60% removal ($FeCl_3$)	39
	TiO_2	Wastewater treatment plant effluent check	98.3% removal	127
Basic water treatment is not sufficient to remove ENM	TiO_2	Wastewater treatment plant effluent monitoring, laboratory tests	70-85% removal by biomass in waste water treatment, but 10-100 µg/L Ti still remained in effluent.	131
	Ag, TiO_2, ZnO	Jar test	10 – 20% Ag and TiO_2 nanoparticles breakthrough without filtration. The amount was lowered greatly by ultrafiltration. However, the cleaned water contained detectable metal concentration. Moreover, dissolved ZnO needs better removal method.	132

Table 4.1. Comparison of the results on breakthrough of different types of ENM in various porous media (*Continued*).

Basic water treatment is not sufficient to remove ENM	TiO_2, ZnO, Fe_2O_3, NiO, and silica NP	Jar test using $Al_2(SO_4)_3 \cdot 16H_2O$ (alum)	Less than 80% removal of nanoparticles However, filtration could improve the efficiency.	126
	TiO_2, ZnO, and Ag NP, CNT, fullerene	Simulation	The predicted environment concentration of Ag, TiO_2, and ZnO NP in sewage treatment plant effluents exceeded the critical value for no effect concentration	133
	Dispersant-stabilized CNT	Jar test using poly aluminium chloride and alum	Positively-charged CTAB-CNT could not be effectively removed	134
	Cerium oxide	Laboratory-scale plant	6% (considered significant) found in the exit stream	135

4.A.III. Dispersed ENM Entrapment by Interpolyelectrolyte Complexes

This study is a continuation of previous study which utilized DNA and chitosan to capture ENM dissolved in water by formation of interpolyelectrolyte complexes (IPEC) (**Figure 4.1**). In the original method, DNA and chitosan were added into the ENM solution in the order of PE with different charge from ENM first and then PE of the same charge as ENM. Previous study showed multi-walled carbon nanotubes (CNT-OH), hydroxylated fullerenes (C_{60}-OH), gold nanorods and several types of Qdots can be entrapped efficiently by the methods. Despite of the method universality, this method depends on the concentration ratio between DNA and chitosan. If both PE charge is not equal stoichiometrically, the neutralization of one type of PE is not optimal and soluble IPEC is formed due to charge imbalance. In this condition, the removal of ENM is not optimal either. However, the ratio between DNA and chitosan in which PE completely precipitates and forms insoluble IPEC (optimum ratio) shifts depending on pH as stated in the paper reported by Zinchenko et al. [19] For instance, optimum ratio of chitosan-DNA was ca. 0.75 in the pH of 3.3 and shifted to 1.5 in the pH of 6.8 and 2.0 in the pH of 10.8. The shift was caused by the change in the protonation degree of the PE functional groups due to the solution pH. For example, in acidic condition, the polycation positive charge is increased and the polyanion negative charge is suppressed and vice versa. [19]

To understand further about the system, a new experiment was conducted using similar methodology, but utilizing different PE, carboxymethyl cellulose (CMC) as polyanion and chitosan as well as poly(diallyldimethylammonium chloride) (PDADMAC) as polycation. The results of the investigation which are summarized in **Table 4.2** show that not all PE can be used in this method, especially the short PE. Furthermore, not only pH, but also, changing of

PE and PE molecular weight can change the optimum ratio. However, the shift due to applying PE of different molecular weight is not significant and depends on the type of the PE.

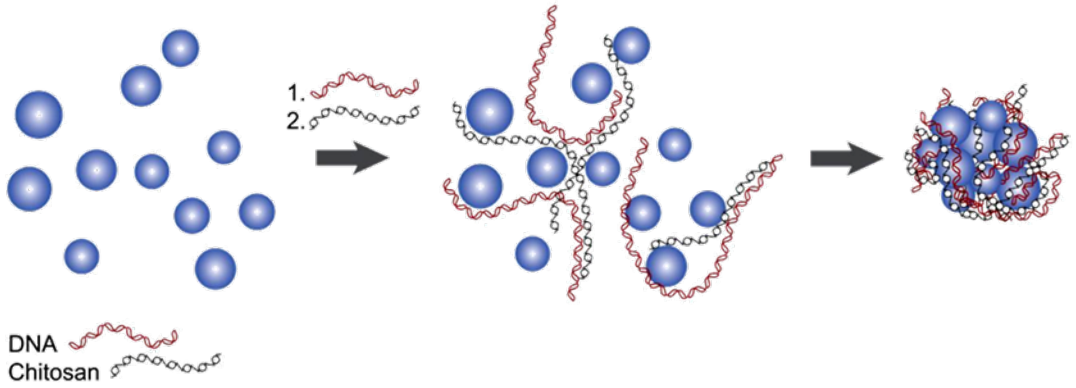

Figure 4.1. Entrapment of ENM dissolved in water by formation of DNA-chitosan IPEC. Reprinted (adapted) with permission from Zinchenko, A. A et al *Environ. Sci. Technol.* **2013**, *47* (9), 4489–4496.[19] Copyright 2013 American Chemical Society.

Since the charge ratio plays an important part in the system. In the current research, a method that is less complex and uses less amount of PE was proposed.

Table 4.2. Optimum charge ratio of carboxymethyl cellulose (CMC) – chitosan pairs and CMC-poly(diallyldimethylammonium chloride) (PDADMAC). High Mw CMC: CMC with molecular weight (Mw) of 700,000 and degree of substitution (DS) of 0.9, low Mw CMC: CMC with Mw of 90,000 and DS of 0.7, high Mw chitosan: chitosan 500 (Mw: 1,200,000)[136], low Mw chitosan: chitosan 10 (Mw: 60,000)[137], high Mw PDADMAC: PDADMAC with Mw of 400,000 – 500,000, low Mw PDADMAC: PDADMAC with Mw < 100,000

PE Pairs	**Removal Efficiency**	**Optimum Charge Ratio**
High Mw CMC – High Mw Chitosan	> 90%	1 to 0.8

Table 4.2. Optimum charge ratio of carboxymethyl cellulose (CMC) – chitosan pairs and CMC-poly(diallyldimethylammonium chloride) (PDADMAC). (Continued)

High Mw CMC – Low Mw Chitosan	> 90%	1 to 1
Low Mw CMC – High Mw Chitosan	IPEC do not precipitate well	1 to 1
Low Mw CMC – Low Mw Chitosan	IPEC do not precipitate well.	No optimum point
High Mw CMC – High Mw PDADMAC	> 90%	1 to 1
High Mw CMC – Low Mw PDADMAC	> 90%	Between 1 to 0.6 and 1 to 1

4.B. Experimental Section

4.B.I. Materials

Chitosan (chitosan 10 of average Mw 60,000; chitosan 50 of Mw 320,000; chitosan 100 of Mw 650,000; chitosan 300 of Mw 1,120,000; chitosan 500 of Mw 1,200,000; the molecular mass was reported earlier[136–139]), sodium hydroxide (NaOH), trisodium citrate dihydrate (Na_3Citrate), Sodium acetate ($NaCH_3COO$), and 6 M hydrochloric acid (HCl) were purchased from Wako Pure Chemical Industries, Ltd (Japan). Acetic acid (CH_3COOH) was purchased from Tokyo Chemical Co., Ltd. (Japan). Hydroxylated multi-walled carbon nanotubes, 10–20 nm in diameter and 0.5–2 µm in length, were purchased from Nanostructured and Amorphous Materials, Inc. (USA). Hydroxylated fullerene (C_{60}-OH) (nanom spectra D100) was purchased from Frontier Carbon Corporation (Japan). Rhodamine-B isothiocyanate (RBITC), gold (III) chloride solution (30% in dilute HCl), 3- aminopropyltriethoxy- silane (99%) (APTES), 28% ammonium hydroxide solution were purchased from Sigma-Aldrich (USA). cyclohexane, 1-hexanol, triton X-100 ($C_{14}H_{22}O(C_2H_4O)_{n\ (n=9\text{-}10)}$), acetone, ethyl silicate were purchased from Kishida Chemical Co., Ltd (Japan). Ethanol (99.5%) was purchased from Nacalai Tesque (Japan). All the chemicals were used without further purification. Milli-Q water was purified by Advantec GSH-200 apparatus followed by purification by a Merck Simplicity Millipore Water Purification System (Germany). Lake water sample was collected from Kagami Lake (Nagoya, Japan, coordinates 35°15’73”63, 136°96’36”02, pH = 7.5 (25 °C), 11 mg/L of suspended solids), tap water sample was collected from tap water in Nagoya university.

4.B.II. Synthesis of Nanoparticles

In this research, C_{60}-OH and CNT-OH were purchased from Frontier Carbon Corporation and Nanostructured and Amorphous Materials, Inc. respectively. In addition to carbon-based ENM, gold NP and silica NP were synthesized as follows.

Gold NP. The synthesis follows the method described by Frens[81] with slight modification. 2 solutions, 0.01% w/w gold (III) chloride solution and 10% w/w Na_3Citrate, were prepared by dilution of the purchased concentrated gold (III) chloride and dissolving Na_3Citrate powder in water respectively. Afterwards, 50 ml of the first solution was boiled on 100 ^oC hot plate stirrer enclosed with aluminum foil, then 0.5 ml of the second solution was added. The solution was stirred vigorously for 2 hours before the process was terminated. The color change from yellow to dark red that shows the change from gold (III) chloride solution to gold NP. The concentration of Gold NP stock solution was based on the amount of reactants used in the synthesis with assumption that the reaction proceeded until all the reactants became product. The concentration of Gold NP stock solution is 5.74×10^{-3} %w/w.

Silica NP. The synthesis done in this research is reverse microemulsion method (Stober method) described by Shahabi et al.[78] For preparation, the dye solution was prepared before NP synthesis. The dye solution was made by dissolving RBITC in 99% ethanol until the solution reached the concentration of 1 mM. APTES is added into the solution with the ratio of RBITC : APTES = 1:1. This solution was stirred in room temperature in the aluminum-foil-wrapped bottle for 12 hours and saved in freezer afterwards.

For the beginning of NP synthesis, 15 ml cyclohexane, 3.6 ml 1-hexanol, 3.54 ml Triton X-100, and 1.1 ml milli-Q water were stirred for 10 minutes. Then, 200 µL of the prepared dye solution was added and stirred for 30 minutes. To begin the NP formation by hydrolysis/ condensation reaction, 200 µL of ethyl silicate and 120 µL of 28% ammonium solution were added, followed with 48 hours stirring. The synthesis was terminated by addition of excess acetone. Centrifugation in 15,000 rpm for 20 minutes was used to recover the NP. The NP were washed several times with ethanol and once with milli-Q water. Silica NP were redispersed in 20 ml of milli-Q water with ultrasonication for 1 hours. The silica NP solution was kept in refrigerator. Concentration of Silica NP was determined by gravimetric analysis. A small amount of silica NP stock solution was transferred into a Petri dish and dried in an open-air oven at 100 °C for 4 h. The weight of the remaining residue was measured to calculate the concentration. The concentration of the stock solution was found to be 0.289 %w/w. The solution was sonicated for 10 minutes before each usage.

4.B.III. Preparation of stock solutions

Chitosan. 10 mM chitosan solution was prepared by dissolution of commercial chitosan in 1% acetic acid by stirring for at least 12 hours. The concentration of chitosan was calculated based on 80% of the degree of deacetylation provided by the manufacturer. The final pH of the solution was 3.3.

Hydroxylated fullerene. A stock solution of hydroxylated fullerene (C_{60}-OH) was prepared by dissolution of 0.003 g of C_{60}-OH in 30 ml Milli-Q water. The nanoparticles were wetted with Milli-Q water for at least 12 hours before sonication for 1 hour (VP-5S Ultra S homogenizer, TAITEC, Japan). To separate insoluble particles, the solution was centrifuged at 10,000 rpm (Kubota 7780, Japan) for 30 minutes. To determine the concentration of the stock solution, a small amount of C_{60}-OH was completely dissolved in 1% w/w NaOH solution. The resulting solution was diluted with water 10, 100, and 1000 times, respectively, and the absorbance was measured by UV-vis spectroscopy at 320 nm to determine the absorptivity. The average concentration of C_{60}-OH in the stock solution was found to be 3.61×10^{-4}% w/w.

Hydroxylated carbon nanotubes. A stock solution of hydroxylated carbon nanotubes (CNT-OH) was prepared by dissolution of 0.1 g CNT-OH in 30 ml Milli-Q water. CNT-OH were wetted with Milli-Q water for at least 12 h and sonicated for 1.5 h. To separate insoluble CNT-OH aggregates, the solution was centrifuged at 10 000 rpm for 30 minutes and the insoluble fraction was discarded. The concentration of CNT-OH in solution was determined by gravimetric analysis. A small amount of the CNT-OH stock solution was transferred into a Petri dish and dried in an open air oven at 75 °C for 6 h. The weight of the remaining residue was measured to calculate the concentration. The concentration of the stock solution was found to be 6.87×10^{-2}% w/w. The CNT-OH stock solution was diluted 10 times before being used for removal experiments.

4.B.IV. Methods

UV-vis spectroscopy. The UV-vis spectra of chitosan and ENM were recorded on a Jasco V-630 Bio Spectrometer in a 1 cm × 1 cm × 5 cm quartz cell at room temperature. The amount of ENM was measured at $\lambda = 320$ nm for both hydroxylated fullerene and hydroxylated carbon nanotubes. The detection limit of the spectrometer is 0.001 OD which corresponds to a maximum of 3% of the experimental error of the removal percentage measurements.

Transmission electron microscopy (TEM). TEM observations were performed at room temperature using a HITACHI H-800 microscope (Japan) at a 200 kV acceleration voltage. A drop of a solution containing nanomaterials co-precipitated with chitosan was placed onto a 3 mm copper grid with a collodion film after 30 min from the moment of pH adjustment to avoid aggregation of the complex into a bulky precipitate. The blotted solution was removed after 3 minutes with a filter paper, and the sample was dried at room temperature before observation.

Zeta potential analysis. The zeta potential of nanomaterials was measured using a Zetasizer Nano ZS (Malvern, England) in aqueous solutions at room temperature.

General protocol of ENM removal. The scheme of this general protocol is shown in **Figure 4.2.** To a diluted solution of CNT-OH or a solution of C_{60}-OH, 10 mM chitosan solution was added. After 30 minutes of stirring, 0.5 M NaOH was added to adjust the solution pH to mildly basic (pH 8.0 ± 0.5 for the hydroxylated fullerene NP's removal process and pH 8.5 ± 1.0 for the hydroxylated carbon nanotubes NP's removal process). The precipitate was allowed to settle for 24 hours before the mother liquid was centrifuged at 1500 rpm for 30 minutes. The concentration of ENM in the mother liquid was measured spectroscopically. The final concentration of CNT-OH, C_{60}-OH and chitosan was 2.22×10^{-4} % w/w, 2.79×10^{-4} % w/w, and 1.6 mM respectively.

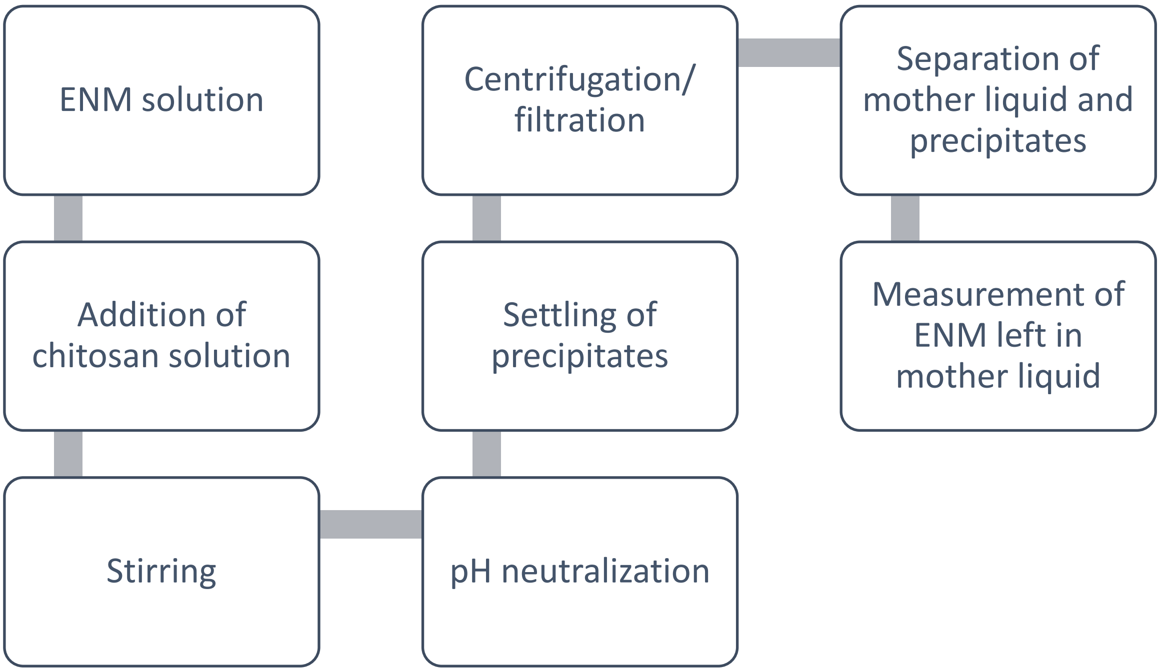

Figure 4.2. Scheme of general protocol of ENM removal.

4.C. Results and Discussions

4.C.I. ENM charge, size and distribution

In this study, four types of ENM with different size were utilized. The biggest one was hydroxylated multi-walled carbon nanotubes (CNT-OH) with outer diameter of 10-20 nm and inside diameter 5-10 nm as well as the length of 500-2,000 nm. they contain mostly carbon atom with the shape of a tube as shown in **Figure 4.3.A and B**. Due to their nucleophilic hydroxyl functional group, they have a negative zeta potential of -19 mV in milli-Q water.

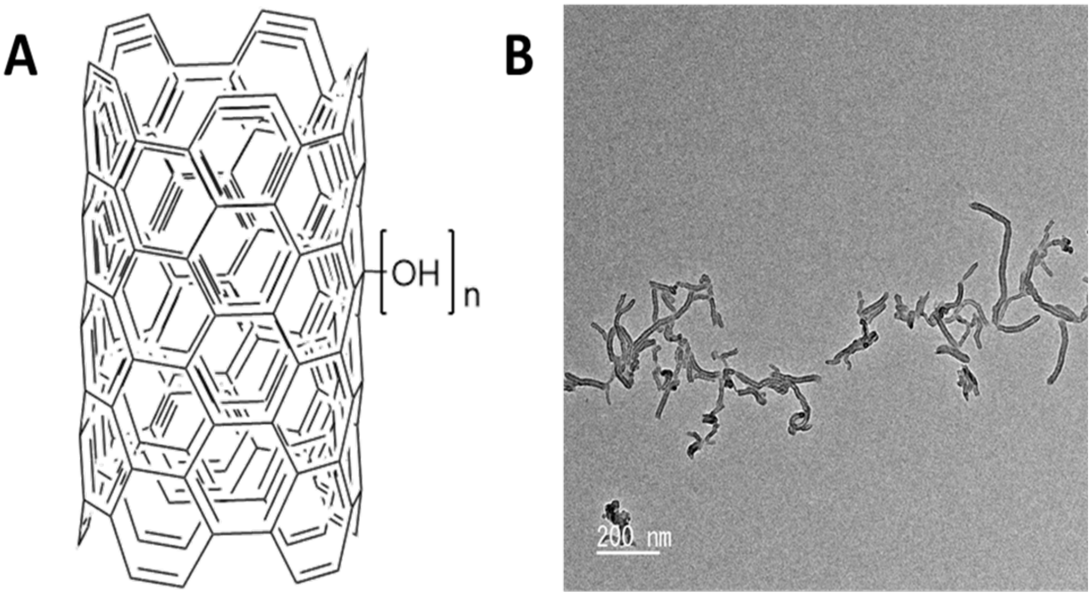

Figure 4.3. A. The chemical structure of CNT-OH. **B**. TEM image of CNT-OH.

The smallest NP were hydroxylated fullerenes (C_{60}-OH) which have ball-like structure with diameter of ca. 1 nm and contain mostly carbon atom as shown in **Figure 4.4**. Similar to CNT-OH, due to their nucleophilic hydroxyl functional group, they have a negative zeta potential of -36 mV in milli-Q water. Due to their infinitesimal size, C_{60}-OH are difficult to be observed under TEM.

Other than those 2 carbon-based ENM, we used metal NP and metal oxide NP. These 2 ENM were synthesized with bottom-up procedure as explained in **Chapter 4.B.II**.

Figure 4.4. Chemical structure of C_{60}-OH.

Gold NP were stabilized by citrate and due to its capping agent, gold NP have a negative zeta potential of -46 mV in solution containing citrate. The shape and the size of the NP were not uniform. Morphology of the gold NP largely varied. The common ones were oval and shapeless as shown in TEM image in **Figure 4.5.A**. The size of the NP ranges from 10 to 60 nm (**Figure 4.5.B**) with the majority at 20-30 nm. Size distributions of NP was built by measuring >100 NP on TEM images.

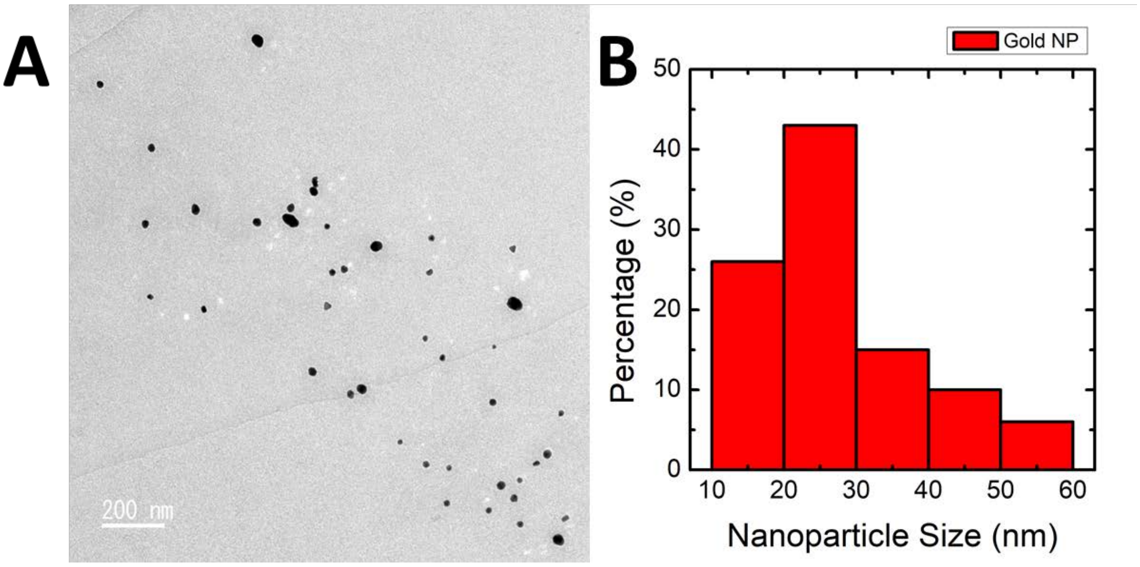

Figure 4.5. A. TEM image of Gold NP. **B**. Size distribution of Gold NP.

Silica NP were stabilized by Triton X-100 and modified by TEOS (**Figure 4.6**) Thus, these NP had negative zeta potential of -32 mV in milli-Q water. The shape of the NP was mostly round with several shapeless figures. The size was more homogenous than gold NP as shown in TEM image in **Figure 4.7.A**. The size of the NP ranges from 35 to 60 nm (**Figure 4.7.B**) with the majority at 45-50 nm. Size distributions of NP was built by measuring >100 NP on TEM images.

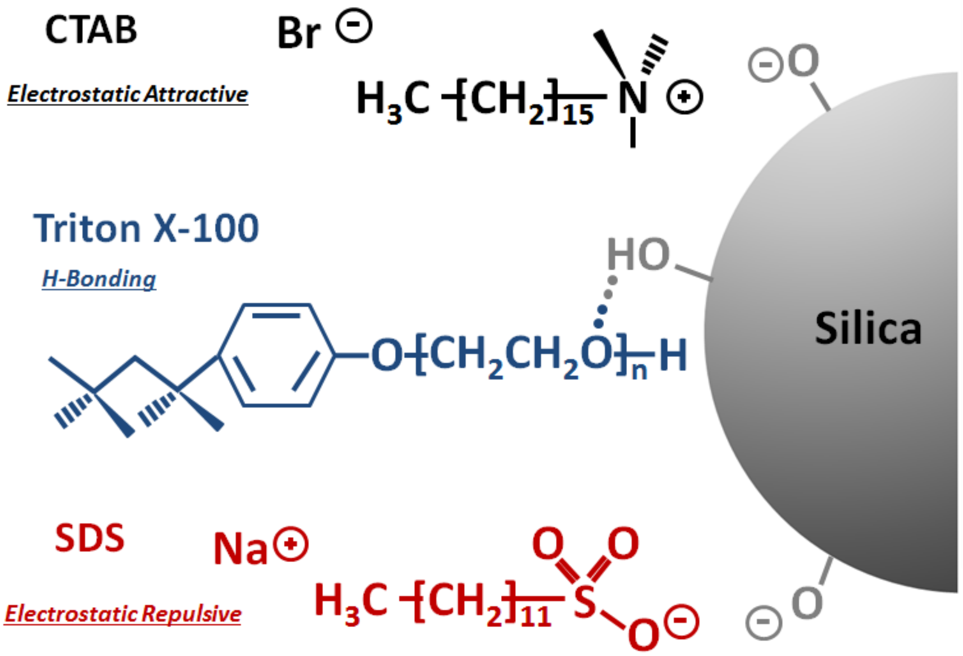

Figure 4.6. Interaction on the surface between silica NP and capping agents. Reproduced from Zhang, T.; Blum, F. D. Cationic Surfactant Blocks Radical-Inhibiting Sites on Silica. *J. Colloid Interface Sci.* **2017**, *504* (May), 111–114[140] with permission from Elsevier (license number: 4421211341527)

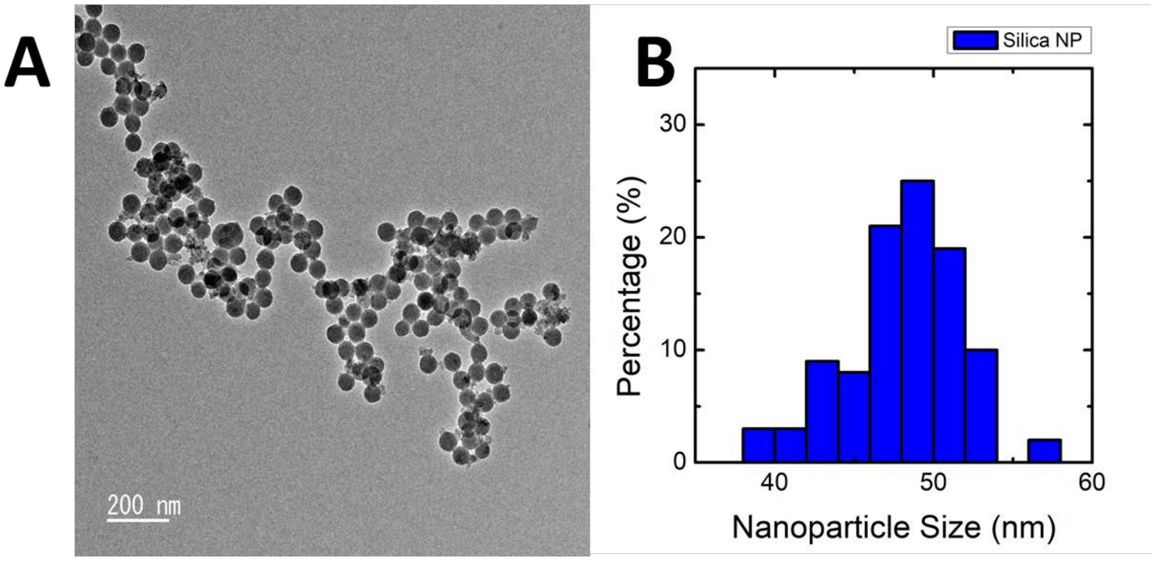

Figure 4.7. A. TEM image of silica NP. **B**. Size distribution of silica NP.

4.C.II. Linearity of Concentration – Absorbance Correlation

In this research, measurement of ENM concentration in solution was mostly done by UV spectroscopy. Therefore, the value of absorbance wavelength should be correlated with concentration of ENM in solution. For current research, wavelength of 320 nm was chosen as there is no overlap of absorbance value due to absorbance of chitosan or acetic acid. **Figure 4.8** shows linear correlation of C_{60}-OH concentration to absorbance value and **Figure 4.9** provides proof about the linearity of CNT-OH concentration to absorbance value. Meanwhile, the peak in gold NP peak (around 525 nm) was chosen as the maximum of surface plasmon absorbance for small Au NP as shown in **Figure 4.10**. The value of the absorbance of the distinctive peak has linear correlation with gold NP concentration. Distinct from the other 3 ENM, the concentration of dyed silica NP was measured by fluorescence spectroscopy because silica NP produce low absorbance value of UV spectra so that it is difficult to be measured with UV spectroscopy accurately. As the dye attached to the silica NP was rhodamine-B isothiocyanate, the wavelength used for excitation was 530 nm and it produced emission around 575 nm. In **Figure 4.11**, the linear dependence of the emission peak on silica NP concentration is shown. As long as there is no adjustment to the measurement tool settings, the linearity is similar in all measurement.

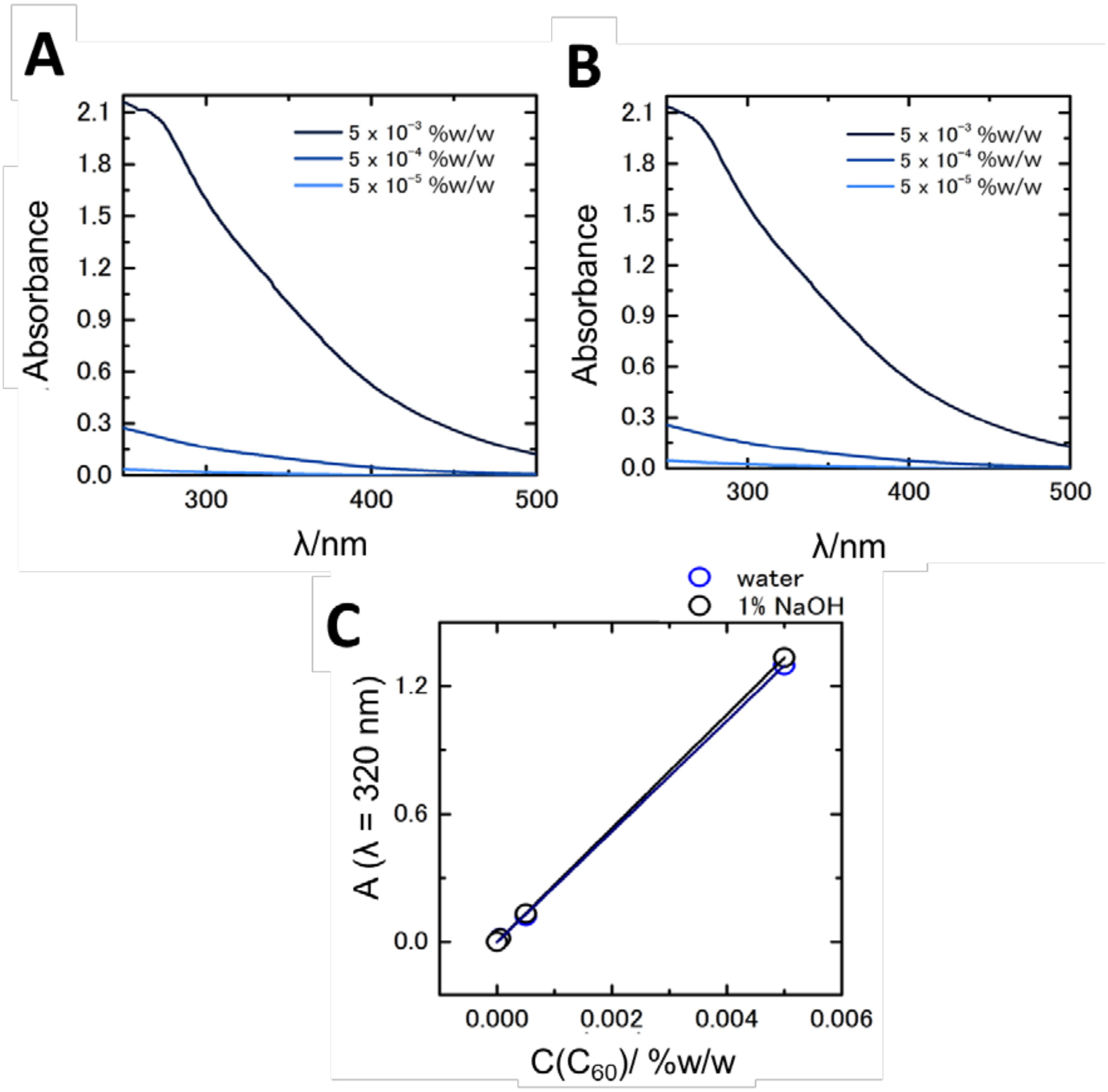

Figure 4.8. A. UV-vis spectra of C_{60}-OH at different C_{60}-OH concentrations. The samples were prepared by dissolving certain amount of C_{60}-OH into 1% w/w NaOH and then the samples were diluted with milli-Q water. **B.** UV-vis spectra of C_{60}-OH at different C_{60}-OH concentrations prepared by dilution of C_{60}-OH stock solution with 1% w/w NaOH. **C.** Dependence of C_{60}-OH UV absorbance at λ= 320 nm on C_{60}-OH concentration.

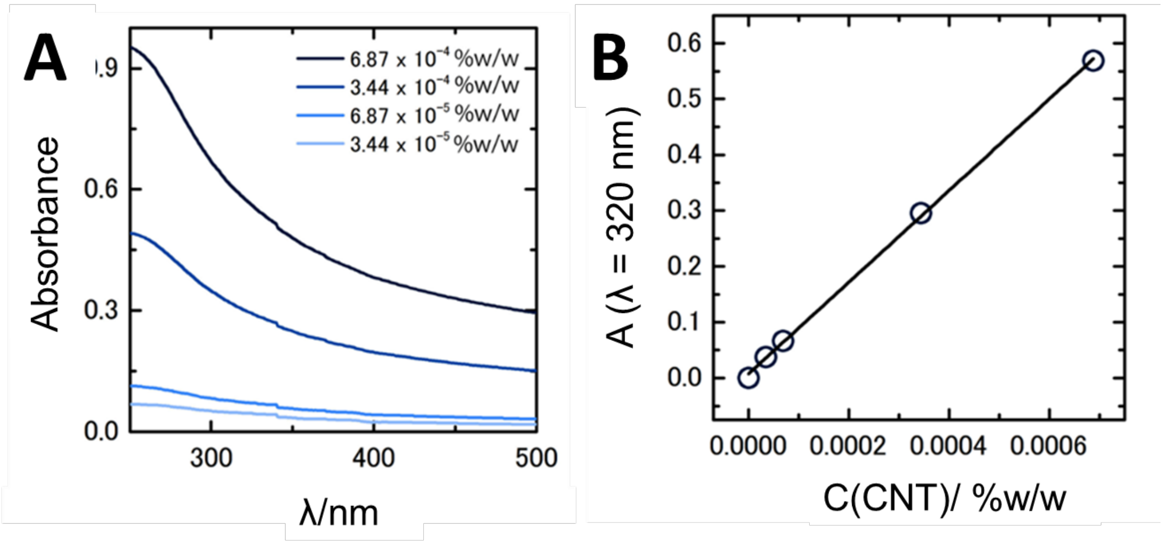

Figure 4.9. A. UV-vis spectra of CNT-OH at different CNT-OH concentrations. CNT-OH samples were prepared by consequent diluting of CNT-OH stock solution with milli-Q water 100, 200, 1000 and 2000 times. **B.** Dependence of CNT-OH UV absorbance at λ= 320 nm on CNT-OH concentration. Concentration of CNT-OH obtained by gravimetric analysis was 6.87×10^{-2} % w/w.

In **Figure 4.8**, both dilution of 1%- NaOH-dissolved-C_{60}-OH solution with water and 1% NaOH solvent were shown. As represented in that Figure, dilution with water and 1% NaOH solvent show similar gradient. Thus, it can be assumed that the dilution of C_{60}-OH stock solution with either 1% NaOH or water will result in similar absorbance value.

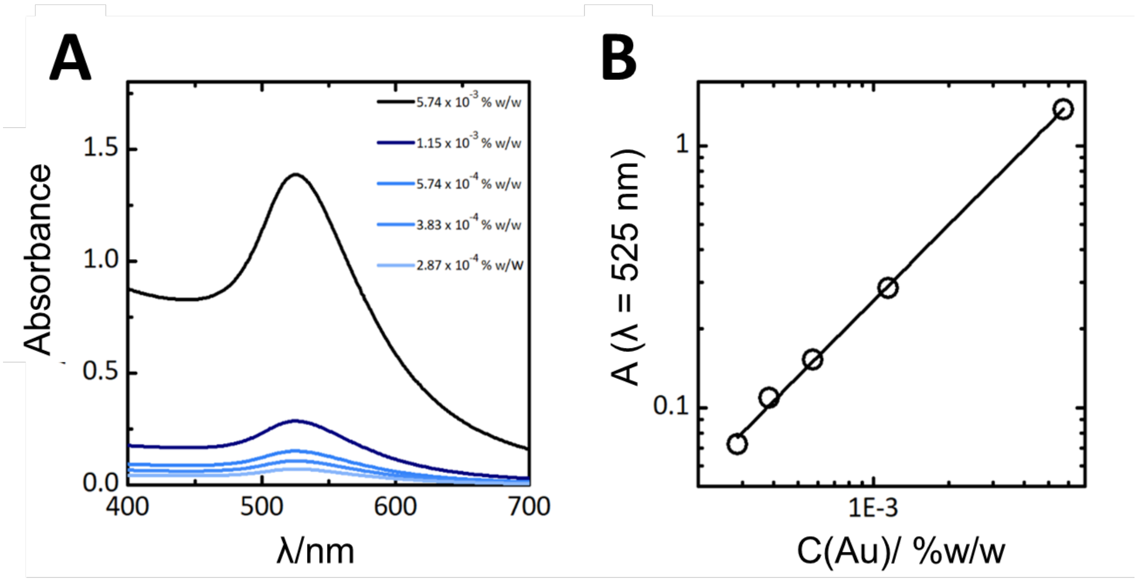

Figure 4.10. A. UV-vis spectra of gold NP at different gold NP concentrations. Gold NP samples were prepared by consequent diluting of gold NP stock solution with Milli-Q water 5, 10, 15, and 20 times, respectively. **B.** Dependence of gold NP absorbance at λ= 525 nm on gold NP concentration. The calculated concentration of gold NP stock solution was 5.74 × 10^{-3} % w/w.

4.C.III. General ENM Removal Protocol and Its Efficiency

Chitosan is a deacetylated form of chitin which can be extracted from crustacean shells and are the second most abundant natural polymers after cellulose. As a natural polymer, chitin and their derivative, chitosan, have no toxicity. As a weak polycation, chitosan cannot be dissolved in water in neutral or basic condition (pH higher than 7). However, chitosan can be dissolved in acidic condition (dilute hydrochloric acid or acetic acid are usually utilized) due to protonation of amino functional group of it. On other hand, pH neutralization of chitosan results in their precipitation.[107,141,142] In current research, 1% acetic acid (CH_3COOH) was used to dissolve various kinds of chitosan with certain polymer length to make 10 mM stock solutions.

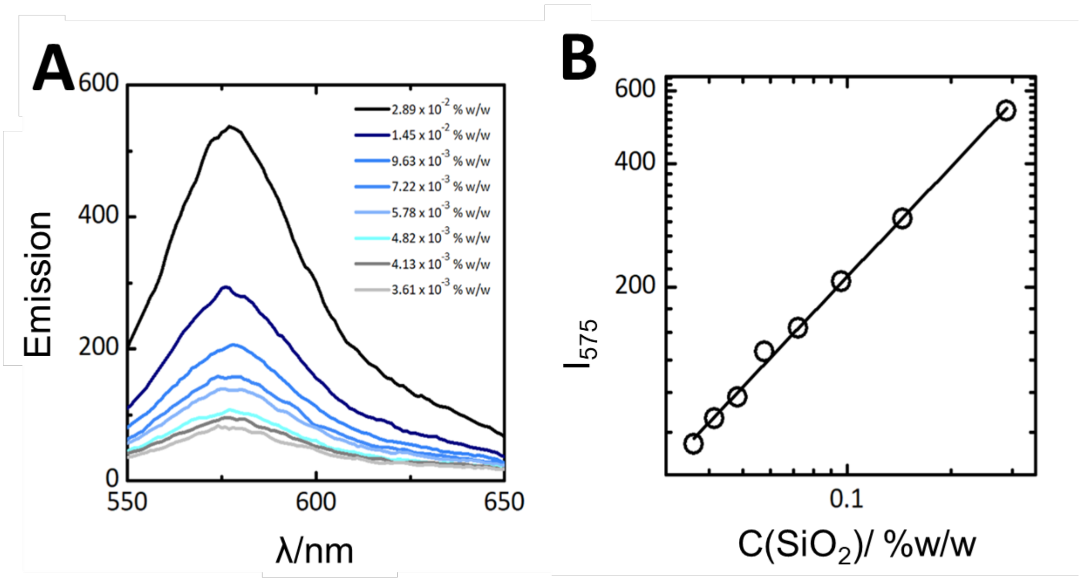

Figure 4.11. A. Fluorescence spectra of rhodamine-labeled silica NP at different silica NP concentrations. Silica NP samples were prepared by consequent dilution of silica NP stock solution with Milli-Q water 10, 20, 30, 40, 50, 60, 70, and 80 times, respectively. **B.** Dependence of silica NP fluorescence emission at λ_{em}= 575 nm (λ_{ex} = 530 nm) on silica NP concentration. Concentration of silica NP in the initial stock solution obtained by gravimetric analysis was 0.334% w/w.

The pH-sensitive solubility of chitosan explained before can be shown through the transmittance spectra of UV spectroscopy of the sample in certain pH. **Figure 4.12** shows the dependence of transmittance spectra of 1.61 mM chitosan on solution acidity level. The acidity level was adjusted by addition of 0.5 M sodium hydroxide dropwise until the required pH was reached. In **Figure 4.12**, the transmittance is around 100% in acidic area. However, between pH 6 to 8, there is a sharp fall in the transmittance indicating the increase of turbidity due to formation of precipitates. The reason of the decrease in turbidity is due to rapid formation of bulk precipitates of chitosan. The pH-sensitive solubility feature of chitosan utilized in current research is in agreement with the research of Sogias et al.[143] By utilizing this characteristic of chitosan, we developed a new method to reduce ENM concentration in solution by pH dependent co-precipitation method by a single reactant, chitosan.

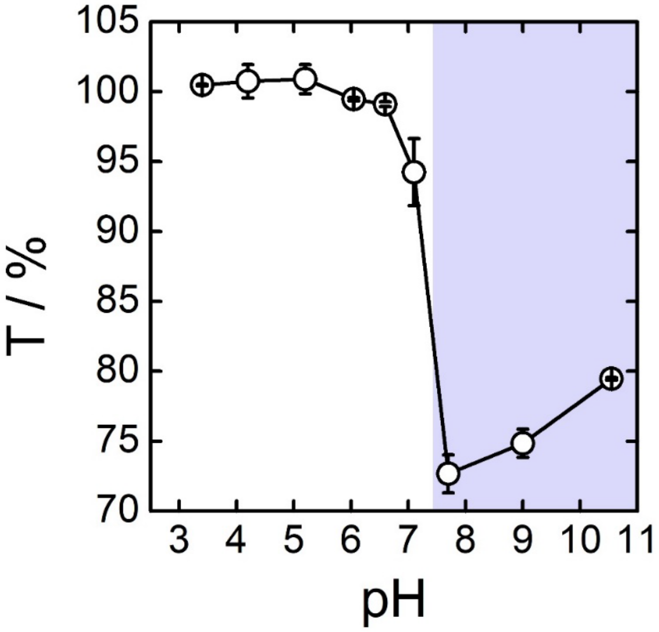

Figure 4.12. The dependence of optical transmittance of UV spectroscopy of 1.61 mM chitosan 500 solution at wavelength of 320 nm on solution pH.

4.C.III.1. ENM Removal Protocol by Co-Precipitation

The current protocol utilized chitosan's pH-dependent solubility to capture and separate ENM from mother liquid (illustrated in **Figure 4.13.A**). In acidic condition, positively-charged chitosan complex with ENM (which are mostly negatively-charged) and form complexes. Then, after neutralization (or alkalization), chitosan complexes cannot be properly protonated, so they agglomerate as well as precipitate. This process will result in bulky precipitates of ENM-chitosan-complex precipitates which can be easily separated from mother liquid.

In this study, the ENM used in the whole process as representatives are hydroxylated multi-walled carbon nanotubes (CNT-OH) and hydroxylated fullerenes (C_{60}-OH) with additional research using gold NP and silica NP. The zeta potentials of each ENM were -36 mV, -19 mV for, -46 mV, and -32 mV for C_{60}-OH, CNT-OH, gold NP, and silica NP respectively. Thus, both carbon-based ENM are negatively-charged due to their hydroxyl functional group and both gold NP and silica NP are negatively-charged due to their capping agents. Each ENM at low concentration (2.22×10^{-4} % w/w for CNT-OH, 2.79×10^{-4} %w/w for C_{60}-OH, 5.55×10^{-4} %w/w for gold NP, 10^{-2} %w/w for silica NP) were treated with 1.61 mM of chitosan solution and left to precipitate for 24 hours followed by centrifugation at 1,500 rpm for 30 minutes to remove precipitates. **Figure 4.13. B and C** show the samples in the condition of before (1), after chitosan addition (2), and after the general protocol treatment with chitosan 500 without centrifugation (3) as explained previously.

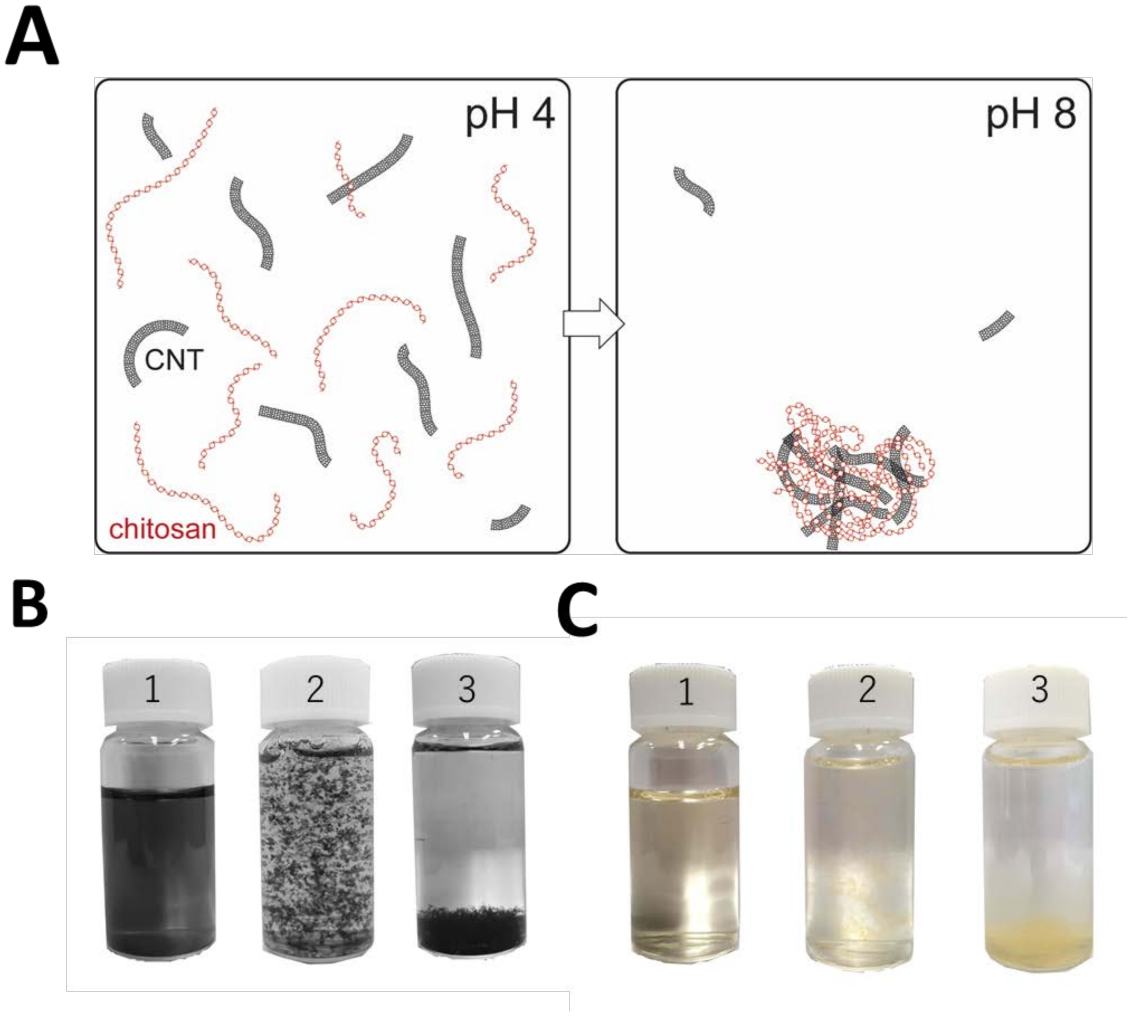

Figure 4.13. A. Illustration of ENM co-precipitation with chitosan. **B.** Photographic image of 2.22 x 10^{-4} % w/w solution of CNT-OH before (1) and after (2) treatment by chitosan 500, followed by settling for 24 hours (3). **C.** Photographic image of 2.79×10^{-4} % w/w solution of C_{60}-OH before (1) and after (2) treatment by chitosan 500, followed by settling for 24 hours (3).

To validate the capability of removal method and measure the efficiency of the removal, UV spectroscopy on the wavelength of 320 nm was used for CNT-OH and C_{60}-OH, 525 nm for gold NP. Fluorescence spectroscopy with excitation wavelength of 530 nm and emission wavelength around 575 nm was used to measure the efficiency of the removal of silica NP.

The linear correlation between the absorbance value and concentration is mentioned in **Chapter 4.C.I.**

Addition of acetic acid-dissolved chitosan solution (pH 3.3, 10 mM) to ENM-dispersed solution induced pH change from pH ca. 6 to pH 3.4. The spectra in **Figure 4.14.C** show the dependance of ENM (2.22×10^{-4} %w/w for CNT-OH, 2.79×10^{-4} %w/w for C_{60}-OH) removal method efficiency utilizing pH-sensitive chitosan on pH solution adjusted with 0.5 M NaOH solution. As shown in **Figure 4.14.C,** addition of chitosan did not affect the transmittance of CNT-OH solution, but induced to 20% increase in absorbance to C_{60}-OH solution. Gradual increase of pH to mild acid condition ($pH < 6$) did not show any changes. However, further adjustment to mild basic condition (8.0 ± 0.5 for solution containing C_{60}-OH and 8.5 ± 1.0 for solution containing CNT-OH) resulted in a significant drop of concentration which was related to the formation of insoluble complexes of chitosan and ENM. In a strong basic condition ($pH > 8.5$), C_{60}-OH solution graph shows a gradual increase of ENM concentration (ca. 50% increase of C_{60}-OH concentration in the solution on pH 10). We speculate that this result is correlated with the higher solubility of C_{60}-OH in basic condition, as stated by the solubility data provided by the manufacturer. Higher solubility may affect the fullerene aggregation behaviour and hinder the adsorption of those ENM to chitosan. On the other hand, there was no remarkable effect of pH adjustment to > 8.5 on removal capability of CNT-OH by chitosan. To complement the graph in **Figure 4.14.C**, **Figure 4.14.A and B** show the corresponding UV vis spectra for each pH condition in the dependence graph of **Figure 4.14.C** for CNT-OH and C_{60}-OH, respectively.

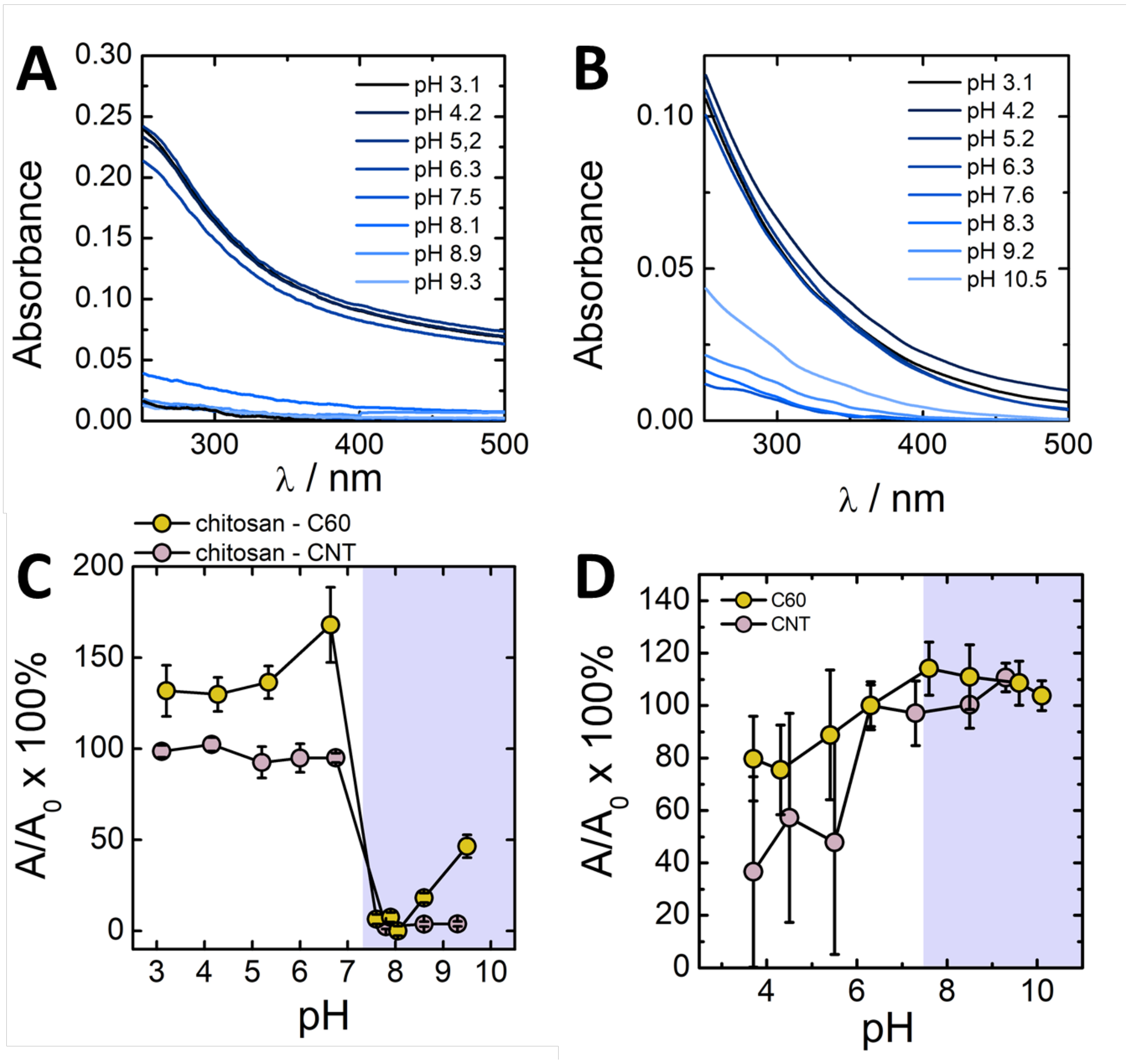

Figure 4.14. A. UV-vis spectra of 1.61 mM chitosan 500 in 2.22×10^{-4} % w/w CNT-OH solutions at pH between 3 to 10 after settling for 24 hours and centrifugation for 30 minutes on 1,500rpm. **B.** UV-vis spectra of 1.61 mM chitosan 500 in 2.79×10^{-4} % w/w CNT-OH solutions at pH between 3 to 10 after settling for 24 hours and centrifugation for 30 minutes on 1,500 rpm. **C.** Dependence of the optical density of ENM solution at λ = 320 nm after being treated with 1.61 mM chitosan 100, left to precipitate for 24 hours and centrifuged on 1,500 rpm for 30 minutes on pH between 3 to 10. **D.** Dependence of the optical density of ENM solution at λ = 320 nm after being left to settle for 24 hours and centrifuged on 1,500 rpm for 30 minutes on pH between 3 to 10 (without chitosan treatment).

In **Figure 4.14.D**, the ENM solution of the same concentration as the one in the previous experiment was subjected to pH adjustment without chitosan. In the absence of chitosan, ca. 60% of CNT-OH and ca. 20% of C_{60}-OH slightly precipitated. On the other hand, the solution containing both chitosan and ENM **(Figure 4.14.C**) showed a different tendency. The solution was stable in acidic condition and unstable in mild basic condition. Thus, the removal of ENM by pH adjustment to mild basic condition was due to the presence of coagulant, chitosan, and not solely by the disruption of colloidal stability of ENM dispersion due to pH change.

Following the formation of insoluble precipitates, the removal of the precipitates was done by natural sedimentation for 24 hours and centrifugation. After settling for 24 hours, the precipitates were separated by decantation. Chitosan added to the solution were chitosan 100 (Mw = 650,000). However, additional treatment (centrifugation at 1,500 rpm for 30 minutes) was performed to measure the maximum capability of the treatment. ENM removal efficiency of chitosan treatment method depends on molecular weight of the chitosan, settling time and additional treatment process, such as filtration and centrifugation. The influence of each of these factors is discussed in the following sections.

4.C.III.2. Influence of Ionic Strength of Solution on the ENM Removal Efficiency

In nature, almost all water bodies contain common salts, such as Na^+, K^+, Mg^{2+}, and Ca^{2+}. Those salts contribute to the ionic strength of the solution which affects colloidal stability of ENM in solution.[144–147] Due to salt effect on colloidal stability, there is a possibility that the above cations may affect the ENM removal method by co-precipitation by changing the solubility of chitosan at certain pH or the process of precipitate formation.[148] Therefore, it is important to investigate the influence of both monovalent and divalent cation on the ENM removal by co-precipitation treatment by chitosan. In this experiment, common salt, amount of which is still relevant to their occurrence in nature,[144,145,149] such as Na^+, K^+, Mg^{2+}, and Ca^2, was dissolved in the solution and the co-precipitation treatment process was applied afterwards. Then, the remaining ENM concentration in the solution was measured. In this experiment, the amount of chitosan applied in the solution was smaller (corresponding to ca. 30% of removal of C_{60}-OH or ca. 75% removal of CNT-OH for the control experiment without any addition of salt) than the required chitosan-ENM ratio to achieve > 90% removal. Thus, a small part of ENM remained in the solution after the treatment but changes due to addition of salt can be easily detected.

The presence of both 10 mM of monovalent and divalent cation in the solution changed the precipitation percentage of CNT-OH but did not hinder the co-precipitation process by chitosan (**Figure 4.15.A** for C_{60}-OH and **B** for CNT-OH). For example, precipitation rate of CNT-OH increased from ca. 75% to 78% due to the presence of NaCl and more than 90% due to the presence of $MgCl_2$. Similarly, precipitation rate of C_{60}-OH increased from ca. 30% to 35% due to the presence of NaCl and ca. 80% due to the presence of $MgCl_2$. Comparing with the salt addition in the absence of chitosan in **Figure 4.15.C** for C_{60}-OH and D for CNT-OH, it can be concluded that addition of 10 mM of monovalent ions (Na^+ and K^+) had only a little or no effect t ENM and the co-precipitation process. On the other hand, 10 mM of divalent cations (Ca^{2+} and Mg^{2+}) promoted agglomeration and thereby it improved the ENM removal efficiency by chitosan co-precipitation method. This finding is in agreement with the available literature.[150]

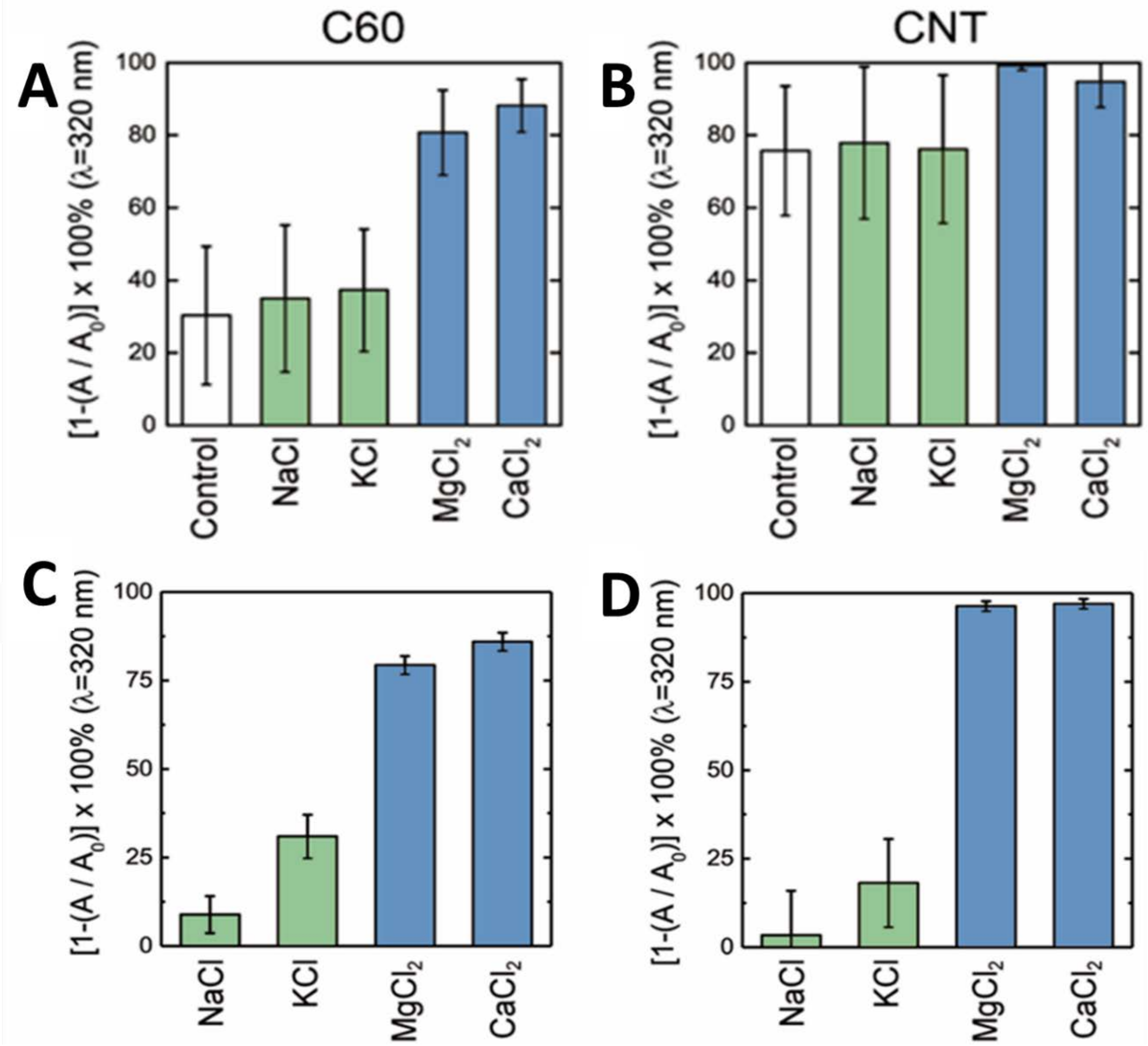

Figure 4.15. Removal percentage of C_{60}-OH (**A**) and CNT-OH (**B**) by co-precipitation method applying chitosan 500 at ratios m(chitosan)/m(ENM) = 0.188 and 0.164 for C_{60}-OH and CNT-OH respectively in a solution containing monovalent cation (green) and divalent cation (blue) with ionic strength of 0.01 M at pH: 8.0 ± 0.5 (C_{60}-OH) and pH: 8.5 ± 1.0 (CNT-OH). Natural sedimentation for 24 hours followed by centrifugation of mother liquid at 1,500 rpm for 30 minutes was applied to separate the mother liquid and precipitates. (**C**) C_{60}-OH and (**D**) CNT-OH removal percentage by addition of 0.01 M monovalent salt (green) and divalent salt (blue) in absence of chitosan. Same separation method (24-hour natural sedimentation followed by centrifugation at 1,500 rpm for 30 minutes) was applied.

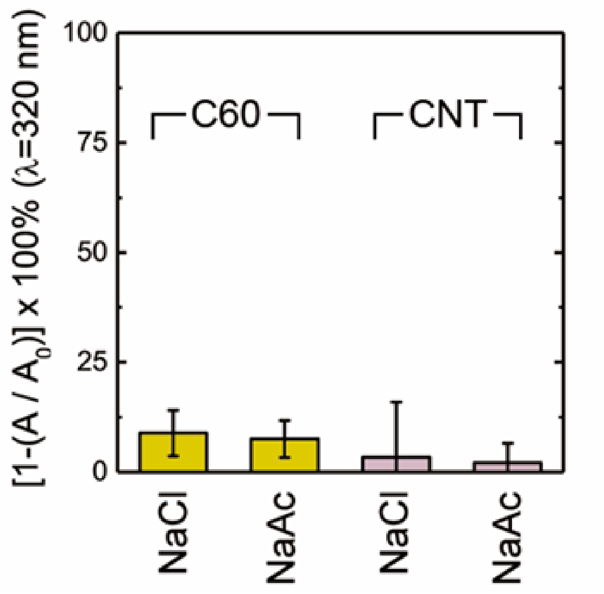

Figure 4.16. Removal percentage of C_{60}-OH and CNT-OH in the presence of 0.01 M of NaCl or $NaCH_3COO$ in the absence of chitosan. 24-hour natural sedimentation and centrifugation at 1,500 rpm for 30 minutes were applied for separation method.

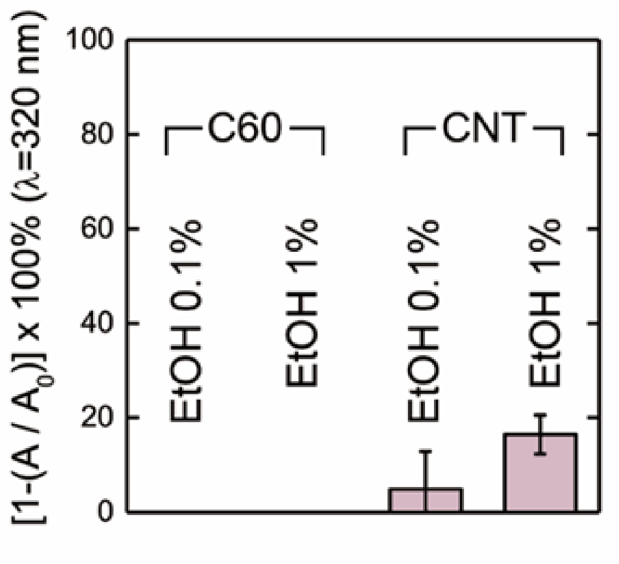

Figure 4.17. Removal percentage of C_{60}-OH and CNT-OH in the presence of 0.1% or 1 % of ethanol in the absence of chitosan. 24-hour natural sedimentation and centrifugation at 1,500 rpm for 30 minutes were applied for separation method.

While cations affected the colloidal stability of ENM, anions did not affect the stability as shown in **Figure 4.16**. In this experiment, both monovalent anion of chloride (Cl^-) and acetate (CH_3COO^-) effect on the stability of ENM was negligible (ca. 10% removal of C_{60}-OH and less than 10% removal of CNT-OH due to addition of sodium chloride or sodium acetate). Therefore, there was hardly some differences in the ENM removal capability for chitosan dissolved in acetic acid and the one dissolved in hydrochloric acid.

4.C.III.3. Influence of Organic Solvent on the Stability of ENM

In contrast to the possibility that some salts are dissolved in solution, the possibility of the presence of an organic solvent in the water is low. Thus, in this study, the effect of small amount of ethanol on the ENM stability was tested (**Figure 4.17**). The presence of 1% or 0.1% of ethanol has a little effect on the stability of CNT-OH but has no effect to the stability of C_{60}-OH.

4.C.III.4. Colloidal stability and ENM Removal Method

As stated earlier, colloidal stability is affected by ionic composition of a solution,[146,147] thereby, it is important to validate that the ENM precipitation was not due to agglomeration of ENM. TEM images of chitosan and CNT-OH precipitates which were formed at early stage of coagulation in **Figure 4.18** shows that CNT-OH were separated from each other and covered by chitosan matrix. Bundles of CNT-OH are not found in the sample which proves that chitosan was the main cause of the ENM separation from solution. The appearance of CNT-OH on the TEM images. The appearance of CNT-OH on the TEM images TEM images also exclude the possibility of self-aggregation of ENM as the main cause of the separation. Due to infinitesimal size of C_{60}-OH, the image of the precipitate of C_{60}-OH is hardly relevant to show both the adsorption process of ENM to chitosan and aggregation of C_{60}-OH.

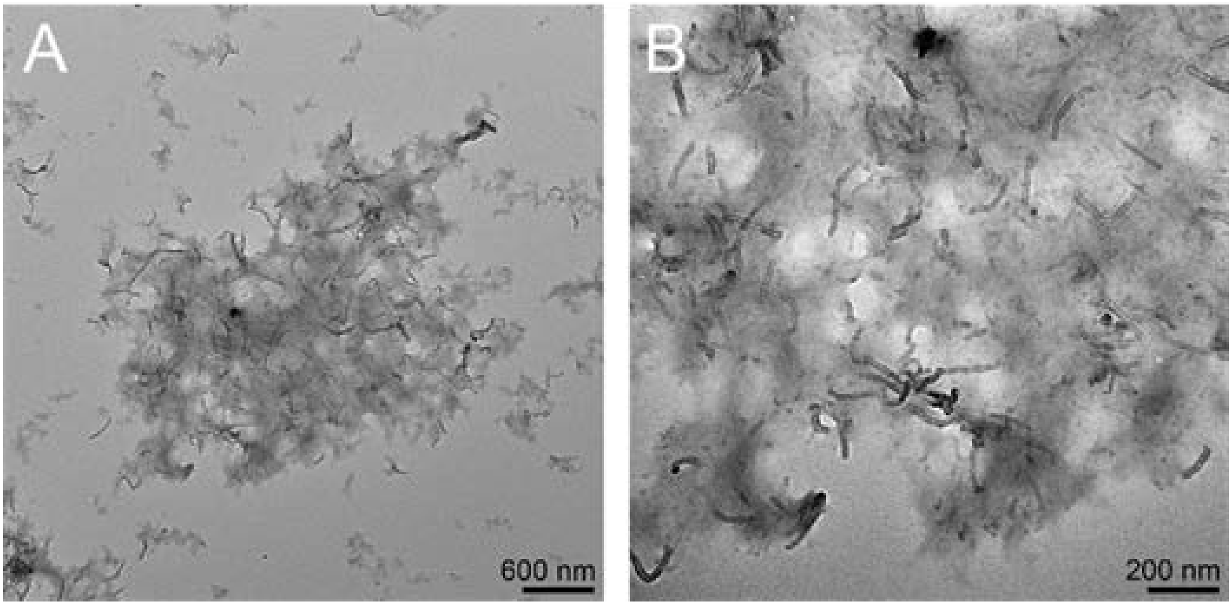

Figure 4.18. TEM images of chitosan-CNT-OH precipitates collected after 60 min from the moment of pH adjustment to 8.5. The concentration of CNT-OH was 2.22×10^{-4} % w/w and the concentration of chitosan 10 was 1.61 mM.

4.C.III.5. Dependence of ENM Removal Percentage on Ratio between Chitosan and ENM

Besides the pH-sensitive solubility of chitosan, interaction between chitosan and ENM is the factor that directly affect the removal of ENM from solution through co-precipitation process. Any excess amount of chitosan will increase the cost of the removal process. On the other hand, any excess amount of ENM will lower the efficacy of the process. Thus, similar to any other process, the optimization of such interaction needs to be studied to achieve cost-effective process.

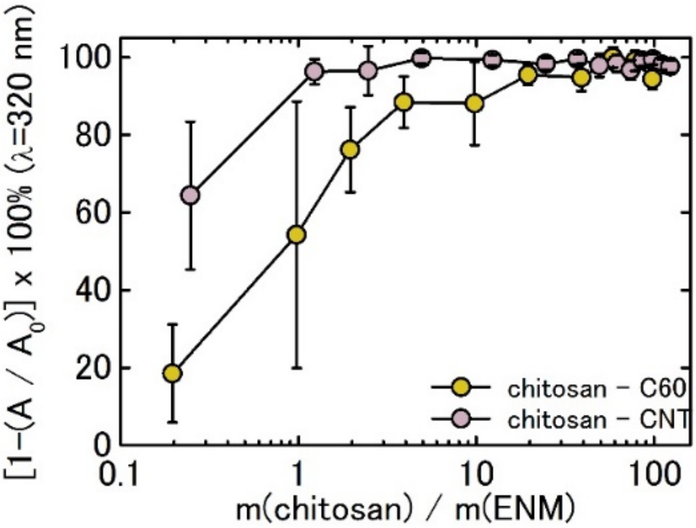

Figure 4.19. Dependence of the percentage of C_{60}-OH and CTN-OH removal at pH =8.0±0.5 (C_{60}-OH) and 8.5±1.0 (CNT-OH) on chitosan 500 to ENM mass ratio. Concentrations of C_{60}-OH and CNT-OH are 2.79�10-4 % w/w and 2.22�10-4 % w/w, respectively. All samples were separated by settling for 24 hours and centrifugation at 1,500 rpm for 30 minutes.

In **Figure 4.19**, the dependence of the removal percentage of ENM (C_{60}-OH and CNT-OH) on the ratio between chitosan and ENM is presented. Each of ENM shows a threshold value under which the maximum efficacy of the method cannot be reached. To achieve >90% removal of CNT-OH at concentration of 2.22×10^{-4} %w/w, ca. 0.02 mM of chitosan 500 was required. On the other hand, to achieve >90% removal of C_{60}-OH at concentration of 2.79×10^{-4} %w/w, ca. 0.32 mM of chitosan 500 was required. If the concentration is converted into weight, the weight of chitosan required to achieve 90% of CNT-OH removal was the same as the weight of the adsorbed ENM. However, 20 times the weight of C_{60}-OH was required to achieve the same removal. The difference in the required amount of chitosan can be related to the surface area of each ENM that can interact with chitosan. The larger the area is, the lower the weight of chitosan required is. Nonetheless, if >80% removal is considered sufficient only 4 times the weight of C_{60}-OH was required.

4.C.III.6. Dependence of ENM Removal Percentage on Chitosan Molecular Weight

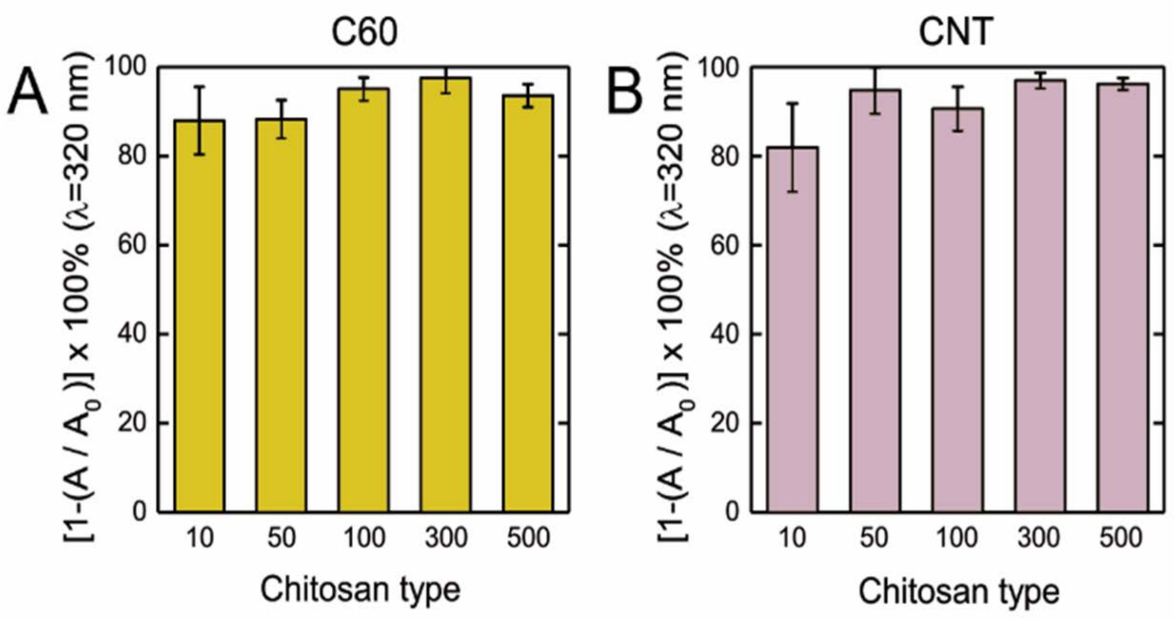

Figure 4.20. Percentages of C_{60}-OH (A) and CNT-OH (B) removal by co-precipitation with chitosan 1.61 mM of different molecular weight at pH 8.0±0.5 (A) or 8.5±1.0 (B) utilizing settling for 24 hours and centrifugation in 1,500 rpm for 30 minutes. Concentration of C_{60}-OH and CNT-OH are 2.79×10^{-4} % w/w and 2.22×10^{-4} % w/w, respectively.

Considering polymer length as a factor that determines the number of sites that are available to interact with ENM, the effect of polymer length deserves investigating. In this study, various types of chitosan with different molecular weight were studied (**Table 4.3**). By applying standard removal procedure consisting of 24-hour-natural sedimentation and 1,500 rpm centrifugation for 30 minutes, there was almost no difference in removal efficiency for chitosan 100, 300, and 500 (>90% removal) as shown in **Figure 4.20**. However, there was a slightly lower removal of both ENM for chitosan 10 and chitosan 50 (only C_{60}-OH). Therefore, it can be concluded that there is a tendency toward higher removal percentage of both ENM applying chitosan of higher molecular weight. Nonetheless, the difference is insignificant.

Table 4.3. Molecular weight of different chitosan samples used in this study.

Type of Chitosan	Molecular Weight (g/mol)	Ref.
Chitosan 10	60,000	137
Chitosan 50	320,000	138
Chitosan 100	650,000	136
Chitosan 300	1,100,000	139
Chitosan 500	1,200,000	136

4.C.III.7. Application of Various Separation Methods and their Influence on Removal Percentage

Even though there was only a slight dependence of removal percentage on molecular weight, this difference can be changed depending on the separation method. Moreover, separation method is a critical step of the removal process. Thus, it is important to investigate the dependence of removal percentage on separation method as well as how chitosan of different molecular weight behaves in different separation method.

In this research, three possible separation methods were investigated. The whole treatment process can be designed either as a single step or multiple steps. The separation methods tested in this study were natural sedimentation, filtration with 0.45-µm filter and centrifugation at 1,500 rpm for 30 minutes.

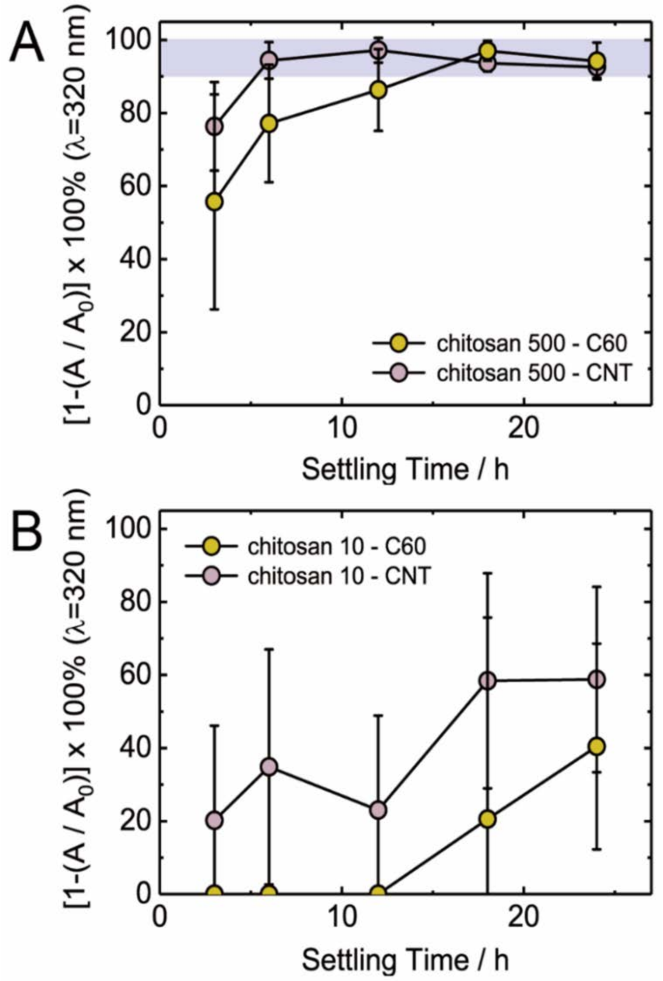

Figure 4.21. Dependence of CNT-OH (purple) and C_{60}-OH (yellow) removal percentage on settling time by high molecular weight chitosan 500 (1,200,000 g/mol)[136] and low molecular weight chitosan 10 (60,000 g/mol)[137]. Concentrations of C_{60}-OH was 2.79×10^{-4} % w/w and concentration of CNT-OH was 2.22×10^{-4} % w/w. Concentration of both chitosan 500 and chitosan 10 were 1.61 mM.

Sedimentation is an important method to form bulky flocs that usually implemented in any wastewater plants due to its low cost. However, it is important to note that natural sedimentation requires certain time which can vary depending on the type of coagulants utilized. For example, in **Figure 4.21**, both chitosan 500 and chitosan 10 had better removal percentage at longer settling time because longer settling time leads to the formation of bulkier flocs and to precipitate (ca. 40% improvement could be achieved by prolonging the settling time from 3 hours to 24 hours). Nevertheless, there was ca. 50% difference in ENM removal capability between chitosan 500 and chitosan 10. ENM removal by chitosan 500 was 75% and 55% for CNT-OH and C_{60}-Oh respectively during 3 hours of settling time. Furthermore, the removal percentage reached >90% ENM removal after 6 hours (CNT-OH) and 18 hours (C_{60}-OH) of settling time.

On the other hand, chitosan 10 didn't remove C_{60}-OH for the first 12 hours of settling time and could only remove 20% of CNT-OH during 3 hours of settling time. Moreover, chitosan 10 only achieved ca. 60% CNT-OH removal and ca. 40% C_{60}-OH removal after 24 hours. This difference in ENM removal capability is because chitosan 500 has almost 20 times higher molecular weight than chitosan 10. This fact indicates that chitosan 500, which has longer polymer length, has better capability to form larger flocks than chitosan 10 so chitosan 500 requires shorter time to separate ENM from its solution after the co-precipitation treatment is applied. The difference in settling time between CNT-OH and C_{60}-OH is due to the fact that the surface of individual filament-like CNT-OH is larger than that of small round-shaped C_{60}-OH. Thus, CNT-OH have more sites to interact with chitosan and it was easier for chitosan and CNT-OH to form bulky and heavy flocs.

In **Figure 4.21**, treatment with chitosan 500 required 6 hours and 18 hours to remove >90% CNT-OH and C_{60}-OH, respectively, and chitosan 10 required more than 24 hours to achieve high removal efficiency. This settling time is below generally accepted to be applied in the water treatment system. To shorten settling time and increase removal efficiency, additional treatment step was used. In this study, filtration with 0.45-μm filter and centrifugation at 1,500 rpm for 30 minutes were used as second step. Centrifugation is an efficient method to force precipitation of flocs in water treatment. However, this method is small-scaled and can only be applied in the laboratory to recover ENM from mother liquid. Therefore, the chance of such method is implemented in water treatment system is low. On the other hand, filtration is a common method to be implemented in water treatment system. There are many types of filter varied in composition (sand, gravel, polymers, etc.) and pore size. Generally, separating ENM from mother liquid by filtration requires membranes with size smaller than ENM. However, smaller pore size membranes require high pressure and frequent cleaning of the separation membrane. Thus, it is common to utilize good coagulant as a pretreatment.[151] The purpose of application of this additional step in wastewater treatment is to increase the removal percentage of the entire treatment.[131]

In this study, three methods were investigated and compared to understand the dependence of ENM removal percentage on separation method. The first one was natural sedimentation for several hours (3, 6, 12, 18 and 24 hours). The second method was 2-step process of natural sedimentation and centrifugation at 1,500 rpm for 20 minutes. The third method was also a 2-step process, but it consists of natural sedimentation and filtration using 0.45-µm cellulose acetate membrane filter.

The removal percentages of the three methods for 3-hour and 24-hour settling time are shown in **Figure 4.22**. As discussed earlier, longer sedimentation time results in better removal percentage and C_{60}-OH need longer sedimentation time to be removed at the same removal percentage as CNT-OH. Additional treatment in second and third method was important to achieve higher ENM removal efficiency, especially for short settling time.

In **Figure 4.22.A'**, settling time for 24 hours after treatment with high molecular weight chitosan 500 achieved more than 90% ENM removal so the effect of additional step was not clear. However, improvement is shown in **Figure 4.22. A, B, and B'**. In **Figure 4.18.A**, 3-hour sedimentation was capable to remove ca. 55% of C_{60}-OH and ca. 75% of CNT-OH. Thus, additional step, low-rate centrifugation or 0.45-µm filtration, was applied to increase the efficiency until it reached >90% removal. In **Figure 4.22.B**, chitosan 10 did not remove C_{60}-OH and could only remove ca. 20% of CNT-OH by 3-hour settling time. Additional 0.45-µm-membrane filtration process increases the ENM removal percentage to ca. 60% and 80% for C_{60}-OH and CNT-OH respectively. On the other hand, low-rate centrifugation increased the percentage to ca. 50% and 70% for C_{60}-OH and CNT-OH, respectively. Thus, between 20% to 50% of ENM remained if chitosan 10, 3-hour settling time, and one of the additional processes are applied. In **Figure 4.22.B'**, chitosan 10 removed ca. 40% of C_{60}-OH and 60% of CNT-OH from solution by 24-hour-settling time. This value can be increased to around 80%-90% by additional treatment, either 0.45-µm-membrane filtration process or low-rate centrifugation process. This value is slightly lower than the value obtained for chitosan 500 which is similar to the result in **Figure 4.20**.

Comparing the result on **Figure 4.20** and **Figure 4.22**, ENM removal percentage of chitosan co-precipitation method depends on both molecular weight of chitosan and separation method. In **Figure 4.20**, the difference in ENM removal efficiency among chitosan samples of different molecular weight was marginal, but, in **Figure 4.21** and **4.21**, the difference in ENM removal efficiency between chitosan 10 and chitosan 500 for 3-hour-sedimentation separation method was significant. Thus, both molecular weight of chitosan and separation method have to be considered together to discuss ENM removal efficiency.

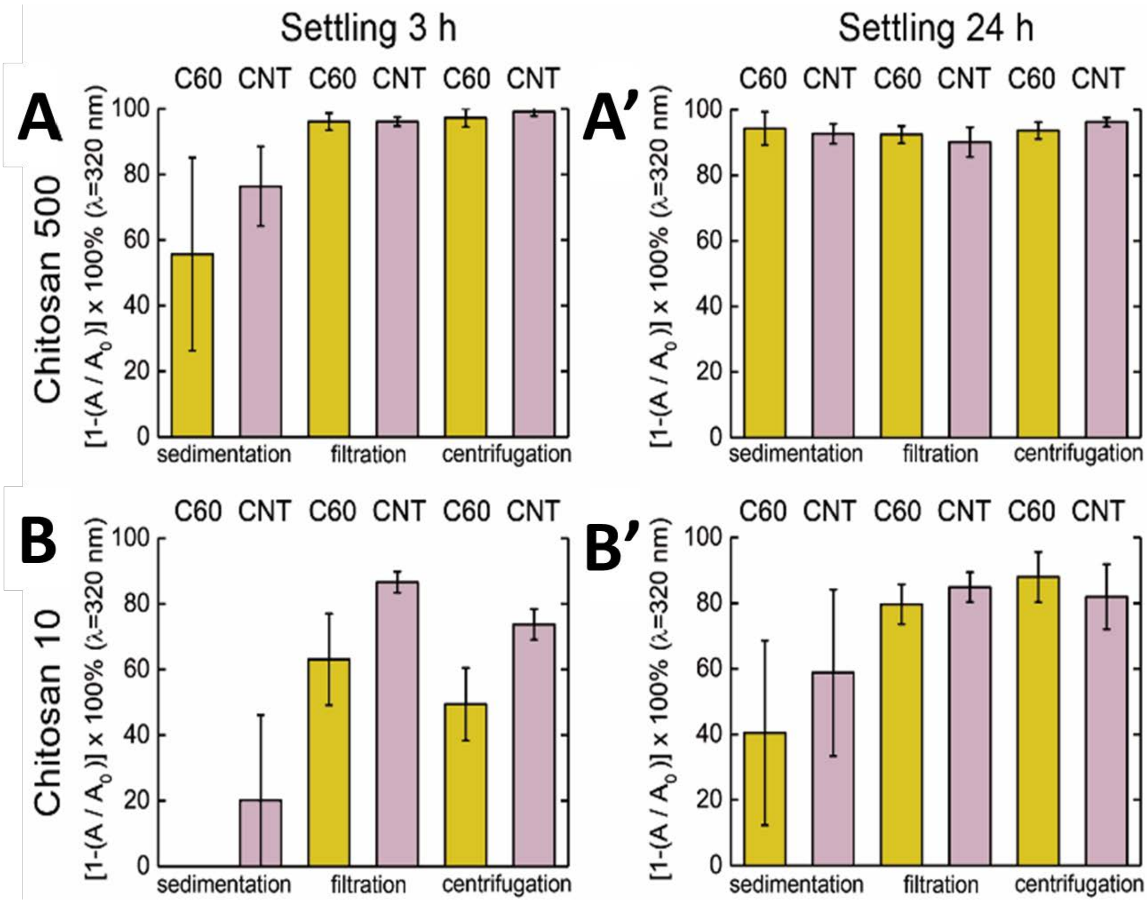

Figure 4.22. Percentage of C_{60}-OH and CNT-OH removal by co-precipitation with chitosan 500 and settling time of 3 h (**A**) or 24 h (**A'**); as well as chitosan 10 and settling time of 3 h (**B**) or 24 h (**B'**) and separation by sedimentation, sedimentation + filtration, or sedimentation + coagulation. Co-precipitation was performed at pH 8.0±0.5 for C_{60}-OH NP and pH 8.5±1.0 for CNT-OH NP. Concentration of C_{60}-OH and CNT-OH were 2.79×10^{-4} % w/w and 2.22×10^{-4} % w/w, respectively. Concentration of chitosan was 1.61 mM. Centrifugation was done at 1,500 rpm for 30 minutes after settling for 3 hours. Filtration was done using 0.45 μm membrane after settling for 3 hours. Sedimentation was done by allowing the precipitates to settle for 24 hours.

From the results shown in **Figure 4.20** to **4.21**, there are several conclusions can be made as follows:

1. Higher molecular weight chitosan is favourable to form heavy and bulky flocs so it is more efficient as a coagulant.
2. Additional filtration process has almost similar efficiency to low-rate centrifugation and both of them can shorten the settling time and increase ENM removal efficiency.
3. Filament-like CNT-OH is easier to form bulky precipitate than small C_{60}-OH because they have more sites to interact with chitosan. Thus, size and surface treatment of ENM affect the capability of certain ENM to be removed.

4.C.III.8. Entrapment of Metal NP and Metal Oxide NP

In this study, in addition to two carbon-based ENM, we also tried the application of chitosan to remove one type of metal ENM and one type of metal oxide ENM by co-precipitation method. Similar to carbon-based ENM, concentration of chitosan was important and worth investigating. The concentration of gold NP was 5.55×10^{-4} %w/w and the concentration of chitosan was 1.61 mM and 0.16 mM so the ratio of m(chitosan):m(ENM) was 49.24 and 4.92, respectively. In the same table, the concentration of silica NP was 10^{-2} %w/w and the concentration of chitosan is similar, which is 1.61 mM and 0.16 mM so the mass ratio of m(chitosan):m(ENM) was 2.74 and 0.27. The final pH of all the solutions was 8.5±1.0.

The process of ENM removal through co-precipitation by chitosan was characterized by high removal percentage. At ratios of m(chitosan):m(ENM) of 49.24 and 4.92, both experiments on gold NP was successful to remove ENM >90% and the amount of chitosan can be lowered even further.

On the other hand, due to high concentration of silica utilized for the experiment, at ratio of m(chitosan):m(ENM) of 0.27, the removal percentage was ca. 90%. At ratio of m(chitosan):m(ENM) of 2.74, >90% of silica NP were removed. In this study, both gold NP and silica NP did not require high amount of chitosan to be entrapped >90% as was observed for C_{60}-OH due to their relatively bigger size. This result is in a good agreement with the dependence of required amount of chitosan to effectively remove ENM on ENM size in **Figure 4.19**.

4.C.III.9. Recycling of Entrapped ENM

In this study, two methods were additionally tested to recycle recovered ENM in order to sustain the availability of ENM and lower their production cost. We found that it is possible to re-solubilize the precipitate of CNT-OH – chitosan complexes by adjusting pH into acidic condition by addition of acid. However, further separation of ENM from coagulants was difficult. This result can be due to the strong interaction between chitosan and ENM.

The two methods that were applied are as follows:

1. Separation of CNT-OH and chitosan by aqueous two-phase separation, polyethylene glycol (PEG)/ magnesium sulphate ($MgSO_4$)[152] and PEG/ dextran.[153] Dissociation of the CNT-OH-chitosan complex was not achieved by this method because both ENM and chitosan was soluble in one phase and not soluble in the other phase.

2. Degradation of chitosan to recover CNT-OH by 2M of hydrochloric acid (HCl) solution or 10% of nitric acid (HNO_3). The degradation was tested by Fourier transform infrared spectroscopy (FTIR). However, complete degradation was not achieved.

4.D. Conclusion

We developed an efficient method for removal of ENM by co-precipitation with chitosan and this method is promising to be applied for ENM removal in water treatment system. In this system, adjusting pH to basic condition is an important step to precipitate chitosan which interacted with ENM beforehand to remove >90% of ENM from solution. The bigger the size of ENM, the smaller the amount of chitosan needed and vice versa, regardless of the type of ENM and the shape of ENM. Monovalent and divalent salts were shown to have the capability to induce agglomeration of ENM. The settling time required to achieve maximum ENM removal efficiency depends on the molecular weight and the availability of an additional separation process, such as filtration and centrifugation. Moreover, both filtration and centrifugation increase the removal efficiency at almost similar efficiency. This proposed method utilizes a derivative of one of the most abundant natural polymers, chitin, which is environmentally friendly, non-toxic, and commercially available. This method can be used not only in wastewater treatment, but also in drinking water treatment. Finally, recycling of the complexes is still challenging. Further development of the method to enable the recycling of the entrapped nanomaterials is a future goal toward a more sustainable use of ENM.

Chapter 5

Entrapment of Engineered Nanomaterials in Soil by Implementing Polyelectrolytes

Most of the content in this chapter is adopted and modified from paper Soenaryo, T.; Murata, S.; Zinchenko, A. Efficient Prevention of Nanomaterials Transport in the Porous Media by Treatment with Polyelectrolytes. *Chemosphere* **2018**, *210*, 567–576.[154]

5.A. Introduction to ENM and Their Contamination to Soil

5.A.I. Contamination of Soil by ENM

30% of earth are land which contains various types of porous media, such as clay, grains of sand, rock, pebbles, etc. They are mostly made of silicon dioxide/ silica, but they may contain organic chemicals and other chemicals as well. As it contains mostly silica, those porous media usually have negative charge. Thus, water and negatively-charged components tend to flow through their pores and reach ground water or other water body. On the other hand, positively-charged components tend to stick to the surface of those media.

As it was discussed in **Chapter 2**, the advancement of nanotechnologies resulted in a rapid increase in the production of engineered nanomaterials (ENM) and, nowadays, ENM are used in various consumer goods.[2,77,116] Furthermore, the market of ENM is expected to keep growing by 25% annually.[9,10] On the other hand, certain ENM can cause genotoxic and cytotoxic effects to human and animal,[20–28] plants,[27,29,30] and microorganisms.[27,31] Due to the lack of toxicological data, the regulations regarding safety and proper handling of ENM lag behind the advancement of ENM production.[13,155,156] Because there is a possibility of ENM to be released into environment during life cycle, including manufacture, use and disposal of ENM,[76,93] their accumulation in water and soil is considered to be an emergent environmental problem.[94,118,125,157,158]

As a sink for many kinds of environmental pollutants, soil will absorb contaminating ENM. Therefore, transport and accumulation of ENM in soil is being increasingly concerned.[33,34,159] According to calculation by Keller et al., there was 22,000 to 80,400 metric tons of 10 most common ENM released in a soil, with TiO_2 nanoparticles (NP) to be the most abundant ENM pollutant.[76] Natural soils have a very complex structure and behaviour[30,55,58,160–162] that results in a complex character of ENM interaction with it. Therefore, it is difficult to design suitable experimental systems to describe the fate of ENM in soil[163,164] and usually the transport of ENM in well-defined porous media, such as silica beads, quartz sands, etc. was investigated instead (**Table 5.1**). Most of these studies (**Table 5.1**) acknowledged a significant ENM transport though the porous media, but no methods have been developed so far to prevent ENM transport.

5.A.II. Application of Polyelectrolytes for Soil Remediation.

Polyelectrolytes (PE) have been extensively used in the field of environmental treatment and remediation. In particular, complexes of oppositely charged polyelectrolytes were used to prevent the erosion of contaminated soils by water or wind, such as the radionuclide-contaminated soils during Chernobyl disaster.[45–47] Being good coagulants, polyelectrolytes were also used for removal of dispersed particulates from solutions upon their precipitation. For example, methods of ENM removal by precipitation of insoluble polyelectrolyte[43] or polyelectrolyte complexes[19] showed a good efficiency in removal of dispersed ENM from aqueous solutions. Similarly, in the presence of solid-liquid interfaces, entrapment of ENM into polyelectrolyte complexes accompanied by their adsorption on a solid surface, can serve as a barrier against diffusion of ENM through a porous media. This suggests an application of PE to prevent ENM transport in soils. Herein, we propose a polyelectrolyte-based treatment method for an efficient retention of ENM in quartz sand used as a simple model of soil that can be used (i) to prevent ENM contaminants from spreading in soils as well as (ii) to locally retain the ENM that are currently used for soil remediation purposes.

Table 5.1. Comparison of the results on breakthrough of different types of ENM in various porous media.

ENM breakthrough	Type of ENM	Porous media	Transport behaviour of ENM	Ref
No or little breakthrough	Single walled carbon nanotubes (SWCNT)	Soil	The maximum depth of CNT penetration into soil was 5.5 cm	165
Significant breakthrough	Quantum dots (CdTe, CdSe), carboxylated polystyrene latex	Saturated quartz sand and loamy sand	The retention of quantum dots in quartz sand was 17-33% at 100 mM KCl concentration and almost 100% at 10 mM $CaCl_2$ concentration. The retention of NP in loamy sand was 80-90% (CdTe), 29-43% (CdSe), and 5-93% (latex NP) at 0.1 to 10 mM KCl concentrations.	64

Table 5.1. Comparison of the results on breakthrough of different types of ENM in various porous media. (Continued)

Significant breakthrough	TiO_2 NP, C_{60}	Saturated quartz sand	At pH 5, TiO_2 NP breakthrough was *ca.* 10% regardless of the presence of C_{60}, but at pH 7, the presence of C_{60} increased the breakthrough of TiO_2 up to 90% depending on the ionic strength. On the other hand, the presence of TiO_2 reduced the breakthrough of C_{60} to *ca.* 50%.	54
	TiO_2 NP	Saturated homogenous soil	In soil with large diameter particles and at low ionic strengths, significant portion of NP (19-83%) passed through the soil. Up to 37 cm depth soil penetration was found.	55
	Carbon black (CB)	Saturated natural soils	Depending on the soil type and the amount of CB, 1.9 to 81.3% of CB was found in the effluent.	66
	Ag NP	Soil	30-70% of Ag NP was found in the effluent of the soil column.	164
	Al_2O_3 NP, TiO_2 NP, SiO_2 NP	Sedimentary rocks	40-90% of NP passed through quartz sand, dolomite, and limestone. The transport characteristics depended on NP charge, medium, NP suspension stability, and roughness of the medium.	166

Table 5.1. Comparison of the results on breakthrough of different types of ENM in various porous media. (Continued)

Significant breakthrough	Al_2O_3 NP	Saturated sand	More than 90% NP breakthrough was found. The mobility and speed depended on ionic strength and NP concentration.	167
	Au NP and nanorods (NR)	Soil	More than 50% Au NP and more than 90 % of Au nanorods released from soil column. The release dated depended on the NP capping agent.	68
	Sb_2O_3 NP, TiO_2 NP	Undisturbed floodplain soil	Both Sb_2O_3 and TiO_2 penetrated deeper than 14 cm into the soil.	168

5.B. Experimental Section

5.B.I. Materials

Chemicals. Hydroxylated multi-walled carbon nanotubes (CNT-OH) of 10-20 nm diameter and 0.5-2 µm length, were purchased from Nanostructured and Amorphous Materials Inc. (USA). Hydroxylated Fullerenes (C_{60}-OH) Nanom Spectra D100 was purchased from Frontier Carbon Corporation (Japan). Poly(diallyldimethylammonium chloride) (PDADMAC) (average Mw 400,000 - 500,000, and Mw < 100,000), poly(acrylic acid) sodium salt (PAANa) (average Mw 15,000 and 1,200), sodium carboxymethyl cellulose (CMC) (average Mw 700,000), gold (III) chloride solution(30% in dilute HCl), 3- aminopropyltriethoxy-silane (99%), rhodamine-B isothiocyanate, 28% ammonium hydroxide solution were purchased from Aldrich (USA). Sodium Alginate (NaAlg) (75,000) was purchased from Funakoshi Co., Ltd. (Japan). Sodium chloride, sodium hydroxide, trisodium citrate dihydrate, coarse sand (600-850 µm diameter) were purchased from Wako Pure Chemical Industries Ltd. (Japan). Fine sand (300-500 µm diameter), cyclohexane, 1-hexanol, triton X-100, acetone, ethyl silicate were purchased from Kishida Chemical Co., Ltd (Japan). Ethanol (99.5%) was purchased from Nacalai Tesque (Japan). All the chemicals were used without further purification.

Synthesis of NP. Gold nanoparticles were synthesized by the method of Frens[81] with a slight modification. Silica nanoparticles were synthesized by the method of Shahabi et al.[78] Both of them are explained in the **Chapter 4**.

Labelling of CNT-OH. CNT-OH were labelled with fluorescein using 5-(4,6-dichlorotriazinyl)aminofluorescein (5-DTAF) reagent (Funakoshi, Japan). To 3 ml of 1.5 g/L CNT-OH dispersion, 100 µL of 0.5 M NaOH solution and 50 µL of 10 mg/L 5-DTAF solution in anhydrous DMSO were added and stirred for 1 hour. Labelled CHT-OH were purified by multiple separation by centrifugation (20,000 rpm, 30 min) and redispersion in 15 ml pure water.

Mobile phase for column experiment. Milli-Q water was purified by Advantec GSH-200 apparatus followed by purification by Merck Simplicity Millipore Water Purification System (Germany). Lake water sample was collected from Kagami Lake (Nagoya, Japan, coordinates 35°15’73”63, 136°96’36”02, pH = 7.5 (25 °C), 11 mg/L of suspended solids). Tap water sample was collected from tap water of Nagoya University.

5.B.II. Preparation of Stock Solutions

C_{60}-OH stock solutions. Stock solution of C_{60}-OH was prepared by stirring overnight 0.1 g of C_{60}-OH in 10 ml 1 wt. % NaOH solution for complete dissolution. The stock solution was further diluted 20 times before use.

CNT stock solutions. Stock solution of hydroxylated carbon nanotube (CNT-OH) was prepared similarly as the one in **Chapter 4**.

5.B.III. Methods

UV-vis spectroscopy. UV-vis spectra of ENM were recorded on a Jasco V-630 Bio spectrometer in a 1 cm × 1 cm × 5 cm quartz cell at a room temperature. The absorbance of ENM was measured at λ= 450 nm for CNT-OH, and C_{60}-OH and at λ= 525 nm for gold NP. The maximum instrumental error in measurements of ENM concentration was 0.02% for CNT-OH, 0.2% for C_{60}-OH, and 0.4% for gold NP.

Fluorescence microscopy. Fluorescence microscopy (FM) observations were performed using ECLIPSE TE2000-U (Nikon, Japan) microscope equipped with 10X lens and a Nikon DS-Ri1 digital camera (Micron Optics, USA). Digital colour pictures were processed using an image-analysis system (Nikon Eclipse 80i microscope) and NIS-Elements BR 3.1 software (Micron Optics, USA).

Zeta-potential analysis. Zeta potential of nanomaterials in aqueous solutions and at room temperature was measured using ELSZ-2000 (Otsuka Electronics Co., Ltd., Japan) particles analyser.

Fluorescence spectroscopy. Fluorescence spectra of silica NP (λ_{ex} = 530 nm, λ_{em} = 575 nm) were recorded on a Jasco FP-6600 spectrofluorimeter in a 1 cm × 1 cm × 5 cm quartz cell at a room temperature. The maximum instrumental error of the measurements was 1%.

Sodium alginate molecular weight measurement. Due to its popular use as a thickener, many manufacturers provide the viscosity of sodium alginate in cps (centipoise second) instead of molecular weight. Thus, molecular weight (M_{vis}) of sodium alginate in this study was determined through Ostwald viscometer method. In this method, sodium alginate was dissolved in 0.1 M NaCl into several concentrations. Then, the relative viscosity (η_t) was calculated as follows:

$$\eta_r = \frac{t}{t_0} \qquad \text{(eq. 7.1)}$$

Where t is the time needed for the sodium alginate solution to reach the starting line and the finish line of the Ostwald viscometer and t_0 is the time needed for the 0.1 M NaCl solution to travel the same distance.

Afterwards, specific viscosity (η_{sp}) can be calculated with following equation:

$$\eta_{sp} = \eta_r - 1 \qquad \text{(eq. 7.2)}$$

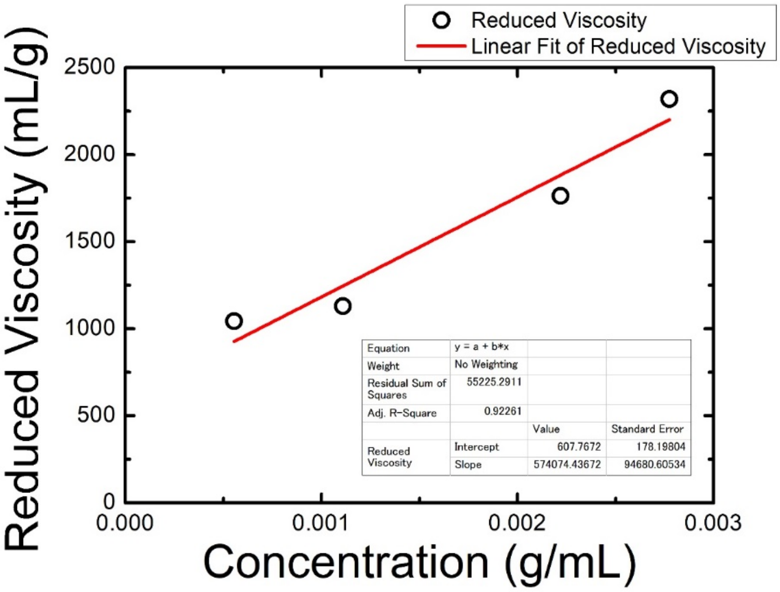

Figure 5.1. Dependence of reduced viscosity to concentration to determine the value of intrinsic viscosity of sodium alginate. The solution to dissolve sodium alginate was 0.1M NaCl.

Reduced viscosity (η_{red}) can be calculated using the following equation:

$$\eta_{red} = \frac{\eta_{sp}}{C} \qquad \text{(eq. 7.3)}$$

From the value of reduced viscosity, we determined the intrinsic viscosity ($[\eta]$) by building a graph of reduced viscosity (η_{red}) against polyelectrolyte concentration (C) and the data were extrapolated to zero concentration (**Figure 5.1**).

$$[\eta] = \left(\frac{\eta_{sp}}{C}\right)_{C \to 0} \qquad \text{(eq. 7.4)}$$

After determining the value of intrinsic viscosity, the M_{vis} was determined by following equation:

$$[\eta] = \mathrm{K}{M_{vis}}^{\alpha} \qquad \text{(eq. 7.5)}$$

Where $\mathrm{K} = 0.01228$ and $\alpha = 0.963$. Determination of these constants were adapted from previous study conducted by Mancini et al.[169,170] The result of the measurement was ca. 75,000 g/mol.

ENM column transport experiments. Quartz sand was repeatedly washed with Milli-Q water before packing columns. Milli-Q water was added to 20.5 g of quartz sand to make sand slurry. The slurry was wet-packed into a glass column with inner diameter of 18 mm and length of 285 mm which was plugged with glass cotton. The column was vibrated to let air escape from the slurry. Next, 0.3 ml of ENM solution was added onto the top surface of the column. One ml of PE solution was introduced to the sand directly after addition of ENM solution. For the control experiment, Milli-Q water was used instead of PE solution. After incubation (0 to 120 min) the water was passed through the column and the effluent (ca. 1.5 ml) was collected in microtubes. The concentration of ENM in each sample was determined by UV-vis spectrometry. In the experiments with tap water and lake water, sand slurry was made by mixing milli-Q water and sand. However, the column was flushed and filled with the corresponding water to condition the sand before adding ENM solution. The whole scheme is illustrated in **Figure 5.2.**

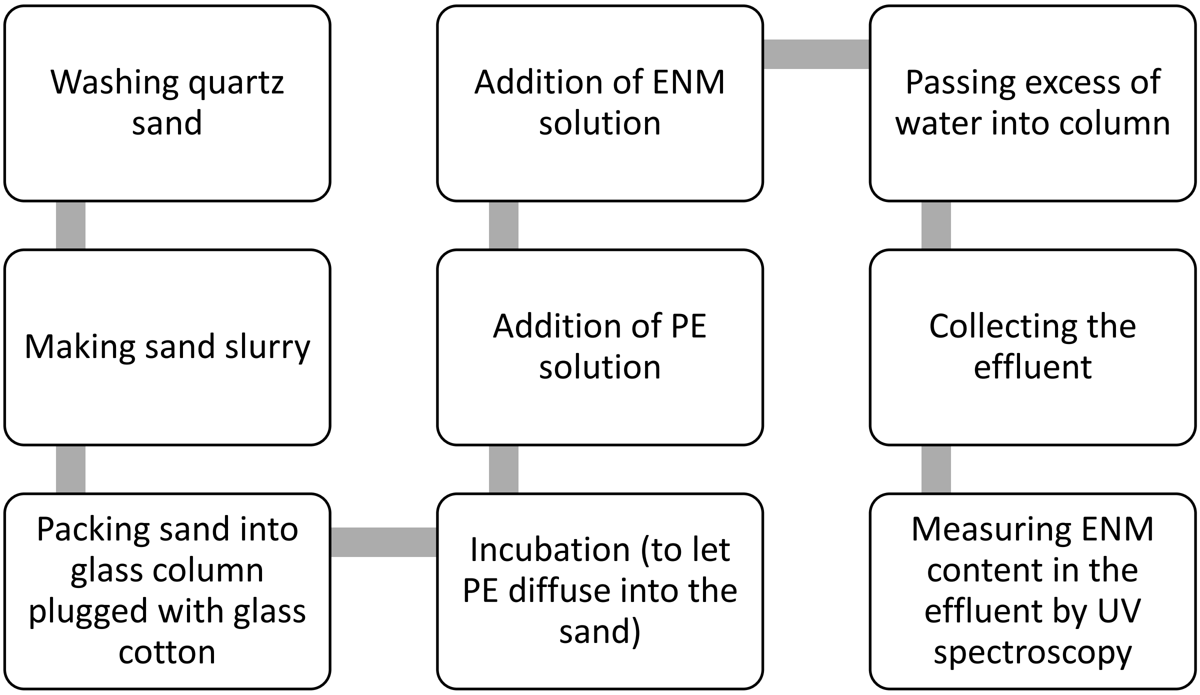

Figure 5.2. Scheme of the ENM column transport experiment.

5.C. Results and Discussion

ENM utilized in this study were the same as the ones in **Chapter 4**, which are CNT-OH, C_{60}-OH, gold NP, and silica NP. However, most of the experiments were conducted with CNT-OH with additional experiments utilizing other types of ENM at **Chapter 5.C.IX.**

5.C.I. Linearity of ENM Concentration – Absorbance Value

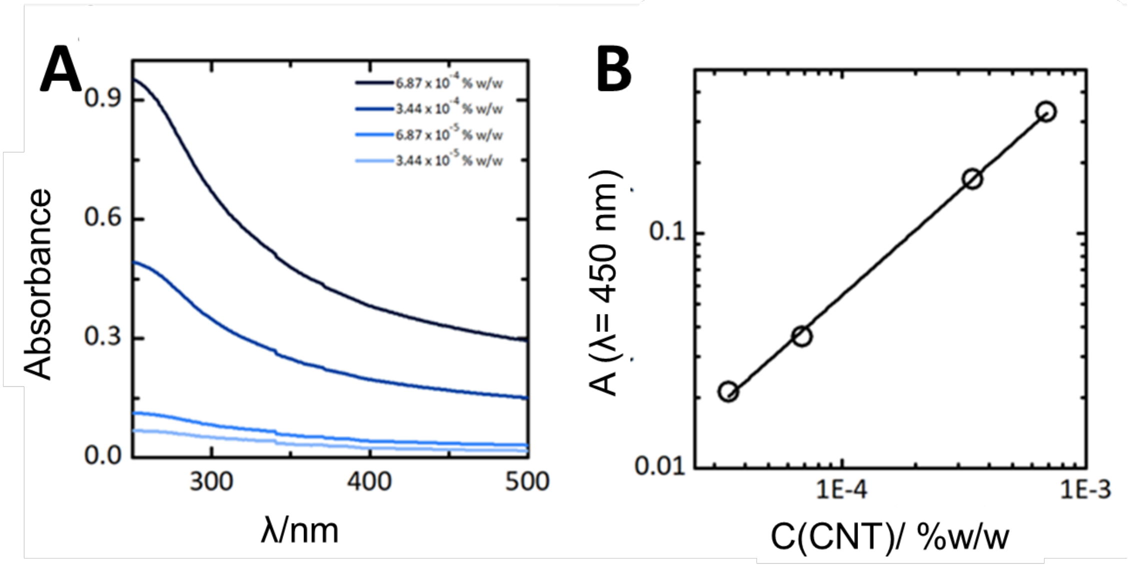

Figure 5.3.A. UV-vis spectra of CNT-OH at different CNT-OH concentrations. CNT-OH samples were prepared by consequent dilution of CNT-OH stock solution with Milli-Q water 100, 200, 1000, and 2000 times, respectively. **B.** Dependence of CNT-OH UV absorbance at λ= 450 nm on CNT-OH concentration. Concentration of CNT-OH in the original most concentrated stock solution was 6.87×10^{-2} % w/w according to gravimetric analysis.

Similar to the method utilized in **Chapter 4**, in this study we also applied UV-vis to measure the amount of ENM in the solution. The wavelengths of the absorbance spectra of UV-vis used to determine the concentration of gold NP and the emission spectra of fluorescence spectroscopy to determine the concentration of silica NP were the same as the one in **Chapter 4.C.2**.

Different from **Chapter 4.C.2**, to determine the concentration of CNT-OH and C_{60}-OH in this study, we utilized the graph of dependence of concentration of ENM on UV spectroscopy absorbance value at wavelength of 450 nm. Longer wavelength was chosen in this study because the absorbance value of polyelectrolytes (PDADMAC, NaAlg, PAANa and CMC) in the region of 400 nm and below can affect the absorbance value of the ENM which, in turn, affects the accuracy of the method.

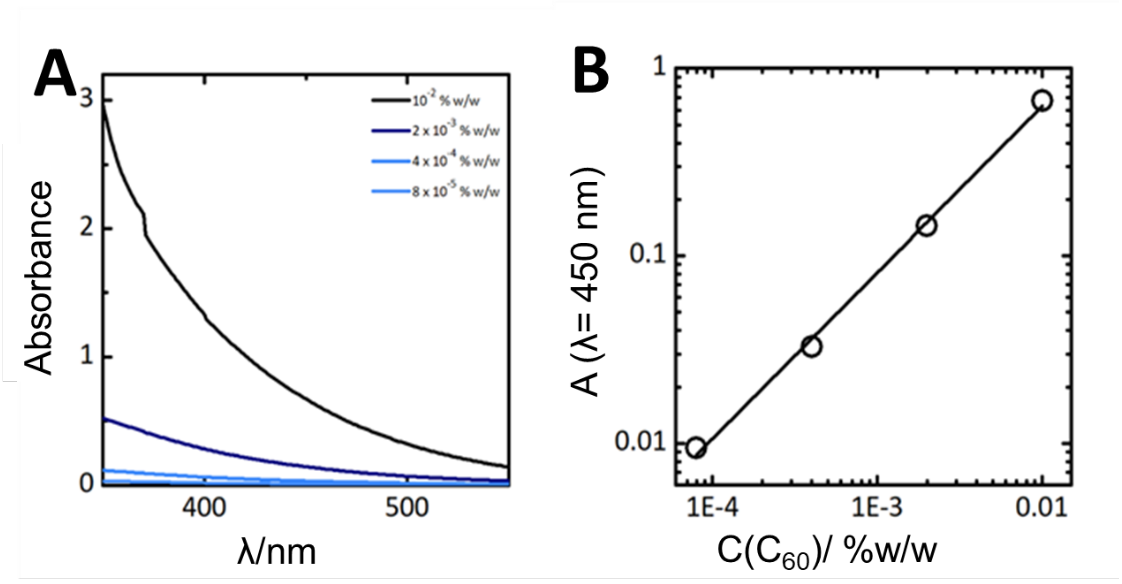

Figure 5.4.A. UV-vis spectra of C_{60}-OH at different C_{60}-OH concentrations. The samples were prepared by dissolving certain amount of C_{60}-OH into 1% w/w NaOH solution to make 0.05% stock solution which was further diluted 5, 25, 125, and 625 times, respectively, with Milli-Q water. **B.** Dependence of C_{60}-OH UV absorbance at λ= 450 nm on C_{60}-OH concentration.

In **Figure 5.3.B**, the absorbance value of CNT-OH at 450 nm is linear to the concentration of CNT-OH. Similarly, in **Figure 5.4.B**, the absorbance value of C_{60}-OH correlates linearly with the concentration of C_{60}-OH. Due to the fact that the absorbance value of UV-Vis spectra of the particular ENM is linear to their concentration, it is possible to measure the concentration of ENM in the retention from the sand column. Thus, the amount of ENM entrapped by this method can be measured and the efficiency of the IPEC method can be determined.

5.C.II. The Influence of Solution Ionic Strength to Interpolyelectrolyte Complexes (IPEC) Formation in Aqueous Solution.

Polymers of opposite charges (polycations and polyanions) can react with each other and form interpolyelectrolyte complexes (IPEC) in aqueous solution.[103,171–173] One of the examples is the polymers that were applied in this study, PDADMAC and PAANa as illustrated in **Figure 5.5.A**. Moreover, the formed complexes, charge of which is neutralized, are usually hydrophobic so that after the formation, they become insoluble in water and precipitate from solution.[19,103,106,172,173] Yet, under influence of high salt content, IPEC are not formed because the salts ion can screen the charge of the two oppositely-charged PE. Nonetheless, upon dilution of salt solution, charge screening weaken and those PE interact electrostatically and form IPEC. This phenomenon is called re-complexation (**Figure 5.5.C**).[174]

5.C.II.1. The Dependence of PE Solubility in Aqueous Solution on Salt Content

To understand the required ionic strength under which the polycations and polyanions do not form insoluble complexes, we built the phase diagram of dependence of optical transmittance of solution at wavelength of 450 nm of PDADMAC and PAANa of the same concentration on NaCl concentration. The phase diagrams can be divided into 2 regions. The low ionic strength solution was usually in the favor of insoluble precipitate formation. On the other hand, the high ionic strength was usually in favor of soluble PE solution. As shown in **Figure 5.5.B**, if the solution contained more than 0.6 M of NaCl, mixing of both of polycation and polyanion did not form IPEC because high ionic strength of NaCl was capable to effectively screen the electrostatic interaction of those two PE. In high ionic strength condition, there was no turbidity of the solution and no precipitation. However, below 0.6 M of NaCl (0.1 M < NaCl concentration < 0.6 M), IPEC could form easily. The phase diagram can be divided into 2 regions depending on the concentration of the PE. If the PE concentration was less than 0.75 M, small flocs were formed slowly, and they showed typical colloidal behavior. Thus, the solution appeared turbid. If the PE concentration was higher than 0.75 M, bulky flocs were formed and precipitated quickly. In this condition, the solution appeared as clear as the solution with high salinity and coexisted with the precipitates.

5.C.II.2. Entrapment of ENM in Porous Media by IPEC Treatment

In previous study, we successfully applied PE of opposite charges to entrap dispersed ENM in a solution through the formation of IPEC precipitates. The formed IPEC precipitates were easily separated from the mother liquid. Considering the outcome of that research, we studied the entrapment of dispersed ENM in porous media, which were quartz sand, utilizing oppositely-charged PE.

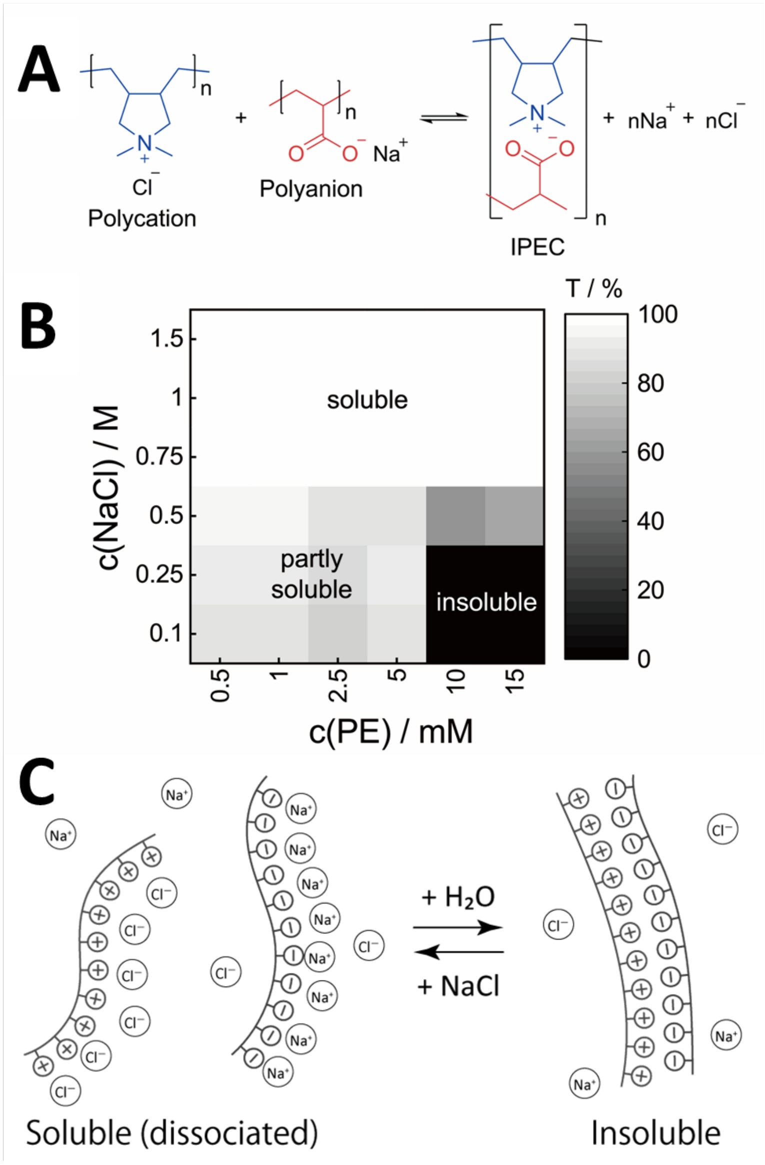

Figure 5.5. A. Formation of the interpolyelectrolyte (IPEC) complex between PDADMAC and PAANa polyelectrolytes. **B**. Phase diagram. Dependence of optical transmittance at λ = 450 nm of a solution containing an equimolar mixture of PDADMAC and PAANa on their concentration and concentration of NaCl. The transmittance of solutions was measured immediately after PE mixing by UV-vis spectroscope. The region on the phase diagram marked as “insoluble” indicates the conditions at which fast precipitation of IPEC takes place, therefore, reliable measurements of the optical transmittance cannot be performed. **C.** Re-complexation process of dissolved PE and charge screening process of oppositely-charged PE by sodium chloride salt.

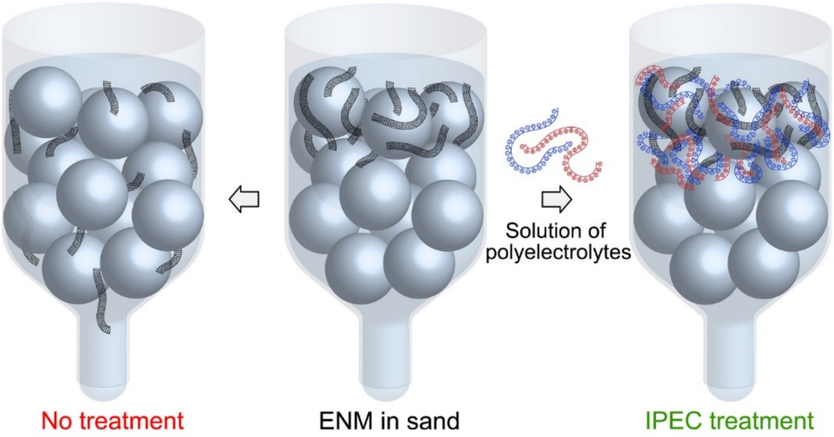

Figure 5.6. Illustration of the difference between ENM transport properties in treated and non-treated column.

To simulate the entrapment of dispersed ENM on porous media process by IPEC method, the simplest model of porous media, quartz sand particles with the size of 600 to 850 µm or 300 to 500 µm were used. The treatment process was designed so that the clear PE solution containing PDADMAC, PAANa (or other polyanion) and high concentration of NaCl (> 0.75 M) salt was applied to the wetted porous media which had been contaminated with ENM solution. On the surface of the porous media, the applied PE solution interacted with both ENM and sand particles. Furthermore, due to the decrease in salt concentration, polycation and polyanion were no longer dissolved and IPEC were formed due to electrostatic interactions. As the interaction of IPEC and ENM as well as IPEC and sand particles proceeded, IPEC promoted the adsorption of ENM on the sand grains and immobilized ENM. The process is illustrated in **Figure 5.6.**

5.C.III. Pre-treatment Aspects

To efficiently entrap ENM inside the porous media, the interaction of PE with sand grains and ENM have to be taken into consideration as an important criterion. Therefore, there are several pre-treatment aspects concerning PE solution that needs to be considered.

1. **PE solubility in a mobile phase.** As the PE needs to diffuse into the porous media and interact efficiently with both surface of sand particles as well as ENM, clear PE solution without precipitate is required for the process. Thus, the concentration of monovalent salts used to maintain high ionic strength should be high enough to prevent the formation of insoluble precipitate during mixing of the two oppositely-charged PE.
2. **Charge ratio of polycation and polyanion.** In previous study, we found that to entrap ENM effectively by IPEC method, the ratio of polycation and polyanion charges should be stoichiometric to provide PE charge neutralization.[19] Thus, in this study, to achieve maximum entrapment percentage, we analyzed the optimum charge ratio of both of polycation and polyanion by measuring the transmittance value (T) of UV vis spectra of the solution containing both PE. In a complete charge-neutralized PE solution, formation of insoluble complex results in the turbidity increase and IPEC precipitation. Thus, the point of the complete PE charge neutralization can be determined as the PE charge ratio with lowest transmittance value. The value differs between different pair of PE and is also influenced by changes in the PE solution condition such as pH. The optimum ratio of the PE pairs applied in this study in normal pH range (5 to 7) and ambient temperature is listed in **Table 5.2**.

Table 5.2. The optimum ratio of pairs of PE in ambient temperature and normal pH range (5 to 7). The concentration of PE applied in the solution is 0.67 M for the ratio of 4.

Polycation	Polyanion	Optimum Ratio
PDADMAC	PAANa	4:4
PDADMAC	NaAlg	5:4
PDADMAC	CMC	7:4

5.C.IV. The Effects of IPEC Treatment on the Mobility of CNT-OH Through Porous Media

The experiment to examine the efficiency of IPEC to entrap ENM in the porous media was conducted on a glass column packed with sand. Wet packing with vibration was applied to release the trapped gas inside the sand slurry. CNT-OH were used in most of column experiments because they can be observed easily due to their dark color appearance so that any changes to their mobility can be observed by naked eyes. **Figure 5.7** illustrates the concept of the experiment of mobility of CNT-OH without treatment **(A)** and the adsorption of CNT-OH on the sand grains promoted by IPEC **(B)**.

To measure the mobility of CNT-OH in sand column, sand slurry was added onto the glass column and it was washed with excess of water. 0.3 ml of CNT-OH with concentration of 0.62 g/L was added on the top of sand column. Afterwards, excess amount of milli-Q water was passed through the glass column and the effluent of the column was taken every 1.5 ml and analyzed to determine the amount of CNT-OH in each collected aliquot. The fact that most of CNT-OH moved out of the column in less than 15 ml of added eluent can be seen clearly.

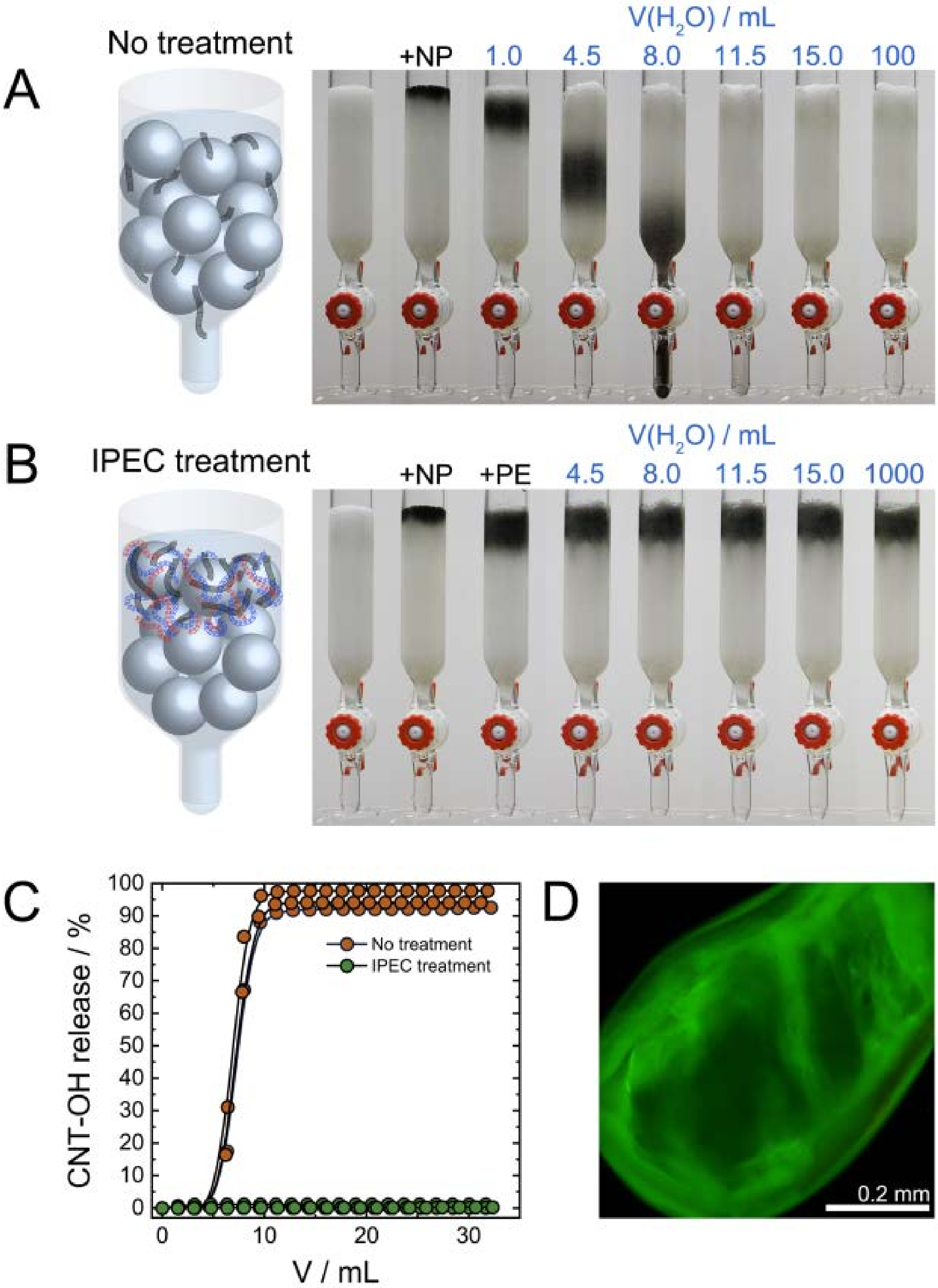

Figure 5.7. Column transport of ENM. (A-B, left) Schematics showing that CNT-OH (black) can diffuse freely through the sand column, while after treatment with a mixture of a polyanion (blue) and a polycation (red) the mobility of CNT in sand is suppressed due to entrapment of CNT-OH into IPEC complex. (A-B, right) Photographic images of 0.3 ml of CNT-OH (0.62 g/L) (black) transport through a

quartz sand column without treatment (A) and after treatment (B) by a mixture of PDADMAC and PAANa (5 mM) in 0.75 M NaCl solution. (right). (C) The corresponding retention curves of CNT-OH in the sand column before and after treatment with 1 ml solution of PDADMAC and PAANa (5 mM each) in 0.75 M NaCl. Column tests were done in triplicates for each condition. (D) Fluorescence microscopy image of a sand grain collected from the top layer of the sand column after CNT-OH deposition and treatment with IPEC. The fluorescence signal (green) is from fluorescein-labelled CNT-OH.

Further experiment was conducted to investigate the ENM entrapment in sand column after IPEC treatment. Similar to the ENM mobility experiment, 0.3 ml of CNT-OH with concentration of 0.62 g/L was added on the top of sand column. For treatment, instead of milli-Q water, 1.0 ml of PE solution containing both PDADMAC and PAANa with concentration of 5 mM (total weight of both PE is 1.28 mg) dissolved in solution containing 0.75 M NaCl was added on the top of sand column. To ensure the completeness of the interaction between IPEC, ENM, and grains of porous media, one hour of incubation time was performed. The effect of incubation time is discussed **Chapter 5.C.V.1**. Afterwards, excess amount of water was added into the glass column and the effluent was collected every 1.5 ml. The concentration of CNT-OH in the effluent samples were measured by UV-Vis spectroscopy at the wavelength of 450 nm. In contrast with the flow of CNT-OH in untreated sand column, CNT-OH in the treated sand column remained at the same position even after addition of 1000 ml of milli-Q water (**Figure 5.7.B**)

The amount of CNT-OH that passed through the column experiment was determined by measuring ENM concentration in the effluent, which was divided into several 1.5-ml samples, with UV-Vis spectroscopy at wavelength of 450 nm. The absorbance value at λ= 450 nm was measured because the absorbance value at 450 nm wavelength correlates linearly with CNT-OH concentration as shown in **Figure 5.3.B**. In addition, the absorbance of PE did not affect the ENM absorbance in the region >450 nm. The results of the measurement of both column experiments with and without IPEC treatment is shown in **Figure 5.7.C.** In **Figure 5.7.C,** the cumulative amount of CNT-OH released from the glass column is represented as a function of amount of water passing through the column. **Figure 5.7.C orange dots** represent the flow of CNT-OH passing through the untreated sand and **Figure 5.7.C green dots** represent the flow of CNT-OH passing through the IPEC-treated sand. Both experiments were conducted 3 times and all the measurement of the amount of CNT-OH breaking through the sand column without treatment showed >90 % release during the first 10 ml. In contrast, the measurement of the amount of CNT-OH breaking through the IPEC-treated sand column was less than 1 % release even after the first 30 ml of effluent. The results are in agreement with our hypothesis which was illustrated in **Figure 5.7.A and B** for untreated sand and IPEC-treated sand, respectively.

To understand whether CNT-OH attached to sand due to IPEC treatment or simple ENM aggregation process, the IPEC-treated sand grains on top of column which contained adsorbed dye-doped fluorescent CNT-OH was taken and observed under fluorescence microscopy. The image of the sample is shown in **Figure 5.7.D**. As shown in that the image the whole sand particle was shining with green fluorescence light which comes from fluorescein-labelled CNT-OH. Since IPEC solution was applied to the upper layer of the sand column, both sand grains and ENM were interacting with PE. After the formation of IPEC, the ENM were attached to the sand and could not move so the ENM were distributed evenly on the surface of the sand grain. In-depth discussion is provided on the **Chapter 5.C.X**.

In the experiment above, CNT-OH was covalently labeled with dye to enable ENM visualization under fluorescence microscope. In general, dye doping can affect the properties of the surface where the dye is attached to. Nevertheless, the concentration of the dye was relatively small (max. 2.25×10^{-7} % w/w) compared to CNT-OH (0.062 % w/w) or less than 10^{-3} % of the total amount of CNT-OH. Therefore, the change is considered scarce and negligible.

In the IPEC-assisted CNT-OH adsorption on the sand, there are 2 main phenomena that took effect. The first one is the agglomeration of CNT-OH by the PE through the formation of water-insoluble IPEC. The phenomenon was observed in our previous study in which addition of oppositely-charged PE into ENM solution assisted ENM entrapment into PE. Afterwards, due to the charge neutralization of PE of opposite charge, the polyelectrolyte complex becomes insoluble in the solution and precipitate together with ENM.[19] The second process is the adsorption of IPEC on the surface of sand grains. The phenomenon was studied in the past by Russian researchers to prevent the erosion of radioactive-nuclide-contaminated soil which was the result of Chernobyl nuclear disaster in 1986. Due to IPEC treatment of the soil, it was found that the soil can be stabilized against erosion by water and wind.[45–47] As the result of the interplay of two above processes, the entrapped CNT-OH are immobilized by IPEC on the surface of each sand grain effectively.

The IPEC treatment that caused CNT-OH attachment to the surface of the sand is the efficient method to not only localize contamination of CNT-OH, but also hinder the flow of the upcoming CNT-OH. For instance, after the IPEC-treatment process, large amount (0.93 mg) of CNT-OH was newly added into the column and ca. 43.5% of that CNT-OH could be entrapped on the sand. Hence, 1 gram of IPEC is capable to entrap more than 3 grams of CNT-OH. The capacity of IPEC to adsorb post-introduced CNT-OH depends on a number of factors, such as concentration of PE, salt concentration, etc. which are discussed in the following section.

5.C.V. Factors Affecting Entrapment Process

In the entrapment process, not only pre-treatment factors affect the efficiency of the treatment, but also some factors during the treatment can determine the percentage of ENM that can be adsorbed on the surface of sand. The factors that are important to be considered during treatment are as follows:

5.C.V.1. Incubation Time

After addition of PE solution on the top of the sand pack, an incubation time was required before eluting the column with excess amount of water. Incubation time is an important factor of the process to ensure the diffusion of PE solution into porous media, interaction between PE solution and either CNT-OH or sand particles, and formation of IPEC to entrap CNT-OH on the sand surface. As shown in **Figure 5.8**, the shortest time needed in the case of 1 ml of 0.5 mM PDADMAC-PAANa pairs in 0.75 M NaCl to entrap 0.3 ml of 0.62 g/L CNT-OH stock solution on 300 – 500 µm sand grains effectively was 15 minutes. Without incubation time, there was ca. 6% of CNT-OH that broke through the IPEC-treated column. In this experiment, 60 minutes were used as the standard incubation time which is significantly longer than the shortest time, 15 minutes, to ensure that the incubation time is sufficient to any kinds of PE as well as any kinds of contaminating ENM.

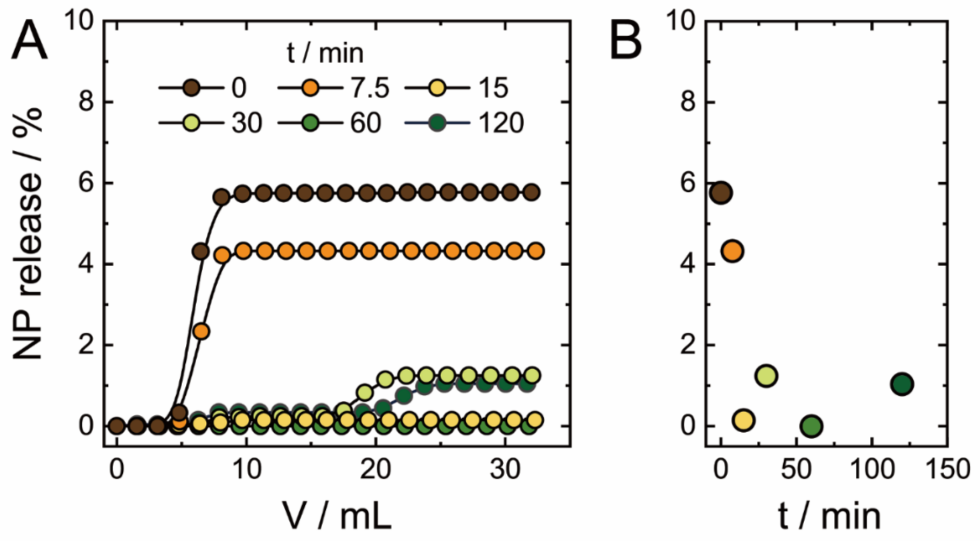

Figure 5.8. Effect of incubation time. (**A**) Retention curves of CNT-OH in the sand column at different incubation times after treatment with PDADMAC and PAANa (0.5 mM) in 0.75 M NaCl and (**B**) the dependence of the total CNT-OH escape from the sand column at different incubations times. The grain diameter was 300 – 500 µm.

5.C.V.2. Solution Ionic Strength

As explained in **Chapter 4.C.III.2**, colloidal stability of ENM is affected by the presence of monovalent and divalent cation. Interaction between ENM and salt may induce aggregation of ENM.[146,175,176] To maintain the solubility of PE solution, high concentration of NaCl (1.0 ml 0.75 M) was used. Thus, there is a possibility that NaCl in the PE solution induced aggregation of CNT-OH which affected the adsorption of CNT-OH on the surface of sand grains. To understand the influence of salts on the CNT-OH entrapment process, CNT-OH transport through the column treated with monovalent (NaCl) and divalent ($MgCl_2$) salt was compared with the CNT-OH transport through untreated sand column (**Figure 5.9.A**).

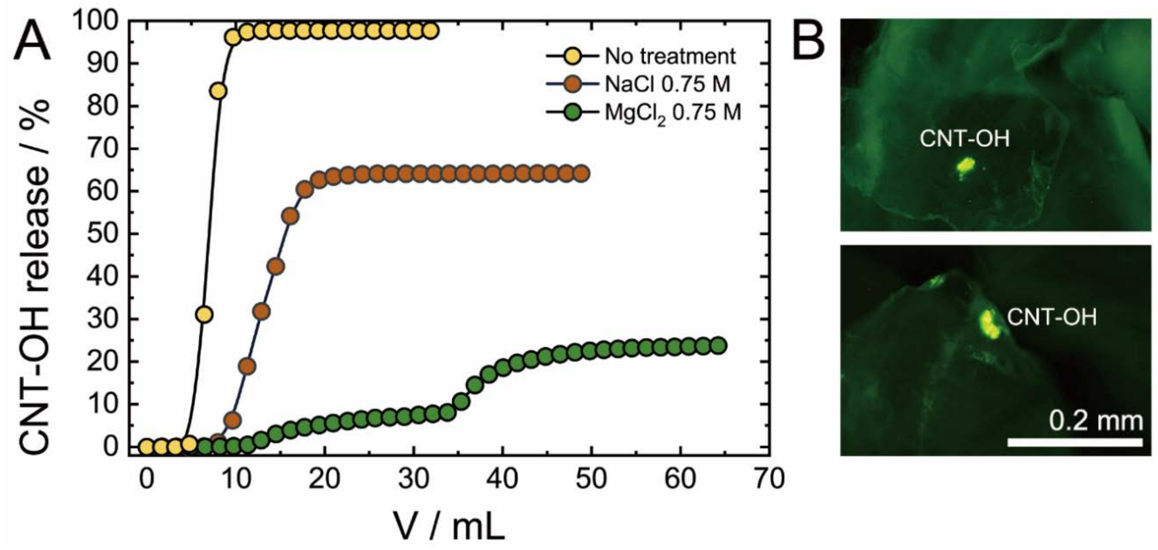

Figure 5.9. Salt effect on ENM transport. (A) Retention curves of CNT-OH in the sand column after treatment pure water, 0.75 M NaCl, and 0.75 mM $MgCl_2$. (B) Fluorescence microscopy image of a sand grain collected from the top layer of the sand column after CNT-OH deposition and treatment with 0.75 M NaCl (upper) and $MgCl_2$ (bottom). The fluorescence signal is from fluorescein-labelled CNT-OH.

As represented in **Figure 5.9.A**, compared to the transport of CNT-OH breakthrough from untreated sand column, addition of salt did hamper the transport of CNT-OH in sand column. In the same figure, the graph of cumulative CNT-OH released from the column shifted to the right and almost 20 ml (2-fold of the required amount of water to wash CNT-OH away from the untreated sand column) of milli-Q water was applied to wash CNT-OH until there was no more CNT-OH released from the column. In addition, the transport of CNT-OH in the sand column treated with 0.75 M NaCl only solution did not reach >90 % release of CNT-OH and ca. 30% of CNT-OH were still left inside the sand column. **Figure 5.9.B, upper Figure** shows the FM image of dye-doped CNT-OH trapped by NaCl treatment. In this figure, slight aggregation of CNT-OH can be seen. Since NaCl was present in all PE solution to screen the electrostatic interaction between polyanion and polycation applied, CNT-OH treated with IPEC solution were trapped in the aggregated form.

In **Figure 5.9.A**, graph of cumulative CNT-OH breakthrough treated with divalent cation (0.75 M of $MgCl_2$) is shown. The graph shows that $MgCl_2$ hampered the flow of CNT-OH stronger than NaCl. In sand column treated with $MgCl_2$ solution, large amount of water was applied to wash CNT-OH and the mobility of CNT-OH through the sand column was drastically slow. Furthermore, the maximum amount of CNT-OH that went out of the glass column after the treatment was ca. 30%. Thus, more than 60% of CNT-OH was trapped inside the sand column. In **Figure 5.9.B bottom image**, the heavy aggregation of CNT-OH treated with $MgCl_2$ is shown. The size of the aggregates was ca. 10 µm. Compared with even distribution of CNT-OH on the surface of the sand grain treated by IPEC in **Figure 5.7.D**, the **Figure 5.9.B** shows that the distribution of CNT-OH was uneven and CNT-OH is immobilized on sand grain surface in form of aggregates.

Unlike the flow of CNT-OH in untreated sand column, the flow of CNT-OH solution treated with $MgCl_2$ salt shows an upward slope of the CNT-OH breakthrough. Hence, the release of CNT-OH after treatment with $MgCl_2$ solution was due to slow gradual degradation of CNT-OH aggregates. The phenomenon was resulted from the dilution of $MgCl_2$ caused by addition of excess milli-Q water. At the same concentration of salt (0.75 M), the retained amount of CNT-OH due to $MgCl_2$ treatment was less than half of retention of CNT-OH by NaCl treatment (ca. 65 %). Thus, it can be concluded that divalent ions cause greater aggregation than monovalent ion as discussed in previous chapter (**Chapter 4.C.III.2**).[43] Since natural water contains both monovalent and divalent ion, it is expected that the natural water can assist the entrapment of ENM in soil.

5.C.V.3. Polymer Concentration

The entrapment of ENM on the surface of sand by IPEC treatment relies on the interaction between ENM and PE as well as PE and sand particles. The amount of PE in the solution as well as the polymer length (molecular weight) may affect the adsorption of ENM on sand grains. Thus, the influence of the above parameters was examined.

Figure 5.10 shows the retention percentage of CNT-OH on sand after treatment with various PE concentrations (5 mM to 0.05 µM) in the solution. In the general protocol, 1 ml solution containing 5 mM PE was utilized and it was found that almost all CNT-OH was affixed to the surface of the grains. The same result was obtained by utilizing the same PE solution diluted by 10 times to 0.5 mM. However, further dilution by 10 times to 0.05 mM reduced the efficiency by ca. 15%. Not only the efficiency decreased, but also the deviation of the result was wider in this concentration which showed that the amount of polymers was no longer enough to provide efficient interaction of IPEC with sand surface. Further dilution by 10 times to polymer concentration of 5 µM dramatically dropped the process efficiency by ca. 65% compared with the general protocol. The CNT-OH retention profile of CNT-OH treated with PE on this concentration resembles the CNT-OH retention profile of CNT-OH treated with 0.75 M NaCl shown in **Figure 5.9**. Therefore, in dilute concentration, IPEC could not form well due to the difficulty for both PE of opposite charge to interact with each other.

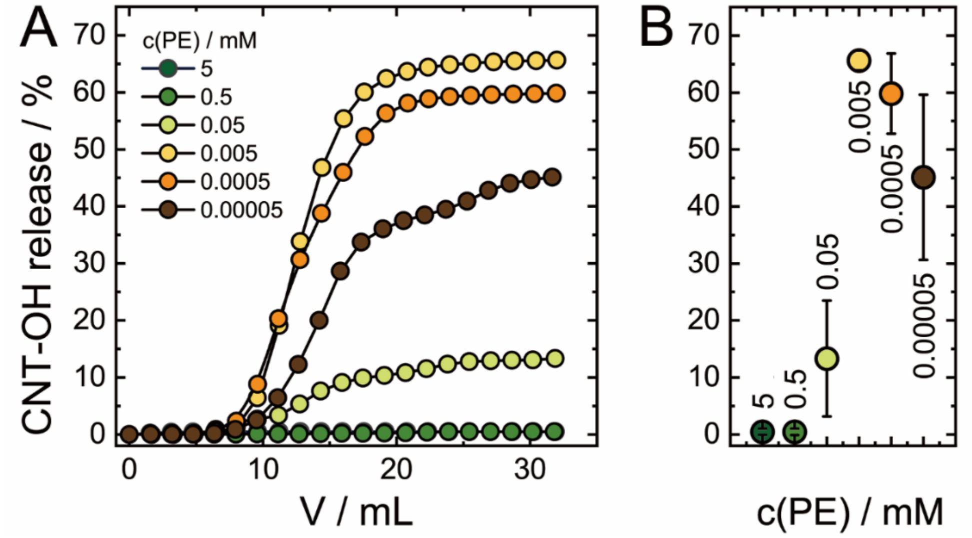

Figure 5.10. PE concentration effect on ENM release. **(A)** Retention curves of CNT-OH in the sand column after treatment with different concentrations of PDADMAC and PAANa in 0.75 NaCl solution. **(B)** The dependence of the total CNT-OH escape from the sand column as a function of PE concentrations. The error bars indicate the standard deviations from the average values CNT-OH cumulative release in three column runs.

From PE concentration of 5 mM to 5 µM, the CNT-OH retention in the sand column kept decreasing and treatment by 5 µM PE solution resulted in the lowest CNT-OH retention percentage as shown in **Figure 5.10**. Further dilution of PE solution concentration did not decrease the retention of CNT-OH percentage. On the contrary, further dilution by 10 times to 0.5 µM and 100 times to 0.05 µM showed better retention of CNT-OH than for 5 µM. At this extremely low concentration, we speculate that the retention process was different than the retention process at higher concentration in where the PE interacted with CNT-OH and sand particles and formed IPEC to assist in adsorption of CNT-OH on sand. In low concentration, PE may act similar to normal salt and induce aggregation of CNT-OH. After the aggregation process, CNT-OH are more difficult to transport through the pores due to their larger size. In contrast to general protocol, the treatment utilizing less than 0.5 µM PE concentration was poorly reproduced and the deviation shown in **Figure 5.10** for cumulative CNT-OH breakthrough graph for treatment with PE concentration of 0.5 and 0.05 µM was wide. The slow release shown in the retention profile for the treatment by 0.05 µM PE solution can be due to the dissociation of CNT-OH aggregates due to dilution by excess water. Therefore, the minimum PE concentration to achieve the highest CNT-OH retention capability in sand column by utilizing IPEC method was 0.5 mM.

5.C.V.4. PE Molecular Weight

As studied in the previous research (**Chapter 4.C.III.7.**), higher molecular weight of PE required less settling time because long polymers are easier to form bulky precipitate. Even though the conclusion may be different, the fact that molecular weight was one of the important factors that determine the formation of IPEC is applicable in both treatments.[174] Thus, in this research, we studied the dependence of CNT-OH treatment efficiency on molecular weight

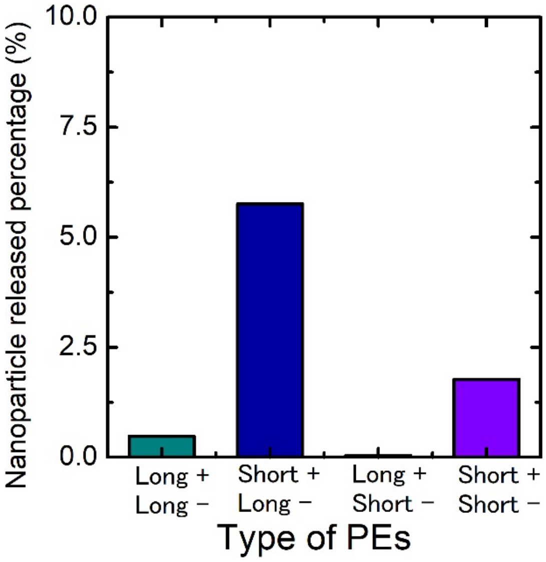

Figure 5.11. PE (PDADMAC and PAANa) molecular weight (polymer length) effect to entrapment of CNT-OH percentage. All PE concentration is 0.5 mM. + refers to polycation which is PDADMAC and – refers to

polyanion which is PAANa. Long + is PDADMAC with Mw 400,000-500,000, Long - is PAANa with Mw 15,000, Short + is PDADMAC with Mw <100,000, Short - is PAANa with Mw 1,200.

In **Figure 5.11**, the amount of CNT-OH released from the sand column treated with pairs of PE with different molecular weight is shown. Treatment by each solution containing PE resulted in more than 90% adsorption on the sand grains surface. However, there was one pair which had more than 5% CNT-OH broken through the treated sand column which was low-Mw PDADMAC and high-Mw PAANa. Even though, all of the PE pairs in **Figure 5.11** showed high CNT-OH entrapment efficiency, there is a tendency that high-Mw PDADMAC produced better entrapment compared with low-Mw PDADMAC. On the other hand, if high-Mw PAANa and low-Mw PAANa were compared, there is a tendency that low-Mw PAANa shows better result. The reasons can be because PDADMAC interacts with both negatively-charged CNT-OH and surface of sand so high Mw of PDADMAC which can provide more areas to interact are better. In contrast, PAANa interacted with PDADMAC to produce IPEC so PAANa with higher Mw may hinder the interaction due to steric effects. Thus, shorter (low-M_w) PAANa is easier to form IPEC.

In the beginning of **Chapter 5.C.IV.**, we mentioned that IPEC can treat immediate contamination of CNT-OH as well as consequent contamination. In this study, we investigated the dependence of the capacity of the PE to entrap CNT-OH added after the treatment on polymer concentration and polymer molecular weight. As shown in **Figure 5.12**, the polymer concentration correlated linearly with the amount of adsorbed newly-added CNT-OH. Out of 0.93 mg of newly-added CNT-OH, 0.87 mg were adsorbed on 5 mM PE solution-treated sand column, 0.4 mg were adsorbed by 0.5 mM PE solution-treated sand column, less than 0.1 mg were adsorbed by 0.05 mM PE solution-treated sand column. The higher the concentration, the higher the available PE sites that can adsorb additional CNT-OH. In contrast, there was no difference of the amount of adsorbed newly-added CNT-OH due to difference in PE molecular weight (0.5 mM solution concentration was capable to entrap additional ca. 0.4 mg of newly-added CNT-OH). In conclusion, only polymer concentration determines the amount of the newly-added CNT-OH that can be adsorbed.

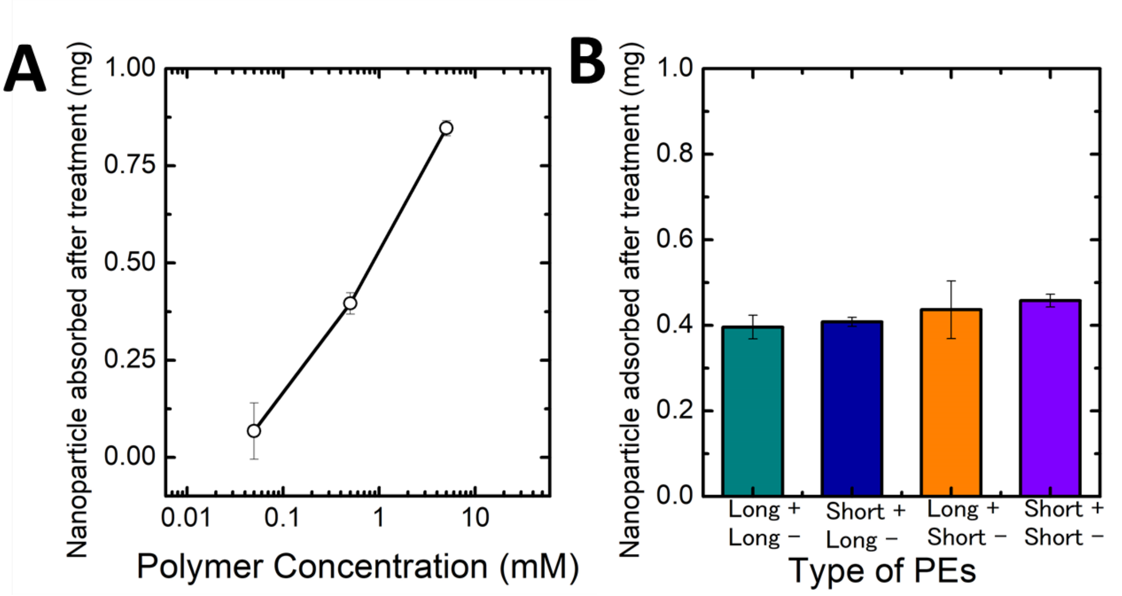

Figure 5.12. Additional CNT-OH that could be adsorbed after treatment by adding 0.93 mg (5 times the amount of CNT-OH applied in general protocol) by the formed IPEC of different polymer concentration (**A**) or different molecular weight (**B**). In **A**, the PE pairs were PDADMAC with Mw 400,000-500,000 and PAANa with Mw 15,000. In **B**, all PE concentration is 0.5 mM. + means polycation which is PDADMAC and – means polyanion which is PAANa. Long + is PDADMAC with Mw 400,000-500,000, Long - is PAANa with Mw 15,000, Short + is PDADMAC with Mw <100,000, Short - is PAANa with Mw 1,200.

5.C.VI. Effect of the Chemical Structure of Polyelectrolytes on the Entrapment of ENM on Sand

Because IPEC are not limited to one single pair of PE, there are many possible PE pairs that can be applied to entrap CNT-OH in sand column. However, not all PE can be applied in the same manner as PDADMAC and PAANa, such as chitosan. Chitosan which was studied in **Chapter 4** cannot be applied in the entrapment of CNT-OH in sand column because chitosan precipitates upon addition of salt. Thus, we investigated several other PE combinations that can be implemented for entrapment of CNT-OH in sand column. Besides PDADMAC and PAANa, PDADMAC and CMC pair as well as PDADMAC and NaAlg pair were investigated.

Figure 5.13 shows the amount of CNT-OH broken through the sand column during treatment with different pairs of PE as well as the capacity of the PE to adsorb newly-added CNT-OH. The ratio between different pairs of PE was adjusted according to **Table 5.2** to ensure complete charge neutralization of the PE which is an important requirement of the entrapment process. In **Figure 5.13.A**, all PE pairs showed almost similar result, i.e. ca. 98% retention of CNT-OH. Furthermore, the amount of the adsorbed newly-added CNT-OH was similar which was ca. 0.4 mg out of 0.93 mg of newly-added CNT-OH after the treatment process (**Figure 5.13.B**). The result suggests that polyanion of the IPEC is interchangeable without lowering the CNT-OH entrapment efficiency.

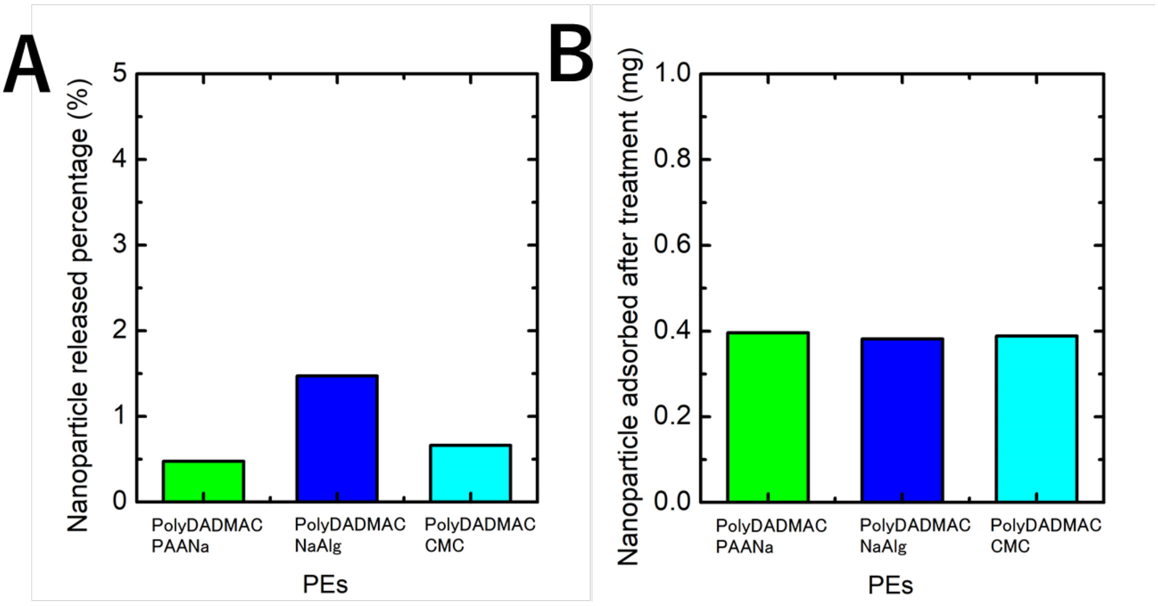

Figure 5.13.A. The entrapment percentage of CNT-OH by different pairs of IPEC. **B.** Additional CNT-OH that could be adsorbed after treatment by adding 0.93 mg (5 times the amount of CNT-OH applied in general protocol) by the formed IPEC with different polyanion. In **B**, the PDADMAC-PAANa pairs were PDADMAC with Mw 400,000-500,000 and PAANa with Mw 15,000 or CMC with Mw 700,000 or NaAlg with Mw 75,000. The PE concentrations were 0.5 mM for both PDADMAC-PAANa, 0.5 mM PDADMAC - 0.4 mM CMC, and 0.5 mM PDADMAC and 0.31 mM of NaAlg.

5.C.VII. CNT-OH Transport in Columns with Different Sand Grain Size

In this study, two kinds of quartz sand with different grain size were used as the stationary phase in column experiment. The small-sized sand was used in most of the experiments and its diameter was 300 – 500 µm. The large-sized sand had the diameter of 600 – 850 µm. In the experiment using the large-sized sand, the amount of the sand was twice of that used in the general protocol so that the height of the sand in the glass column was twice than the height of the sand in the glass column used in the general protocol. **Figure 5.14.A** illustrates the CNT-OH transport in untreated and IPEC-treated large-sized sand and **Figure 5.14.B** shows the cumulative amount of CNT-OH that could break through the column of untreated and IPEC-treated large-sized sand and small-sized sand. As shown in **Figure 5.14.A**, compared to the flow of CNT-OH in small-sized sand (**Figure 5.7.C**), the speed of CNT-OH release from the column containing untreated large-sized sand was faster. Even though the height of the large-sized sand column was twice than the small-sized sand column, the volumes of eluent corresponding to the beginning and the end of CNT-OH release were similar. The reason for the higher speed of the transport was larger pores in the column packed with sand particles of larger diameter. Hence, the space between the sand particles were bigger, so that the physical straining of CNT-OH by the sand particles was less effective.

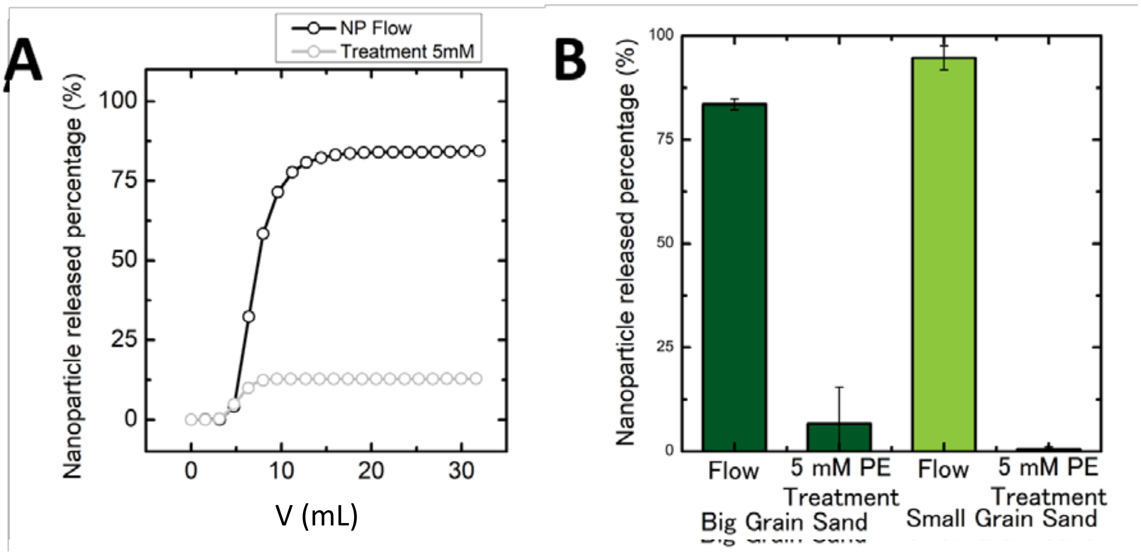

Figure 5.14.A. The flow of CNT-OH through quartz sand with grain diameter of 600 – 850 µm (black) and the flow after being treated with 5 mM solution of PDADMAC with 400,000<Mw< 500,000 and PAANa with Mw of 15,000. The amount of the sand used was 43.0 g. **B.** The comparison of the percentage of CNT-OH flown out of column through sand grain with grain diameter of 600 – 850 µm (dark green) and 300 – 500 µm (light green) with or without IPEC treatment.

Even though CNT-OH can flow through both small-sized sand and large-sized sand, more than 10% of CNT-OH was entrapped in untreated large-sized sand column (**Figure 5.14 A and B**).

The inability of CNT-OH to break through of the sand column can correlate with the condition of the surface of the large-sized sand.

Even though ca. 10% of CNT-OH were entrapped in the untreated large-sized sand column, the CNT-OH entrapment by IPEC method on the sand resulted in ca. 10% of CNT-OH released from the column. Compared to breakthrough rate of CNT-OH in the IPEC-treated small-sized sand column which was less than 5%, the treatment on the large-sized sand column was ineffective. The high breakthrough rate could be related to the fact that the pore size of the sand was so large that PE had difficulty to interact with both CNT-OH and sand particles. Thus, the formed IPEC did not entrapped CNT-OH efficiently. It can be concluded that there is a limit of sand grain size at which the ENM entrapment by IPEC method can be efficient. Nevertheless, most natural soil contains various components with different grain sizes, so the porosity of soil is relatively small. Therefore, IPEC method should be efficient in natural environment.

5.C.VIII. Application of Entrapment Process with Natural Water as the Mobile Phase in the Column

Water around us, such as tap and lake water, contains salts and other organic matters which may affect the colloidal stability of ENM.[146,175,176] Thus, it is important to understand the impact of eluent type on the performance of the entrapment of CNT-OH process by IPEC method. In this study, three types of water with different salt concentration and amount of organic matter were used as eluent for the column experiment. Those types of water are: milli-Q water which contains no organic matter and salt ionic strength, tap water which contains small amount of salt and organic matter, and lake water which contains high concentration of salt and natural organic matter. The packing of the sand was conducted in the same way as in the general protocol, but the wet-packed sand was conditioned by washing them with the corresponding eluent before CNT-OH was added on the top of the sand column.

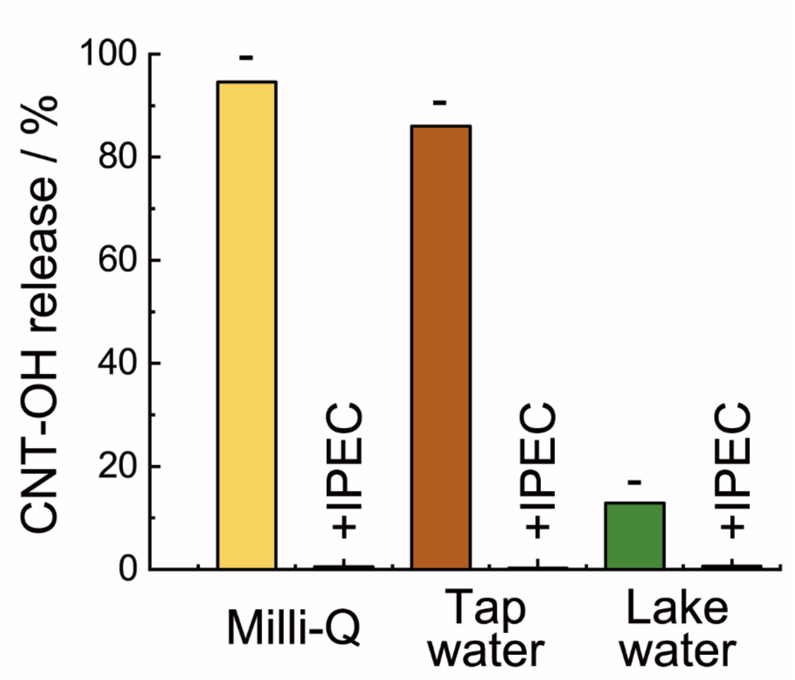

Figure 5.15. Effect of eluent on CNT-OH transport. Release percentages of CNT-OH from quartz sand column for different types of eluents before (−) and after treatment (+IPEC) by PDADMAC and PAANa (0.5 mM) in 0.75 NaCl solution.

Figure 5.15 shows the cumulative amount of CNT-OH released through IPEC-treated or untreated small-sized sand column using different type of eluent. As shown in **Figure 5.15**, the breakthrough of CNT-OH in the untreated sand column with milli-Q water was ca. 95% and this value decreased by 10% upon changing the eluent to tap water. If the eluent was changed to lake water, there was a considerable decrease to ca. 13% of CNT-OH breakthrough (or ca. 80% of CNT-OH retention). This tendency is in agreement with the CNT-OH transport in salt-treated sand column in **Figure 5.9**. Due to high salinity of lake water, CNT-OH aggregated and were blocked by the sand particles. On the other hand, changing the eluent to tap water did not result in a large difference which might be due to low salinity of tap water as well. In **Figure 5.15**, after the treatment by 0.5 mM PE, almost no CNT-OH were found to be broken through the sand column. Thus, the treatment is effective regardless of the type of eluent flowing through the sand column and the result implies that this treatment can be applied in nature.

5.C.IX. Entrapment of Other Types of ENM by IPEC Method

There are various types of ENM that are currently being used in various daily products and with 25% growth of ENM production, those ENM will contribute to the contamination of land and water in a progressive manner.[76] To test the universality of the entrapment process, it is essential to check the capability of IPEC method to entrap other types of ENM in the sand column. In current study, we used silica dioxide as a representative of the ceramic ENM (oxide NP), fullerene as a representative of small-sized ENM and gold NP as a representative of the metal ENM.

Table 5.3 summarizes all the diameter data of all NP (CNT-OH, C_{60}-OH, Au NP and SiO_2 NP), as well as their zeta potential, concentration of stock solution, and the breakthrough percentage through IPEC-treated or untreated 300 – 500 µm sand column. As shown in the diameter column of each ENM, the size observed by TEM was smaller than the size that were acquired by Dynamic Light Scattering (DLS) observation. Since the diameter observed by TEM was a single particle size and the diameter observed through DLS was the size of the particle in solution, the difference in size observed by two different instruments points to the aggregation of ENM in solution.

Table 5.3. Morphological and hydrodynamic characteristics of ENM used in column experiments, ENM concentrations in stock solutions, and ENM release percentages before and after treatment of quartz sand columns with PDADMAC (5 mM) and PAANa (5 mM) solution in 0.75 M NaCl. Milli-Q water was used as an eluent for all experiments. The error of ENM release percentage is a standard deviation from the average value obtained in three independent experiments.

ENM	Size and charge	c(ENM) g/L	Release / % (no IPEC)	Release/ % (+ IPEC)
CNT-OH	d = 50 ± 13 nm (DLS) $\xi = -19$ mV[a]	0.62	94.6 ± 2.9	0.5 ± 0.6
C_{60}-OH	d = 6 ± 1 nm (DLS) $\xi = -39.6$ mV[b]	0.46	91.0 ± 12.0	10.5 ± 7.2
Au NP	d = 27.5 ± 10.5 (TEM), d = 40 ± 25 nm (DLS) $\xi = -46$ mV[c]	0.057	80.4 ± 8.5	0.3 ± 0.6
SiO_2	d = 56.3 ± 4.2 (TEM), d = 102 ± 46(DLS) $\xi = -32$ mV[d]	3.1	84.6 ± 1.3	<1[e]

[a]Milli-Q water, pH 3.9; [b]0.01% NaOH solution; pH 11, [c]0.1% sodium citrate solution; pH 7; [d]Milli-Q water, pH 9.3; [e] the standard deviation value is smaller than the instrumental error.

All NP showed a high release percentage (80-90% release) which was due to the repulsive interaction between NP and like-charged sand grains. The repulsive interaction was caused by the negativity of the surface of both NP and sand grains. Nonetheless, carbon-based NP had >90% release, meanwhile, SiO_2 and Au NP had >80% release. The fact that carbon-based NP showed higher release compared to the Au NP and SiO_2 NP might be ascribed to the difference in surface properties of each NP. Carbon-based NP were grafted with hydroxylated functional group to make it more soluble in water. On the other hand, Au NP were capped with citrate and SiO_2 NP were capped with Triton X-100. We speculate that those capping agents can be destabilized upon dilution with water in the column so that some NP aggregated and were entrapped in the column.

In the release percentage column of IPEC-treated sand column experiment, except C_{60}-OH, the other NP were entrapped efficiently by 5 mM of PDADMAC-PAANa solution. The less efficient C_{60}-OH entrapment percentage is because C_{60}-OH size is infinitesimal so that the active area to contact with PE is limited compared to the other NP. Therefore, it was more difficult for the PE pairs to adsorb C_{60}-OH which resulted in reduced entrapment ratios by ca. 10%. This result is consistent with the results described in **Chapter 4.C.III.5.** However, CNT-OH, Au NP and SiO_2 NP had a very high percentage of entrapment in the sand column. The result clearly demonstrates the universality of the method towards different classes of ENM.

Even though various ENM can be entrapped using this method, we tried to entrap carbon dots, several NP carbon clusters, in the same manner. However, in contrast to other type of ENM described above, carbon dots diffuse though the column easy even after one-hour incubation time and finally released with effluent. The reason can be due to the high solubility of carbon dots in milli-Q water which was used as the mobile phase in column as well as their small size[75] that renders them molecule-like species rather than colloidal particles. Thus, although the proposed method can contribute to solution of environmental problem associated with currently mass-produced ENM, the application of the method for removal of newly-discovered ENM might be limited might require further modification for a specific target.

5.C.X. The Difference between Entrapped ENM in the Column Due to IPEC Method and Aggregation

In this method, the entrapment of ENM was predominantly due to the interaction between ENM, NP and the sand particles and not due to strong aggregation of ENM because the size of the pores (the grains are 300 – 500 μm) were significantly bigger than the size of ENM (less than 0.1 μm (**Table 5.3**)). In addition, there are 2 results that support our proposed mechanism First is FM figures in **Figure 5.7.D** and **Figure 5.9.B** and the difference in optical transmittance of sand column effluent of solution containing formed-IPEC and solution containing PE which formed IPEC inside the sand column as shown in **Figure 5.16**

The results of FM in **Figure 5.7.D** and **Figure 5.9.B** showed different types of CNT-OH distribution on sand grain. If we compare the sand grain images taken by FM in **Figure 5.7.D** and **Figure 5.9.B**, we can see the difference in the distribution of CNT-OH on the surface of sand grains due to different treatment solution composition. In **Figure 5.7.D**, the distribution of ENM was even on the surface of the grain, meanwhile in **Figure 5.9.B**, the aggregates can be clearly observed. If CNT-OH was attached on sand because aggregation and physical constraints, the distribution of the ENM should be more localized as shown in **Figure 5.9.B**. Thus, the equal distribution of dye-doped fluorescent CNT-OH shown by fluorescence microscopy proved that aggregation could not be the main cause of the CNT-OH attachment on the sand grain. Therefore, the main reason of the attachment is the IPEC-treatment that promoted adsorption of CNT-OH on the surface of the sand. This result is in agreement with the UV-Vis measurement result shown in **Figure 5.7.C**.

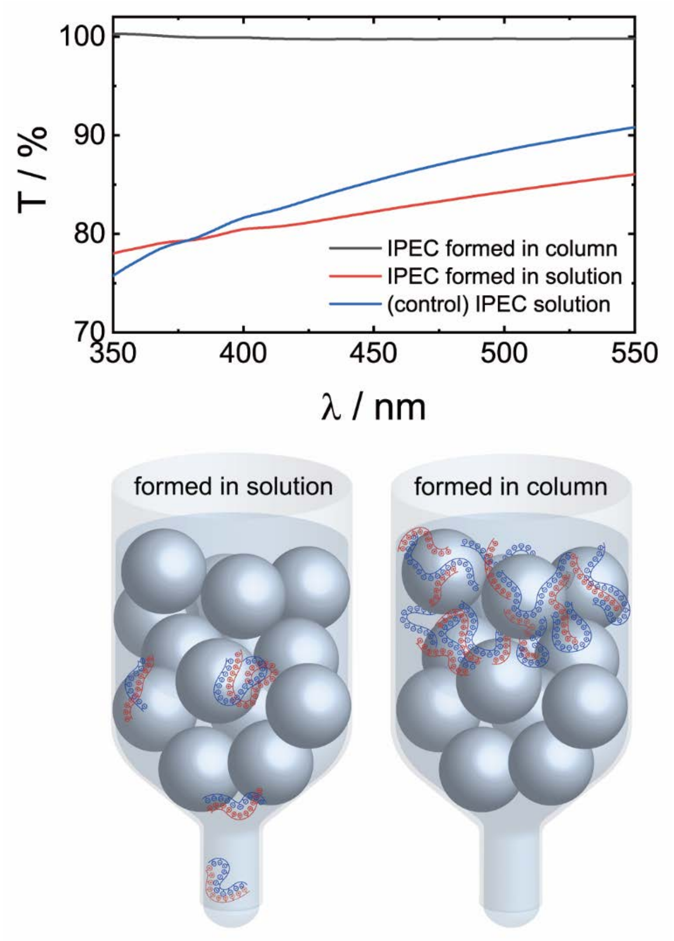

Figure 5.16. Optical transmittance (T) spectra of a solution containing an equimolar mixture of PDADMAC and PAANa (5 mM) after incubation in column and elution (red) and the same solution after dilution with water and passing through the column (grey). The former sample was prepared by injection and incubation of 1 ml 0.75 M of NaCl solution of PDADMAC and PAANa (5 mM) in column for 1 h and elution with 30 ml of water. The latter sample was prepared by dilution of 1 ml PDADMAC and PAANa solution by 9 ml of water, injection into column and elution with 20 ml of Milli-Q water. The control sample (blue) was prepared by dilution of PDADMAC and PAANa solution with 30 ml of water. The drawings below illustrate the difference between IPEC transport depending on preparation method.

Formation of IPEC inside the sand column is important for the entrapment process. Thus, to prove the significance of IPEC formation in the column role on the entrapment of ENM on the surface of grains, in **Figure 5.16**, we compared the transmittance of the eluted sample of IPEC formed outside and inside the sand column. In **Figure 5.16**, sample of IPEC formed inside the column did not show any turbidity. On the contrary, the IPEC pre-formed before addition to the column showed certain decrease of optical transmittance. Thus, it can be concluded that IPEC formed before addition to column did not attach to the sand grains. In order to be attached to the sand grains which are negatively-charged, PE should be cationic. Meanwhile, in the solution of IPEC formed before addition to column, both polycation and polyanion neutralized the charge of each other and the formed IPEC was neutral. The above results indicate that the formation of IPEC inside the column assisted the adsorption of ENM on the sand grains. If IPEC is pre-formed separately, the ENM could break through together with the formed IPEC.

ss

5.D. Conclusions

The uprising production of various types of ENM, an emergent contaminant has been recognized an environmental threat to soil considering its role as a sink ENM accumulation. Thus, an efficient yet low cost method is demanded to solve these emerging problems. In present study, a method utilizing oppositely-charged polyelectrolytes showed an excellent performance in entrapment of ENM on sand grains. The IPEC treatment promotes agglomeration and adsorption of ENM on the surface of sand grains. It is essential that PE are solubilized in treatment solution that was achieved by using high concentration of salt to screen the electrostatic between oppositely-charged PE. In order to efficiently suppress the ENM mobility through the column, the total charge on IPEC has to be neutral that is achieved by adjusting the charge ratio between polycations and polyanions. Additionally, incubation time after applying of PE solution is essential for PE to efficiently form polymer network interconnecting ENM and sand particles. Polycation plays an important role in bridging ENM and porous media particles, therefore, longer polycations provide better ENM retention efficiency. In contrast, longer polyanion may have unfavorable steric effect and the use of short polyanions provides better efficiency. There are three other findings in this study. Firstly, chemical structure of polyanion does not affect the efficiency of the method. Secondly, in this method, concentration of PE is important to entrap ENM efficiently. Thirdly, this method can be applied to various types of ENM and in various water conditions.

Finally, besides the direct remediation of contaminated soil, this method can be utilized to assist the remediation of soil by NP, such as zerovalent Fe NP by limiting their mobility.

Chapter 6

General Conclusions

In the present study, we have shown that natural and synthetic polyelectrolytes can be used to effectively remediate water and soil from ENM contamination. Specifically, we developed a methodology for entrapment and removal of four types of ENM: hydroxylated fullerene, hydroxylated carbon nanotubes, gold NP and silica NP dispersed in water. Another treatment method was developed to prevent ENM diffusion in a porous media by immobilizing ENM on the surface of porous media particles. We demonstrated that both methods can be applied under conditions close to natural environment.

For the first method, chitosan, a derivative of natural polymer chitin, was utilized for ENM removal from aqueous media. Due to pH-dependent solubility of chitosan, ENM can be entrapped by coprecipitation with chitosan induced by a solution pH change. This method is more easy-to-implement and cost-effective compared to the one based on formation of insoluble complex between oppositely-charged polyelectrolytes that has been developed earlier in our laboratory. Generally, removal of smaller size ENM requires higher concentration of chitosan due to smaller surface area per particle that limits the number of interaction sites of ENM particle with chitosan. To increase ENM removal efficiency, use of chitosan with higher molecular weight and longer sedimentation time are preferable treatment conditions.

Moreover, additional treatment, such as filtration can be applied to further improve the removal efficiency of ENM from solution.

In the second method, formation of IPEC between oppositely charged polyelectrolytes was used to entrap ENM in the sand column as a simple model of soil. Treatment solution was prepared by dissolving PE in solution with high concentration of salt to screen the electrostatic charge of both oppositely-charged PE. To enable efficient suppression of ENM transport in the porous media, PE mixture have to be incubated after treatment to enable formation of insoluble IPEC binding ENM to sand particles. Due to the dependence of IPEC solubility on PE charge neutralization degree, charge ratio between polycation and polyanion has to be stoichiometrically equal to ensure charge neutralization and formation of insoluble IPEC. Use of high-molecular-weight polycation and low-molecular-weight polyanion in the treatment solution gave the highest ENM retention efficiency. Polyanion utilized in this treatment is not limited to certain type of PE. This method is less effective for ENM retention in porous media with big pores, but since natural soil is less porous than the sand used in our study, the implementation of the method for treatment of natural soil is apparently possible.

The development of nanotechnology is still on going. Novel ENM will keep being developed further. Thus, suitable methods of safe handling and remediation needs to be developed on the similar pace to protect the environment.

References

(1) RAY, P. C.; YU, H.; Fu, P. P. Toxicity and Environmental Risks of Nanomaterials: Challenges and Future Needs. *J. Environ. Sci. Heal. Part C* **2009**, *27* (1), 1–35.

(2) Ju-Nam, Y.; Lead, J. R. Manufactured Nanoparticles: An Overview of Their Chemistry, Interactions and Potential Environmental Implications. *Sci. Total Environ.* **2008**, *400* (1–3), 396–414.

(3) Wang, Y.; Hu, A. Carbon Quantum Dots: Synthesis, Properties and Applications. *J. Mater. Chem. C* **2014**, *2* (34), 6921.

(4) Tuerhong, M.; XU, Y.; YIN, X. B. Review on Carbon Dots and Their Applications. *Chinese J. Anal. Chem.* **2017**, *45* (1), 139–150.

(5) Burks, J.; Nadella, S.; Mahmud, A.; Mankongpaisarnrung, C.; Wang, J.; Hahm, J. I.; Tucker, R. D.; Shivapurkar, N.; Stern, S. T.; Smith, J. P. Cholecystokinin Receptor-Targeted Polyplex Nanoparticle Inhibits Growth and Metastasis of Pancreatic Cancer. *Cmgh* **2018**, *6* (1), 17–32.

(6) Amin, M. T.; Alazba, A. A.; Manzoor, U. A Review of Removal of Pollutants from Water/Wastewater Using Different Types of Nanomaterials. *Advances in Materials Science and Engineering*. 2014, pp 1–24.

(7) FIFA. FIFA Quality Concept-Handbook of Requirements for Football Turf. **2012**, No. January, 1–39.

(8) Ehrenhauser, F.; Aragon, D.; Gaudet, C.; Tishechkina, I. Size Matters: Crystal Size Analysis for the Louisiana Sugar Industry http://www.lsuagcenter.com/profiles/lbenedict/articles/page1491324916020 (accessed Mar 15, 2018).

(9) Roco, M. C. The Long View of Nanotechnology Development: The National Nanotechnology Initiative at 10 Years. *J. Nanoparticle Res.* **2011**, *13* (2), 427–445.

(10) Wiesner, M. R.; Lowry, G. V.; Alvarez, P.; Dionysiou, D.; Biswas, P. Assessing the Risks of Manufactured Nanomaterials. *Environ. Sci. Technol.* **2006**, *40* (14), 4336–4345.

(11) Steph. "Why all the nano-hype?" or "Do nanoparticles fall in love?"

(12) Pulicharla, R.; Zolfaghari, M.; Brar, S. K.; Cledon, M.; Drogui, P.; Surampalli, R. Y. Cosmetic Nanomaterials in Wastewater: Titanium Dioxide and Fullerenes. *J. Hazardous, Toxic, Radioact. Waste* **2016**, *20* (1), B4014005.

(13) Strand, R.; Kjølberg, K. L. Regulating Nanoparticles: The Problem of Uncertainty. *Eur. J. Law Technol.* **2011**, *2* (3).

(14) Observatorynano. Developments in Nanotechnologies Regulation & Standards - 2011. **2011**, No. July, 21.

(15) Park, Y. Nano-regulation in China, Japan, Korea, USA and EU http://www.egg2012.de/tl_files/pdf/Paper/EGG2012_C6_1_Park_presentation_slides.pdf (accessed Jun 12, 2018).

(16) Lecoanet, H. F.; Bottero, J.; Wiesner, M. R. Laboratory Assessment of the Mobility of Nanomaterials in Porous Media Laboratory Assessment of the Mobility of Nanomaterials in Porous Media. *Environ. Sci. Technol.* **2004**, *38* (August), 5164–5169.

(17) Rico, C. M.; Majumdar, S.; Duarte-gardea, M.; Peralta-videa, J. R.; Gardea-torresdey, J. L. Interaction of Nanoparticles with Edible Plants and Their Possible Implications in the Food Chain. *J. Agric. food Chem.* **2011**, *59*, 3485–3498.

(18) Judy, J. D.; Unrine, J. M.; Bertsch, P. M. Evidence for Biomagnification of Gold Nanoparticles within a Terrestrial Food Chain. *Environ. Sci. Technol.* **2011**, *45* (2), 776–781.

(19) Zinchenko, A. A.; Maeda, N.; Pu, S.; Murata, S. Entrapping of Fullerenes, Nanotubes, and Inorganic Nanoparticles by a DNA-Chitosan Complex: A Method for Nanomaterials Removal. *Environ. Sci. Technol.* **2013**, *47* (9), 4489–4496.

(20) Golbamaki, N.; Rasulev, B.; Cassano, A.; Marchese Robinson, R. L.; Benfenati, E.; Leszczynski, J.; Cronin, M. T. D. Genotoxicity of Metal Oxide Nanomaterials: Review of Recent Data and Discussion of Possible Mechanisms. *Nanoscale* **2015**, *7* (6), 2154–2198.

(21) Borm, P. J. A.; Robbins, D.; Haubold, S.; Kuhlbusch, T.; Fissan, H.; Donaldson, K.; Schins, R.; Stone, V.; Kreyling, W.; Lademann, J.; et al. The Potential Risks of Nanomaterials: A Review Carried out for ECETOC. *Part. Fibre Toxicol.* **2006**, *3* (1), 11.

(22) Reijnders, L. Cleaner Nanotechnology and Hazard Reduction of Manufactured Nanoparticles. *J. Clean. Prod.* **2006**, *14* (2), 124–133.

(23) Ramskov, T.; Selck, H.; Banta, G.; Misra, S. K.; Berhanu, D.; Valsami-Jones, E.; Forbes, V. E. Bioaccumulation and Effects of Different-Shaped Copper Oxide Nanoparticles in the Deposit-Feeding Snail Potamopyrgus Antipodarum. *Environ. Toxicol. Chem.* **2014**, *33* (9), 1976–1987.

(24) Yoo-iam, M.; Chaichana, R.; Satapanajaru, T. Toxicity, Bioaccumulation and Biomagnification of Silver Nanoparticles in Green Algae (Chlorella Sp.), Water Flea (Moina Macrocopa), Blood Worm (Chironomus Spp.) and Silver Barb (Barbonymus Gonionotus). *Chem. Speciat. Bioavailab.* **2014**, *26* (4), 257–265.

(25) Ates, M.; Demir, V.; Adiguzel, R.; Arslan, Z. Bioaccumulation, Subacute Toxicity, and Tissue Distribution of Engineered Titanium Dioxide Nanoparticles in Goldfish (Carassius Auratus). *J. Nanomater.* **2013**, *2013*, 2–7.

(26) Shoults-Wilson, W. A.; Reinsch, B. C.; Tsyusko, O. V; Bertsch, P. M.; Lowry, G. V; Unrine, J. M. Effect of Silver Nanoparticle Surface Coating on Bioaccumulation and Reproductive Toxicity in Earthworms (Eisenia Fetida). *Nanotoxicology* **2011**, *5* (3), 432–444.

(27) Lee, W.; Kim, S. W.; Kwak, J. Il; Nam, S.; Shin, Y.; An, Y. Research Trends of Ecotoxicity of Nanoparticles in Soil Environment. *Toxicol. Res.* **2010**, *26* (4), 253–259.

(28) Shi, H.; Magaye, R.; Castranova, V.; Zhao, J. Titanium Dioxide Nanoparticles: A Review of Current Toxicological Data. *Part. Fibre Toxicol.* **2013**, *10* (1), 15.

(29) Sweet, M. J.; Singleton, I. Soil Contamination with Silver Nanoparticles Reduces Bishop Pine Growth and Ectomycorrhizal Diversity on Pine Roots. *J. Nanoparticle Res.* **2015**, *17* (11), 1–8.

(30) Anjum, N. A.; Gill, S. S.; Duarte, A. C.; Pereira, E.; Ahmad, I. Silver Nanoparticles in Soil–plant Systems. *J. Nanoparticle Res.* **2013**, *15* (9), 1896.

(31) Li, M.; Lin, D.; Zhu, L. Effects of Water Chemistry on the Dissolution of ZnO Nanoparticles and Their Toxicity to Escherichia Coli. *Environ. Pollut.* **2013**, *173*, 97–102.

(32) Oberdörster, G.; Oberdörster, E.; Oberdörster, J. Nanotoxicology: An Emerging Discipline Evolving from Studies of Ultrafine Particles. *Environ. Health Perspect.* **2005**, *113* (7), 823–839.

(33) Gogos, A.; Moll, J.; Klingenfuss, F.; van der Heijden, M.; Irin, F.; Green, M. J.; Zenobi, R.; Bucheli, T. D. Vertical Transport and Plant Uptake of Nanoparticles in a Soil Mesocosm Experiment. *J. Nanobiotechnology* **2016**, *14* (1), 40.

(34) Nickel, C.; Gabsch, S.; Hellack, B.; Nogowski, A.; Babick, F.; Stintz, M.; Kuhlbusch, T. A. J. Mobility of Coated and Uncoated TiO2 Nanomaterials in Soil Columns - Applicability

of the Tests Methods of OECD TG 312 and 106 for Nanomaterials. *J. Environ. Manage.* **2015**, *157*, 230–237.

(35) Park, C. M.; Chu, K. H.; Heo, J.; Her, N.; Jang, M.; Son, A.; Yoon, Y. Environmental Behavior of Engineered Nanomaterials in Porous Media: A Review. *J. Hazard. Mater.* **2016**, *309*, 133–150.

(36) Buzea, C.; Pacheco, I. I.; Robbie, K. Nanomaterials and Nanoparticles: Sources and Toxicity. *Biointerphases* **2007**, *2* (4), MR17-R71.

(37) United States Environmental Protection Agency. *In Situ Treatment Technologies for Contaminated Soil: Engineering Forum Issue Paper*; Washington D.C., 2006.

(38) Gasperi, J.; Laborie, B.; Rocher, V. Treatment of Combined Sewer Overflows by Ballasted Flocculation: Removal Study of a Large Broad Spectrum of Pollutants. *Chem. Eng. J.* **2012**, *211–212* (2012), 293–301.

(39) Honda, R. J.; Keene, V.; Daniels, L.; Walker, S. L. Removal of TiO2 Nanoparticles During Primary Water Treatment: Role of Coagulant Type, Dose, and Nanoparticle Concentration. *Environ. Eng. Sci.* **2014**, *31* (3), 127–134.

(40) Frimmel, F. H.; Doll, T. E. Xenobiotic Pharmaceuticals in Water and Methods To Prevent Their Appearance in Drinking Water: Photolytic and Photocatalytic Degradation of Pharmaceuticals Fritz. In *Soil and Water*; Twardowska, I., Allen, H. E., Häggblom, M. M., Stefaniak, S., Eds.; Springer Netherlands, 2006; pp 339–350.

(41) Farhaoui, M.; Derraz, M. Review on Optimization of Drinking Water Treatment Process. *J. Water Resour. Prot.* **2016**, *08* (08), 777–786.

(42) Pu, S. Y.; Zinchenko, A.; Chen, N.; Murata, S. Entrapment and Removal of Carbon Nanotubes and Fullerenes by Coprecipitation with Calcium Carbonate Beads. *ACS Sustain. Chem. Eng.* **2014**, *2* (10), 2275–2282.

(43) Soenaryo, T.; Zinchenko, A.; Murata, S. Removal of Carbon Nanomaterials by Co-Precipitation with Chitosan: A Facile Method for Water Pre-Treatment. *Environ. Sci. Water Res. Technol.* **2018**, *4* (2), 265–271.

(44) Yao, Z.; Li, J.; Xie, H.; Yu, C. Review on Remediation Technologies of Soil Contaminated by Heavy Metals. *Procedia Environ. Sci.* **2012**, *16*, 722–729.

(45) Zezin, A. B.; Mikheikin, S. V.; Rogacheva, V. B.; Zansokhova, M. F.; Sybachin, A. V.; Yaroslavov, A. A. Polymeric Stabilizers for Protection of Soil and Ground against Wind and Water Erosion. *Adv. Colloid Interface Sci.* **2015**, *226*, 17–23.

(46) Panova, I. G.; Sybachin, A. V.; Spiridonov, V. V.; Kydralieva, K.; Jorobekova, S.; Zezin, A. B.; Yaroslavov, A. A. Non-Stoichiometric Interpolyelectrolyte Complexes: Promising Candidates for Protection of Soils. *Geoderma* **2017**, *307* (January), 91–97.

(47) Pergushov, D. V; Zezin, A. A.; Zezin, A. B.; Müller, A. H. E. Advanced Functional Structures Based on Interpolyelectrolyte Complexes. In *Polyelectrolyte Complexes in the Dispersed and Solid State I: Principles and Theory*; Müller, M., Ed.; Springer Berlin Heidelberg: Berlin, Heidelberg, 2014; pp 173–225.

(48) Balaguru, R. J. B.; Jeyaprakash, B. G. Introduction to Materials and Classification of Low Dimensional Materials School of Electrical & Electronics Engineering http://www.nptel.ac.in/courses/115106076/Module 5/Module 5.pdf (accessed Mar 16, 2018).

(49) Balaguru, R. J. B.; Jeyaprakash, B. G. Quantum size effect , electrical conductivity and Quantum transport School of Electrical & Electronics Engineering http://www.nptel.ac.in/courses/115106076/Module 6/Module 6.pdf (accessed Mar 16, 2018).

(50) Kjeld, P. Quantum Size Effects in Nanostructures http://homes.nano.aau.dk/kp/Quantum size effects in nanostructures.pdf (accessed Mar 16, 2018).

(51) Takagahara, T.; Takeda, K. Theory of the Quantum Confinement Effect on Excitons in Quantum Dots of Indirect-Gap Materials. *Phys. Rev. B* **1992**, *46* (23), 15578–15581.

(52) Khan, I.; Saeed, K.; Khan, I. Nanoparticles : Properties , Applications and Toxicities. *Arab. J. Chem.* **2017**.

(53) Bhatia, S. *Natural Polymer Drug Delivery Systems: Nanoparticles, Plants, and Algae*; Springer International Publishing: Cham, 2016.

(54) Cai, L.; Tong, M.; Ma, H.; Kim, H. Cotransport of Titanium Dioxide and Fullerene Nanoparticles in Saturated Porous Media. *Environ. Sci. Technol.* **2013**, *47* (11), 5703–5710.

(55) Fang, J.; Shan, X. quan; Wen, B.; Lin, J. ming; Owens, G. Stability of Titania Nanoparticles in Soil Suspensions and Transport in Saturated Homogeneous Soil Columns. *Environ. Pollut.* **2009**, *157* (4), 1101–1109.

(56) Chen, X.; Mao, S. S. Titanium Dioxide Nanomaterials: Synthesis, Properties, Modifications and Applications. *Chem. Rev.* **2007**, *107* (7), 2891–2959.

(57) Kessler, R. Engineered Nanoparticles in Consumer Products: Understanding a New Ingredient. *Environ. Health Perspect.* **2011**, *119* (3).

(58) Tourinho, P. S.; van Gestel, C. A. M.; Lofts, S.; Svendsen, C.; Soares, A. M. V. M.; Loureiro, S. Metal-Based Nanoparticles in Soil: Fate, Behavior, and Effects on Soil Invertebrates. *Environ. Toxicol. Chem.* **2012**, *31* (8), 1679–1692.

(59) Kim, I. Y.; Joachim, E.; Choi, H.; Kim, K. Toxicity of Silica Nanoparticles Depends on Size, Dose, and Cell Type. *Nanomedicine Nanotechnology, Biol. Med.* **2015**, *11* (6), 1407–1416.

(60) Murugadoss, S.; Lison, D.; Godderis, L.; Van Den Brule, S.; Mast, J.; Brassinne, F.; Sebaihi, N.; Hoet, P. H. Toxicology of Silica Nanoparticles: An Update. *Arch. Toxicol.* **2017**, *91* (9), 2967–3010.

(61) Liu, X.; Zhong, Z.; Tang, Y.; Liang, B. Review on the Synthesis and Applications of Fe 3 O 4 Nanomaterials. **2013**, *2013*.

(62) Singh, N.; Jenkins, G. J. S.; Asadi, R.; Doak, S. H. Potential Toxicity of Superparamagnetic Iron Oxide Nanoparticles (SPION). *Nano Rev.* **2010**, *1* (1), 5358.

(63) Kolosnjaj, J.; Szwarc, H.; Moussa, F. Toxicity Studies of Fullerenes and Derivatives. In *Bio-Applications of Nanoparticles*; Chan, W. C. W., Ed.; Springer New York: New York, 2007; pp 168–180.

(64) Quevedo, I. R.; Tufenkji, N. Mobility of Functionalized Quantum Dots and a Model Polystyrene Nanoparticle in Saturated Quartz Sand and Loamy Sand. *Environ. Sci. Technol.* **2012**, *46* (8), 4449–4457.

(65) Hardman, R. A Toxicologic Review of Quantum Dots: Toxicity Depends on Physicochemical and Environmental Factors. *Environ. Health Perspect.* **2006**, *114* (2), 165–172.

(66) Lohwacharin, J.; Takizawa, S.; Punyapalakul, P. Carbon Black Retention in Saturated Natural Soils: Effects of Flow Conditions, Soil Surface Roughness and Soil Organic Matter. *Environ. Pollut.* **2015**, *205*, 131–138.

(67) Koike, E.; Kobayashi, T. Chemical and Biological Oxidative Effects of Carbon Black Nanoparticles. *Chemosphere* **2006**, *65* (6), 946–951.

(68) Lohse, S. E.; Abadeer, N. S.; Zoloty, M.; White, J. C.; Newman, L. A.; Murphy, C. J. Nanomaterial Probes in the Environment: Gold Nanoparticle Soil Retention and Environmental Stability as a Function of Surface Chemistry. *ACS Sustain. Chem. Eng.* **2017**, *5* (12), 11451–11458.

(69) Guo, Z.; Fan, X.; Xu, L.; Lu, X.; Gu, C.; Bian, Z.; Gu, N.; Zhang, J.; Yang, D. Shape Separation of Colloidal Gold Nanoparticles through Salt-Triggered Selective Precipitation. *Chem. Commun. (Camb).* **2011**, *47* (c), 4180–4182.

(70) Alkilany, A. M.; Murphy, C. J. Toxicity and Cellular Uptake of Gold Nanoparticles: What We Have Learned so Far? *J. Nanoparticle Res.* **2010**, *12* (7), 2313–2333.

(71) Zhang, Z.; Gao, P.; Qiu, Y.; Liu, G.; Feng, Y.; Wiesner, M. Transport of Cerium Oxide Nanoparticles in Saturated Silica Media: Influences of Operational Parameters and Aqueous Chemical Conditions. *Sci. Rep.* **2016**, *6* (1), 34135.

(72) Pakrashi, S.; Kumar, D.; Iswarya, V.; Bhuvaneshwari, M.; Chandrasekaran, N.; Mukherjee, A. A Comparative Ecotoxicity Analysis of α- and γ-Phase Aluminium Oxide Nanoparticles towards a Freshwater Bacterial Isolate Bacillus Licheniformis. *Bioprocess Biosyst. Eng.* **2014**, *37* (12), 2415–2423.

(73) Pakrashi, S.; Dalai, S.; T.C., P.; Trivedi, S.; Myneni, R.; Raichur, A. M.; Chandrasekaran, N.; Mukherjee, A. Cytotoxicity of Aluminium Oxide Nanoparticles towards Fresh Water Algal Isolate at Low Exposure Concentrations. *Aquat. Toxicol.* **2013**, *132–133*, 34–45.

(74) Zaytseva, O.; Neumann, G. Carbon Nanomaterials: Production, Impact on Plant Development, Agricultural and Environmental Applications. *Chem. Biol. Technol. Agric.* **2016**, *3* (1), 1–26.

(75) Lim, S. Y.; Shen, W.; Gao, Z. Carbon Quantum Dots and Their Applications. *Chem. Soc. Rev.* **2015**, *44* (1), 362–381.

(76) Keller, A. A.; McFerran, S.; Lazareva, A.; Suh, S. Global Life Cycle Releases of Engineered Nanomaterials. *J. Nanoparticle Res.* **2013**, *15* (6).

(77) Vance, M. E.; Kuiken, T.; Vejerano, E. P.; McGinnis, S. P.; Hochella, M. F.; Hull, D. R. Nanotechnology in the Real World: Redeveloping the Nanomaterial Consumer Products Inventory. *Beilstein J. Nanotechnol.* **2015**, *6* (1), 1769–1780.

(78) Shahabi, S.; Treccani, L.; Dringen, R.; Rezwan, K. Modulation of Silica Nanoparticle Uptake into Human Osteoblast Cells by Variation of the Ratio of Amino and Sulfonate Surface Groups: Effects of Serum. *ACS Appl. Mater. Interfaces* **2015**, *7* (25), 13821–13833.

(79) Ema, M.; Kobayashi, N.; Naya, M.; Hanai, S.; Nakanishi, J. Reproductive and Developmental Toxicity Studies of Manufactured Nanomaterials. *Reprod. Toxicol.* **2010**, *30* (3), 343–352.

(80) Valizadeh, A.; Mikaeili, H.; Samiei, M.; Farkhani, S. M.; Zarghami, N.; Kouhi, M.; Akbarzadeh, A.; Davaran, S. Quantum Dots: Synthesis, Bioapplications, and Toxicity. *Nanoscale Res. Lett.* **2012**, *7* (1), 1.

(81) FRENS, G. Controlled Nucleation for the Regulation of the Particle Size in Monodisperse Gold Suspensions. *Nat. Phys. Sci.* **1973**, *241* (105), 20–22.

(82) Jana, N. R.; Gearheart, L.; Murphy, C. J. Seeding Growth for Size Control of 5-40 Nm Diameter Gold Nanoparticles. *Langmuir* **2001**, *17* (22), 6782–6786.

(83) Neouze, M.-A.; Schubert, U. Surface Modification and Functionalization of Metal and Metal Oxide Nanoparticles by Organic Ligands. *Monatshefte für Chemie - Chem. Mon.* **2008**, *139* (3), 183–195.

(84) Kango, S.; Kalia, S.; Celli, A.; Njuguna, J.; Habibi, Y.; Kumar, R. Surface Modification of Inorganic Nanoparticles for Development of Organic-Inorganic Nanocomposites - A Review. *Prog. Polym. Sci.* **2013**, *38* (8), 1232–1261.

(85) Vengatesan, M. R.; Mittal, V. Surface Modification of Nanomaterials for Application in Polymer Nanocomposites: An Overview. In *Surface Modification of Nanoparticle and Natural Fiber Fillers*; Wiley-VCH Verlag GmbH & Co. KGaA: Weinheim, Germany, 2015; pp 1–28.

(86) Qie, Y.; Yuan, H.; Von Roemeling, C. A.; Chen, Y.; Liu, X.; Shih, K. D.; Knight, J. A.; Tun, H. W.; Wharen, R. E.; Jiang, W.; et al. Surface Modification of Nanoparticles Enables Selective Evasion of Phagocytic Clearance by Distinct Macrophage Phenotypes. *Sci. Rep.* **2016**, *6* (April), 1–11.

(87) Makarova, O. V.; Rajh, T.; Thurnauer, M. C.; Martin, A.; Kemme, P. A.; Cropek, D. Surface Modification of TiO2 Nanoparticles for Photochemical Reduction of Nitrobenzene. *Environ. Sci. Technol.* **2000**, *34* (22), 4797–4803.

(88) Rajh, T.; Makarova, O. V.; Thurnauer, M. C.; Cropek, D. Surface Modification of TiO2: A Route for Efficient Semiconductor Assisted Photocatalysis. In *Synthesis, Functionalization and Surface Treatment of NANOPARTICLES*; Baraton, M.-I., Ed.; American Scientific Publishers, 2003; pp 147–172.

(89) Georgakilas, V.; Otyepka, M.; Bourlinos, A. B.; Chandra, V.; Kim, N.; Kemp, K. C.; Hobza, P.; Zboril, R.; Kim, K. S. Functionalization of Graphene: Covalent and Non-Covalent Approaches, Derivatives and Applications. *Chem. Rev.* **2012**, *112* (11), 6156–6214.

(90) Pakrashi, S.; Dalai, S.; Humayun, A.; Chakravarty, S.; Chandrasekaran, N.; Mukherjee, A. Ceriodaphnia Dubia as a Potential Bio-Indicator for Assessing Acute Aluminum Oxide Nanoparticle Toxicity in Fresh Water Environment. *PLoS One* **2013**, *8* (9).

(91) Doane, T.; Burda, C. Nanoparticle Mediated Non-Covalent Drug Delivery. *Adv. Drug Deliv. Rev.* **2013**, *65* (5), 607–621.

(92) Sun, T. Y.; Gottschalk, F.; Hungerbühler, K.; Nowack, B. Comprehensive Probabilistic Modelling of Environmental Emissions of Engineered Nanomaterials. *Environ. Pollut.* **2014**, *185*, 69–76.

(93) Boyes, W. K.; Thornton, B. L. M.; Al-Abed, S. R.; Andersen, C. P.; Bouchard, D. C.; Burgess, R. M.; Hubal, E. A. C.; Ho, K. T.; Hughes, M. F.; Kitchin, K.; et al. A Comprehensive Framework for Evaluating the Environmental Health and Safety Implications of Engineered Nanomaterials. *Crit. Rev. Toxicol.* **2017**, *47* (9), 771–814.

(94) Kim, J. G.; Lee, S. S.; Moon, H.; Kang, I. M.; Kang, I. I. M. Land Application of Alum Sludge from Water Purification Plant to Acid Mineral Soil Treated with Acidic Water. *Soil Sci. Plant Nutr.* **2002**, *48* (1), 15–22.

(95) Caballero-Guzman, A.; Sun, T.; Nowack, B. Flows of Engineered Nanomaterials through the Recycling Process in Switzerland. *Waste Manag.* **2015**, *36*, 33–43.

(96) Kang, D.; Kim, J. E. Fine, Ultrafine, and Yellow Dust: Emerging Health Problems in Korea. *J. Korean Med. Sci.* **2014**, *29* (5), 621–622.

(97) RAY, P. C.; YU, H.; FU, P. P. Toxicity and Environmental Risks of Nanomaterials: Challenges and Future Needs. *J. Environ. Sci. Heal. Part C* **2009**, *27* (1), 1–35.

(98) Allegri, M.; Perivoliotis, D. K.; Bianchi, M. G.; Chiu, M.; Pagliaro, A.; Koklioti, M. A.; Trompeta, A. F. A.; Bergamaschi, E.; Bussolati, O.; Charitidis, C. A. Toxicity

Determinants of Multi-Walled Carbon Nanotubes: The Relationship between Functionalization and Agglomeration. *Toxicol. Reports* **2016**, *3*, 230–243.

(99) Balasubramanian, K.; Burghard, M. Chemically Functionalized Carbon Nanotubes. *Small* **2005**, *1* (2), 180–192.

(100) Madani, S. Y.; Mandel, A.; Seifalian, A. M. A Concise Review of Carbon Nanotube’s Toxicology. *Nano Rev.* **2013**, *4* (1), 21521.

(101) Voigt, N.; Henrich-Noack, P.; Kockentiedt, S.; Hintz, W.; Tomas, J.; Sabel, B. A. Toxicity of Polymeric Nanoparticles in Vivo and in Vitro. *J. Nanopart. Res.* **2014**, *16* (6), 1–22.

(102) Verma, A.; Verma, A. POLYELECTROLYTE COMPLEX- AN OVERVIEW. *Int. J. Pharm. Sci. Res.* **2013**, *4* (5), 1684–1691.

(103) Meka, V. S.; Sing, M. K. G.; Pichika, M. R.; Nali, S. R.; Kolapalli, V. R. M.; Kesharwani, P. A Comprehensive Review on Polyelectrolyte Complexes. *Drug Discov. Today* **2017**, *22* (11), 1697–1706.

(104) Rojas, O. J.; Claesson, P. M.; Muller, D.; Neuman, R. D. The Effect of Salt Concentration on Adsorption of Low-Charge-Density Polyelectrolytes and Interactions between Polyelectrolyte-Coated Surfaces. *J. Colloid Interface Sci.* **1998**, *205* (1), 77–88.

(105) Boustta, M.; Leclercq, L.; Vert, M.; Vasilevskaya, V. V. Experimental and Theoretical Studies of Polyanion-Polycation Complexation in Salted Media in the Context of Nonviral Gene Transfection. *Macromolecules* **2014**, *47* (11), 3574–3581.

(106) Dragan, S.; Cristea, M.; Luca, C.; Simionescu, B. C. Polyelectrolyte Complexes. I. Synthesis and Characterization of Some Insoluble Polyanion-Polycation Complexes. *J. Polym. Sci. Part A Polym. Chem.* **1996**, *34* (17), 3485–3494.

(107) Kim, K. M.; Son, J. H.; Kim, S.; Weller, C. L.; Hanna, M.; Hanna, M. a. Properties of Chitosan Films as a Function of PH and Solvent Type. *J. Food Scince E Food Eng. Phys. Prop.* **2006**, *71* (3), 119–124.

(108) Kumbar, S.; Laurencin, C.; Deng, M. *Natural and Synthetic Biomedical Polymers*; 2014.

(109) Lu, S.; Song, X.; Cao, D.; Chen, Y.; Yao, K. Preparation of Water-Soluble Chitosan. *J. Appl. Polym. Sci.* **2004**, *91*, 3497–3503.

(110) Bolto, B.; Gregory, J. Organic Polyelectrolytes in Water Treatment. *Water Res.* **2007**, *41* (11), 2301–2324.

(111) Das, B. P.; Tsianou, M. From Polyelectrolyte Complexes to Polyelectrolyte Multilayers: Electrostatic Assembly, Nanostructure, Dynamics, and Functional Properties. *Adv. Colloid Interface Sci.* **2017**, *244*, 71–89.

(112) Kawamura, S. Effectiveness of Natural Polyelectrolytes in Water Treatment. *J. Am. Water Work. Assoc.* **1991**, *83* (10), 88–91.

(113) Dixit, R.; Wasiullah; Malaviya, D.; Pandiyan, K.; Singh, U. B.; Sahu, A.; Shukla, R.; Singh, B. P.; Rai, J. P.; Sharma, P. K.; et al. Bioremediation of Heavy Metals from Soil and Aquatic Environment: An Overview of Principles and Criteria of Fundamental Processes. *Sustain.* **2015**, *7* (2), 2189–2212.

(114) Troester, M.; Brauch, H.-J.; Hofmann, T. Vulnerability of Drinking Water Supplies to Engineered Nanoparticles. *Water Res.* **2016**, *96*, 255–279.

(115) Nam, D. H.; Lee, B. C.; Eom, I. C.; Kim, P.; Yeo, M. K. Uptake and Bioaccumulation of Titanium- and Silver-Nanoparticles in Aquatic Ecosystems. *Mol. Cell. Toxicol.* **2014**, *10* (1), 9–17.

(116) Nel, A.; Xia, T.; Mädler, L.; Li, N. Toxic Potential of Materials at the Nanolevel. *Science* **2006**, *311* (February 2006), 622–627.

(117) Liu, Y.; Tourbin, M.; Lachaize, S.; Guiraud, P. Nanoparticles in Wastewaters: Hazards, Fate and Remediation. *Powder Technol.* **2014**, *255*, 149–156.

(118) Farré, M.; Gajda-Schrantz, K.; Kantiani, L.; Barceló, D. Ecotoxicity and Analysis of Nanomaterials in the Aquatic Environment. *Anal. Bioanal. Chem.* **2009**, *393* (1), 81–95.

(119) Eckelman, M. J.; Mauter, M. S.; Isaacs, J. A.; Elimelech, M. New Perspectives on Nanomaterial Aquatic Ecotoxicity: Production Impacts Exceed Direct Exposure Impacts for Carbon Nanotoubes. *Environ. Sci. Technol.* **2012**, *46* (5), 2902–2910.

(120) Gottschalk, F.; Sondere, T.; Schols, R.; Nowack, B. Modeled Environmental Concentrations of Engineered Nanomaterials for Different Regions. *Environ. Sci. Technol.* **2009**, *43* (24), 9216–9222.

(121) Klaine, S. J.; Koelmans, A. A.; Horne, N.; Carley, S.; Handy, R. D.; Kapustka, L.; Nowack, B.; von der Kammer, F. Paradigms to Assess the Environmental Impact of Manufactured Nanomaterials. *Environ. Toxicol. Chem.* **2012**, *31* (1), 3–14.

(122) Collin, B.; Oostveen, E.; Tsyusko, O. V.; Unrine, J. M. Influence of Natural Organic Matter and Surface Charge on the Toxicity and Bioaccumulation of Functionalized Ceria Nanoparticles in Caenorhabditis Elegans. *Environ. Sci. Technol.* **2014**, *48* (2), 1280–1289.

(123) Salari Joo, H.; Kalbassi, M. R.; Yu, I. J.; Lee, J. H.; Johari, S. A. Bioaccumulation of Silver Nanoparticles in Rainbow Trout (Oncorhynchus Mykiss): Influence of Concentration and Salinity. *Aquat. Toxicol.* **2013**, *140–141*, 398–406.

(124) Zhu, X.; Chang, Y.; Chen, Y. Toxicity and Bioaccumulation of TiO2 Nanoparticle Aggregates in Daphnia Magna. *Chemosphere* **2010**, *78* (3), 209–215.

(125) Boxall, A. B. a; Tiede, K.; Chaudhry, Q. Engineered Nanomaterials in Soils and Water: How Do They Behave and Could They Pose a Risk to Human Health? *Nanomedicine (Lond).* **2007**, *2* (6), 919–927.

(126) Zhang, Y.; Chen, Y.; Westerhoff, P.; Hristovski, K.; Crittenden, J. C. Stability of Commercial Metal Oxide Nanoparticles in Water. *Water Res.* **2008**, *42* (8–9), 2204–2212.

(127) Westerhoff, P.; Song, G.; Hristovski, K.; Kiser, M. A. Occurrence and Removal of Titanium at Full Scale Wastewater Treatment Plants: Implications for TiO2 Nanomaterials. *J. Environ. Monit.* **2011**, *13* (5), 1195–1203.

(128) Shon, H. K.; Phuntsho, S.; Chaudhary, D. S.; Vigneswaran, S.; Cho, J. Nanofiltration for Water and Wastewater Treatment - A Mini Review. *Drink. Water Eng. Sci.* **2013**, *6* (1), 47–53.

(129) AWWA Subcommittee on Periodical Publications. Microfiltration and Ultrafiltration Membranes for Drinking Water (M53). *J. Am. Water Work. Assoc.* **2008**, *100* (12), 84–97.

(130) Kozisek, F. 12. HEALTH RISKS FROM DRINKING DEMINERALISED WATER. In *Nutrients in Drinking Water*; World Health Organization, Ed.; World Health Organization: Geneva, 2005; pp 148–163.

(131) Kiser, M. A.; Westerhoff, P.; Benn, T.; Wang, Y.; Pérez-Rivera, J.; Hristovski, K. Titanium Nanomaterial Removal and Release from Wastewater Treatment Plants. *Environ. Sci. Technol.* **2009**, *43* (17), 6757–6763.

(132) Abbott Chalew, T. E.; Ajmani, G. S.; Huang, H.; Schwab, K. J. Evaluating Nanoparticle Breakthrough during Drinking Water Treatment. *Environ. Health Perspect.* **2013**, *121* (10), 1161–1166.

(133) Gottschalk, F.; Sonderer, T.; Scholz, R. W.; Nowack, B. Modeled Environmental Concentrations of Engineered Nanomaterials (TiO2, ZnO, Ag, CNT, Fullerenes) for Different Regions. *Environ. Sci. Technol.* **2009**, *43* (24), 9216–9222.

(134) Liu, N.; Liu, C.; Zhang, J.; Lin, D. Removal of Dispersant-Stabilized Carbon Nanotubes by Regular Coagulants. *J. Environ. Sci. (China)* **2012**, *24* (8), 1364–1370.

(135) Limbach, L. K.; Bereiter, R.; Müller, E.; Krebs, R.; Gälli, R.; Stark, W. J. Removal of Oxide Nanoparticles in a Model Wastewater Treatment Plant: Influence of Agglomeration and Surfactants on Clearing Efficiency. *Environ. Sci. Technol.* **2008**, *42* (15), 5828–5833.

(136) Tachaboonyakiat, W.; Serizawa, T.; Endo, T.; Akashi, M. The Influence of Molecular Weight over the Ultrathin Films of Biodegradable Polyion Complexes between Chitosan and Poly (γ-Glutamic Acid). *Polymer Journal*. 2000, pp 481–485.

(137) Vishu Kumar, A. B.; Varadaraj, M. C.; Gowda, L. R.; Tharanathan, R. N. Low Molecular Weight Chitosans-Preparation with the Aid of Pronase, Characterization and Their Bactericidal Activity towards Bacillus Cereus and Escherichia Coli. *Biochim. Biophys. Acta - Gen. Subj.* **2007**, *1770* (4), 495–505.

(138) Ishii, D.; Ohashi, C.; Hayashi, H. Facile Enhancement of Deactylation Degree of Chitosan by Hydrothermal Treatment in Imidazolium-Based Ionic Liquid. *Green Chem.* **2014**.

(139) Dobashi, T.; Tomita, N.; Maki, Y.; Chang, C. P.; Yamamoto, T. An Analysis of Anisotropic Gel Forming Process of Chitosan. *Carbohydr. Polym.* **2011**, *84* (2), 709–712.

(140) Zhang, T.; Blum, F. D. Cationic Surfactant Blocks Radical-Inhibiting Sites on Silica. *J. Colloid Interface Sci.* **2017**, *504* (May), 111–114.

(141) Dutta, P. K.; Joydeep, D.; Tripathi, V. S. Chitin and Chitosan: Properties and Applications. *J. Sci. Ind. Res. (India).* **2004**, *63*, 20–31.

(142) Chawla, S. P.; Kanatt, S. R.; Sharma, A. K. Chitosan. In *Polysaccharides*; Springer International Publishing: Cham, 2014; pp 1–24.

(143) Sogias, I. A.; Khutoryanskiy, V. V.; Williams, A. C. Exploring the Factors Affecting the Solubility of Chitosan in Water. *Macromol. Chem. Phys.* **2010**, *211* (4), 426–433.

(144) Azoulay, A.; Garzon, P.; Eisenberg, M. J. Comparison of the Mineral Content of Tap Water and Bottled Waters. *J. Gen. Intern. Med.* **2001**, *16* (3), 168–175.

(145) Rawson, D. S. The Total Mineral Content of Lake Waters. *Ecology* **1951**, *32* (4), 669–672.

(146) Pfeiffer, C.; Rehbock, C.; Huhn, D.; Carrillo-Carrion, C.; de Aberasturi, D. J.; Merk, V.; Barcikowski, S.; Parak, W. J. Interaction of Colloidal Nanoparticles with Their Local Environment: The (Ionic) Nanoenvironment around Nanoparticles Is Different from Bulk and Determines the Physico-Chemical Properties of the Nanoparticles. *J. R. Soc. Interface* **2014**, *11* (96), 20130931–20130931.

(147) Zhang, X.; Servos, M. R.; Liu, J. Ultrahigh Nanoparticle Stability against Salt, PH, and Solvent with Retained Surface Accessibility via Depletion Stabilization. *J. Am. Chem. Soc.* **2012**, *134* (24), 9910–9913.

(148) Dautzenberg, H.; Kriz, J. Response of Polyelectrolyte Complexes to Subsequent Addition of Salts with Different Cations. *Langmuir* **2003**, *19* (13), 5204–5211.

(149) Azlan, A.; Khoo, H. E.; Idris, M. A.; Ismail, A.; Razman, M. R. Evaluation of Minerals Content of Drinking Water in Malaysia. *Sci. World J.* **2012**, *2012*, 1–10.

(150) Peng, X.; Jia, J.; Gong, X.; Luan, Z.; Fan, B. Aqueous Stability of Oxidized Carbon Nanotubes and the Precipitation by Salts. *J. Hazard. Mater.* **2009**, *165* (1–3), 1239–1242.

(151) Van der Bruggen, B.; Mänttäri, M.; Nyström, M. Drawbacks of Applying Nanofiltration and How to Avoid Them: A Review. *Sep. Purif. Technol.* **2008**, *63* (2), 251–263.

(152) Kim, C. W.; Rha, C. Phase Separation of Polyethylene Glycol/Salt Aqueous Two-Phase Systems. *Phys. Chem. Liq.* **2000**, *38* (2), 181–191.

(153) Iqbal, M.; Tao, Y.; Xie, S.; Zhu, Y.; Chen, D.; Wang, X.; Huang, L.; Peng, D.; Sattar, A.; Shabbir, M. A. B.; et al. Aqueous Two-Phase System (ATPS): An Overview and Advances in Its Applications. *Biol. Proced. Online* **2016**, *18* (1), 1–18.

(154) Soenaryo, T.; Murata, S.; Zinchenko, A. Efficient Prevention of Nanomaterials Transport in the Porous Media by Treatment with Polyelectrolytes. *Chemosphere* **2018**, *210*, 567–576.

(155) Hansen, S. F.; Baun, A. European Regulation Affecting Nanomaterials - Review of Limitations and Future Recommendations. *Dose-Response* **2012**, *10* (3), 364–383.

(156) Rauscher, H.; Rasmussen, K.; Sokull-Klüttgen, B. Regulatory Aspects of Nanomaterials in the EU. *Chemie-Ingenieur-Technik* **2017**, *89* (3), 224–231.

(157) Gottschalk, F.; Nowack, B. The Release of Engineered Nanomaterials to the Environment. *J. Environ. Monit.* **2011**, *13*, 1145–1155.

(158) Holder, A. L.; Vejerano, E. P.; Zhou, X.; Marr, L. C. Nanomaterial Disposal by Incineration. *Environ. Sci. Process. Impacts* **2013**, *15* (9), 1652–1664.

(159) Heidmann, I. Metal Oxide Nanoparticle Transport in Porous Media – an Analysis about (Un)Certainties in Environmental Research. *J. Phys. Conf. Ser.* **2013**, *429*, 012042.

(160) Babakhani, P.; Bridge, J.; Doong, R. an; Phenrat, T. Continuum-Based Models and Concepts for the Transport of Nanoparticles in Saturated Porous Media: A State-of-the-Science Review. *Adv. Colloid Interface Sci.* **2017**, *246* (June), 75–104.

(161) Whitley, A. R.; Levard, C.; Oostveen, E.; Bertsch, P. M.; Matocha, C. J.; Kammer, F. Von Der; Unrine, J. M. Behavior of Ag Nanoparticles in Soil: Effects of Particle Surface Coating, Aging and Sewage Sludge Amendment. *Environ. Pollut.* **2013**, *182*, 141–149.

(162) Duffy, P.; Cullen, R. J.; Jayasundara, D. R.; Murphy, D. M.; Fonda, E.; Colavita, P. E. Electroless Deposition and Characterization of Fe/FeOx Nanoparticles on Porous Carbon Microspheres: Structure and Surface Reactivity. *J. Mater. Chem. A* **2013**, *1* (19), 6043–6050.

(163) Darlington, T. K.; Neigh, A. M.; Spencer, M. T.; Nguyen, O. T.; Oldenburg, S. J. Nanoparticle Characteristics Affecting Environmental Fate and Transport through Soil. *Environ. Toxicol. Chem.* **2009**, *28* (6), 1191–1199.

(164) Sagee, O.; Dror, I.; Berkowitz, B. Transport of Silver Nanoparticles (AgNPs) in Soil. *Chemosphere* **2012**, *88* (5), 670–675.

(165) Jaisi, D. P.; Elimelech, M. Single-Walled Carbon Nanotubes Exhibit Limited Transport in Soil Columns. *Environ. Sci. Technol.* **2009**, *43* (24), 9161–9166.

(166) Esfandyari Bayat, A.; Junin, R.; Shamshirband, S.; Tong Chong, W. Transport and Retention of Engineered Al2O3, TiO2, and SiO2 Nanoparticles through Various Sedimentary Rocks. *Sci. Rep.* **2015**, *5* (April), 1–12.

(167) Rahman, T.; George, J.; Shipley, H. J. Transport of Aluminum Oxide Nanoparticles in Saturated Sand: Effects of Ionic Strength, Flow Rate, and Nanoparticle Concentration. *Sci. Total Environ.* **2013**, *463–464*, 565–571.

(168) Duester, L.; Prasse, C.; Vogel, J. V; Vink, J. P. M.; Schaumann, G. E. Translocation of Sb and Ti in an Undisturbed Floodplain Soil after Application of Sb2O3 and TiO2 Nanoparticles to the Surface. *J. Environ. Monit.* **2011**, *13* (5), 1204–1211.

(169) Mancini, M.; Moresi, M.; Sappino, F. Rheological Behaviour of Aqueous Dispersions of Algal Sodium Alginates. *J. Food Eng.* **1996**, *28* (3–4), 283–295.

(170) Masuelli, M. A.; Illanes, C. O. Review of the Characterization of Sodium Alginate by Intrinsic Viscosity Measurements . Comparative Analysis between Conventional and Single Point Methods. *Int. J. Biomater. Sci. Eng.* **2014**, *1* (1), 1–11.

(171) Márquez-Beltrán, C.; Castañeda, L.; Enciso-Aguilar, M.; Paredes-Quijada, G.; Acuña-Campa, H.; Maldonado-Arce, A.; Argillier, J. F. Structure and Mechanism Formation of Polyelectrolyte Complex Obtained from PSS/PAH System: Effect of Molar Mixing Ratio, Base-Acid Conditions, and Ionic Strength. *Colloid Polym. Sci.* **2013**, *291* (3), 683–690.

(172) Lankalapalli, S.; Kolapalli, V. R. M. Polyelectrolyte Complexes: A Review of Their Applicability in Drug Delivery Technology. *Indian J. Pharm. Sci.* **2009**, *71* (5), 481–487.

(173) Kabanov, V. A.; Zezin, A. B.; Rogacheva, V. B.; Gulyaeva, Z. G.; Zansochova, M. F.; Joosten, J. G. H.; Brackman, J. Interaction of Astramol Poly(Propyleneimine) Dendrimers with Linear Polyanions. *Macromolecules* **1999**, *32* (6), 1904–1909.

(174) Vasilevskaya, V. V.; Leclercq, L.; Boustta, M.; Vert, M.; Khokhlov, A. R. Study of Interpolymer Complexes of Oppositely Charged Macromolecules with Different Affinity to Solvent. *Macromolecules* **2007**, *40* (16), 5934–5940.

(175) Raza, G.; Amjad, M.; Kaur, I.; Wen, D. Stability and Aggregation Kinetics of Titania Nanomaterials under Environmentally Realistic Conditions. *Environ. Sci. Technol.* **2016**, *50* (16), 8462–8472.

(176) Mui, J.; Ngo, J.; Kim, B. Aggregation and Colloidal Stability of Commercially Available Al2O3 Nanoparticles in Aqueous Environments. *Nanomaterials* **2016**, *6* (12), 90.